INFORMATION TO USERS

This manuscript has been reproduced from the microfilm master. UMI films the text directly from the original or copy submitted. Thus, some thesis and dissertation copies are in typewriter face, while others may be from any type of computer printer.

The quality of this reproduction is dependent upon the quality of the copy submitted. Broken or indistinct print, colored or poor quality illustrations and photographs, print bleedthrough, substandard margins, and improper alignment can adversely affect reproduction.

In the unlikely event that the author did not send UMI a complete manuscript and there are missing pages, these will be noted. Also, if unauthorized copyright material had to be removed, a note will indicate the deletion.

Oversize materials (e.g., maps, drawings, charts) are reproduced by sectioning the original, beginning at the upper left-hand corner and continuing from left to right in equal sections with small overlaps.

ProQuest Information and Learning
300 North Zeeb Road, Ann Arbor, Mi 48106-1346 USA
800-521-0600

UMI®

PHOTOINITIATED DESTABILIZATION OF STERICALLY STABILIZED LIPOSOMES FOR ENHANCED DRUG DELIVERY

by

Paul Anthony Spratt

A Dissertation Submitted to the Faculty of the

DEPARTMENT OF CHEMISTRY

In Partial Fulfillment of the Requirements
For the Degree of

DOCTOR OF PHILOSOPHY

In the Graduate College

THE UNIVERSITY OF ARIZONA

2002

UMI Number: 3073259

UMI®

UMI Microform 3073259
Copyright 2003 by ProQuest Information and Learning Company.
All rights reserved. This microform edition is protected against
unauthorized copying under Title 17, United States Code.

ProQuest Information and Learning Company
300 North Zeeb Road
P.O. Box 1346
Ann Arbor, MI 48106-1346

THE UNIVERSITY OF ARIZONA ®
GRADUATE COLLEGE

As members of the Final Examination Committee, we certify that we have read the dissertation prepared by Paul Anthony Spratt

entitled Photoinitiated Destabilization of Sterically Stabilized Liposomes for Enhanced Drug Delivery

and recommend that it be accepted as fulfilling the dissertation requirement for the Degree of Doctor Of Philosophy

Eugene A. Mash Jr.	10-23-02 Date
S. S. Saavedra	10/23/02 Date
Indraneel Ghosh	10/23/02 Date
K. McGovern	10/23/02 Date
J. Rupley	10/23/02 Date
Bruce Armitage	10/23/02

Final approval and acceptance of this dissertation is contingent upon the candidate's submission of the final copy of the dissertation to the Graduate College.

I hereby certify that I have read this dissertation prepared under my direction and recommend that it be accepted as fulfilling the dissertation requirement.

Eugene A. Mash Jr.	10-28-02
Dissertation Director	Date

STATEMENT BY AUTHOR

This dissertation has been submitted in partial fulfillment of requirements for an advanced degree at The University of Arizona and is deposited in the University Library to be made available to borrowers under rules of the Library.

Brief quotations from this dissertation are allowable without special permission, provided that accurate acknowledgment of source is made. Requests for permission for extended quotation from or reproduction of this manuscript in whole or in part may be granted by the head of the major department or the Dean of the Graduate College when in his or her judgment the proposed use of the material is in the interests of scholarship. In all other instances, however, permission must be obtained from the author.

SIGNED: 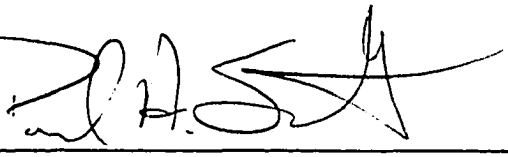

ACKNOWLEDGEMENTS

The research described in this dissertation is not the result of my effort alone, but could only be achieved with the support of many people. Above all, I wish to recognize my research advisor Dr. David F. O'Brien. His skillful leadership, understanding, and patience made it possible to keep going even in the most difficult times. Losing Dr. O'Brien was a terrible tragedy and his presence is surely missed in the completion of this work. I will always remember Dr. O'Brien fondly as a friend and mentor who expected the best from his students and gave his best to the community.

I would like to also recognize the other graduate students and post doctoral fellows with whom I worked: Dr. Bruce Bondurant, Dr. Rachel LaBell, Dr. Tony Drager, Dr. Steve Arzberger, and Da Yang. In addition the personnel at the University of Arizona Cancer Center were key to some of my successes and I would like to acknowledge them also: Dr. Kathy McGovern, Joe Divijak, Sara, and Jessica.

One final special thanks must be made to Dr. Bruce Armitage. In our hour of need, Dr. Armitage was there to lend assistance as best he could even in the difficult circumstances of being 2,000 miles away. His presence and guidance in writing this dissertation cannot be overvalued. His help will always be appreciated and a debt will always be owed to him for his help.

DEDICATION

This dissertation is dedicated to my wife and daughter. When you are a small child, you dream of what your future could hold. My dream was to have a beautiful and intelligent wife who would always be there for me and be an excellent mother of my children. She would also be a friend who would comfort me when needed and who would kick me on the rear when needed as well. I have that. My daughter is now two years old and she grants me sanity and perspective in those times when I am in most need. A simple smile on her face along with the word "Daddy" makes everything else seem inconsequential. I am truly blessed.

TABLE OF CONTENTS

TABLE OF CONTENTS – *Continued*

TABLE OF CONTENTS – *Continued*

TABLE OF CONTENTS – *Continued*

TABLE OF CONTENTS – *Continued*

TABLE OF CONTENTS – *Continued*

LIST OF ILLUSTRATIONS

CHAPTER 1

CHAPTER 2

CHAPTER 3

LIST OF ILLUSTRATIONS - *Continued*

CHAPTER 4

CHAPTER 5

LIST OF ILLUSTRATIONS - *Continued*

CHAPTER 6

CHAPTER 7

LIST OF ILLUSTRATIONS - *Continued*

LIST OF TABLES

CHAPTER 4

CHAPTER 5

CHAPTER 6

LIST OF TABLES - *continued*

CHAPTER 7

ABSTRACT

The use of liposomes for the delivery of therapeutic agents to tumor sites took a major step forward with the introduction of sterically stabilized liposomes (PEG-liposomes). Several research groups reported the increased localization of PEG-liposomes at tumor sites. Once PEG-liposomes reach these sites, it can be desirable to increase the rate of release of encapsulated compound(s). The use of radiation for this purpose is attractive, because it can be delivered in a spatially and temporally selective manner. An effective strategy for the photopertubation of PEG-liposomes relies on the photoinitiated polymerization of reactive lipids in the liposomal bilayer. Previous studies indicated that the inclusion of the photoreactive 1,2-bis[10-(2',4'-hexadienoyloxy)decanonyl]-*sn*-glycero-3-phosphocholine (bis-SorbPC$_{17,17}$) among the lipids of PEG-liposomes had little effect on their permeability until the PEG-liposomes were exposed to UV light. Photoexposure increased the permeability of the PEG-liposomes 200-fold.

Research in this dissertation was focused upon increasing the reactivity of PEG-liposomes to UV and ionizing radiations. Additionally, the most favorable formulations were then used for the encapsulation of chemotherapeutic compounds that are currently on the market. Results in this dissertation indicate the ability to encapsulate water soluble compounds with high efficiency and subsequently release those compounds with minimal UV light exposure and with ionizing radiation doses that approach therapeutic levels.

1 INTRODUCTION

1.1 Properties of Amphiphiles, Bilayers, and Liposomes

Amphiphiles are a class of organic molecules that contain both polar (or in most cases charged) and nonpolar segments and are therefore simultaneously hydrophobic and hydrophilic. Typical examples of these molecules are detergents and phospholipids. Due to hydrophobic and hydrophilic interactions, these molecules orient and self-associate in polar and nonpolar solvents. Aqueous systems of amphiphiles exhibit a very diverse phase behavior, and some of the structures formed are schematically shown in Figure 1.1. The most common structures that most phospholipids adopt spontaneously are the concentric bilayer vesicles (lamellar phase) in excess water (Figs. 1.1, 1.2). In the bilayer structure the lipid hydrophilic head groups orient toward the aqueous phase, and the nonpolar hydrocarbons are associated at the center, away from bulk water. In comparison most detergents and lysophospholipids (Fig. 1.4) form micelles that vary in size and shape depending on the type of detergents. Certain amphiphiles, such as long-chain phosphatidylethanolamine (PE) (Fig. 1.4), do not form bilayers but adopt a structure known as the inverted hexagonal (Hexagonal II) phase (Fig. 1.1). Various types of cubic phases have also been discovered [1]. In drug delivery, the dispersed, self-closed lamellar phase — the liposome — is most important and used for most applications. In other applications, such as gene transfer and regional drug delivery applications, other structures such as the dispersed H_{II} and cubic phases, and the micelles, may be also important.

The ability of lipids to adopt structures other than the bilayers upon hydration is known as lipid polymorphism. A generalized concept of geometric shape properties can be ascribed to various amphiphilic molecules that reflect the phase structure they prefer under given conditions, as illustrated in Figure 1.3. Molecules, such as lipids, that prefer the bilayer structure, have cylindrical shapes, i.e., similar areas of polar heads and the cross sections of nonpolar chains. In the case of a larger polar head with respect to a smaller nonpolar tail, the molecules tend to pack into structures with high radii of curvature, such as micelles.

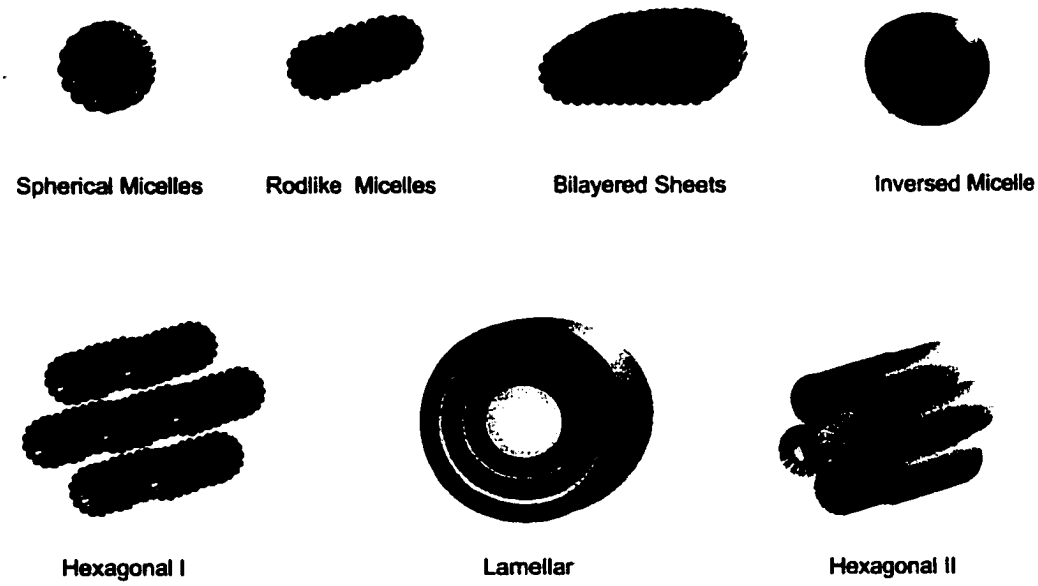

Figure 1.1. Common types of structures (phases) formed by amphiphiles in aqueous solution [2].

Liposomes are simply lipid vesicles in which an aqueous volume is entirely enclosed by a membrane composed of lipid molecules. Alec D. Bangham first discovered liposomes in the early 1960s when investigating the role of phospholipids in the clotting cascade [3]. The bilayer structure of the liposome is in principle

identical to the lipid portion of natural cell membranes — the "sea of phospholipids" in the Singer and Nicholson mosaic model [4]. Since then, liposomes have been used as models of biological membranes because liposomes can be prepared from natural constituents and membrane proteins can be reconstituted using these systems.

With respect to the size and number of membranes (lamellarity), we distinguish large multilamellar vesicles (LMV or MLV) and unilamellar vesicles (UV), which can be small (SUV), large (LUV), or giant (GUV), as shown in Figure 1.2. MLVs are normally formed when dry lipid is hydrated in aqueous solution. Small liposomes are normally defined as the ones where curvature effects are important for their properties. This curvature depends on the lipid composition and can vary from 50 nm in diameter for liquid crystalline bilayers to 80 to 100 nm for mechanically very cohesive bilayers typically in the solid phase as described in section 1.3.1. Giant vesicles are normally those with diameters above 1 μm. The thickness of the bilayer depends on the type of lipids, the hydrocarbon chain length, and the temperature, but is usually around 4 nm.

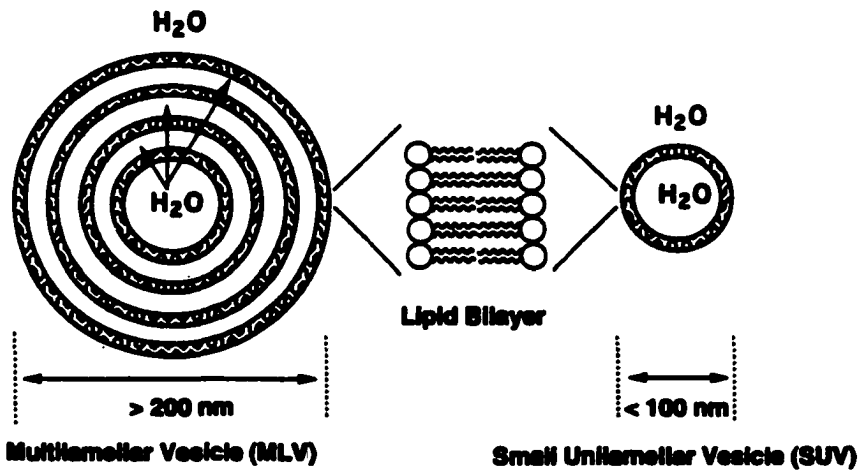

Figure 1.2. Schematic representation of multilamellar vesicles (MLV) vs. small unilamellar vesicles (SUV).

1.2 Chemical Structure of Lipids

Lipids used for lipid vesicles are extracted from natural sources or chemically synthesized. The most common natural lipids are lecithins (phosphatidylcholines, PC), sphingomyelins, and phosphatidylethanolamines (PE), which are zwitterionic at physiological pH (Fig. 1.4). The common sources for these lipids are egg yolks, soya beans, and (ox) brains. Natural lipids are less commonly used for liposome/vesicle preparations for several reasons. First, membranes prepared from natural lipids tend to be more permeable to solutes, due to the low main phase transition temperatures, and therefore they are not suitable for drug delivery when drug retention and carrier stability are emphasized. Second, for basic biophysical studies involving artificial lipid membranes, synthetic lipids are preferred, since in most cases one would like to be able to control the physical properties of the membranes and be able to better interpret the experimental results. One serious drawback of the natural lipids is that they contain a mixture of acyl chains. The last problem in using natural lipids particularly as drug carriers for human use concerns the possible contamination from the source, especially if it is animal in origin.

The stability of natural lipids can be increased by hydrogenation of naturally occurring double bonds within the hydrophobic tails. The degree of hydrogenation is described by the iodine value (*I.V.*), where *I.V.* = 1 for fully saturated chains [5]. A typical high *I.V.* number suggesting high unsaturation amounts is 65 of EPC (Egg PC). Commercially, *I.V.* values of 1, 10, 20, 30, and 40 are normally available.

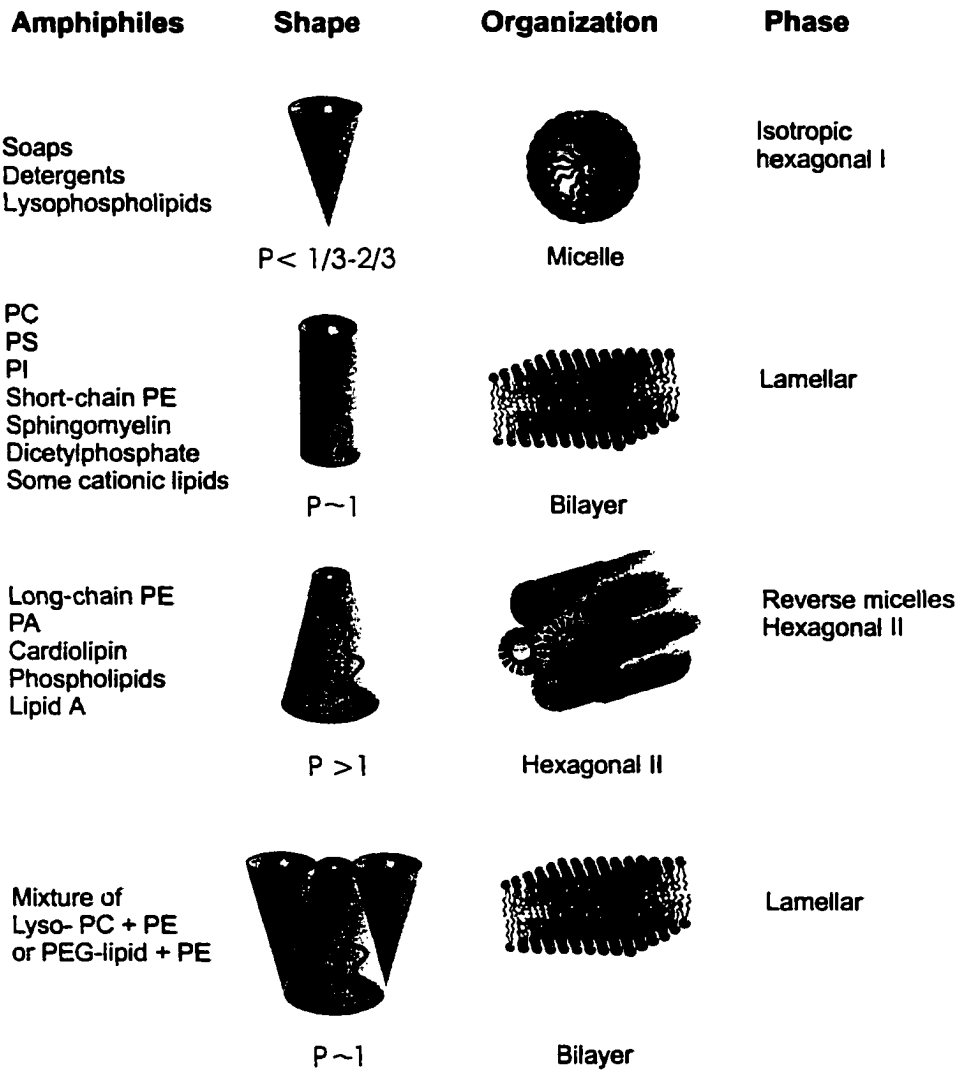

Figure 1.3. The molecular geometry and structure of lipid assemblies as determined by steric effects [2]. The P value represents the area horizontal cross section area of the tail divided by the area of the horizontal cross section of the head group.

In contrast, to lipids obtained from natural sources, chemical synthesis can produce lipids with well-defined acyl chains (number of carbons on the chains and degree of saturation) attached to the same polar heads. The most commonly used acyl chains are dimyristoyl (C14:0, a 14 carbon chain with no double bonds), dipalmitoyl

(C16:0), distearoyl (C18:0), dioleoyl (C18:1), and diarachidoyl (C20:0). The structures of some common phospholipids are shown in Figure 1.4. Cholesterol is a very important component in lipid vesicles for improving the mechanical stability of lipid bilayers and therefore increasing the retention of encapsulated agents.

Charged lipids may be included in the membrane for a large number of reasons. First, inclusion of a charged lipid may increase the surface charge density to prevent close approach between liposomes and, hence, prevent aggregation, fusion, etc. Secondly, like charges in membranes within a multilamellar liposome may push adjacent layers further apart and thus increase the internal aqueous volume. The most suitable phospholipids for either of these purposes are probably the negatively charged phosphatidyl glycerols (PG). Other negative phospholipids such as PA or PS may be unsuitable because they cause aggregation in the presence of calcium. No natural positively charged phospholipids exist, and inclusion of cationic lipids of any class gives rise to liposomes that bind strongly to proteins and other molecules. Incorporation of PG at a 10% mol ratio of total lipids is usually sufficient to reduce intermembrane interactions.

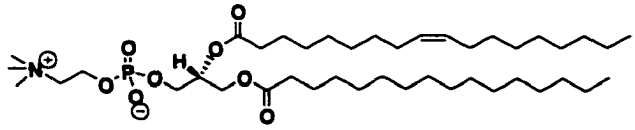

1-pamitoyl-2-oleoyl-sn-phosphatidylcholine (POPC)

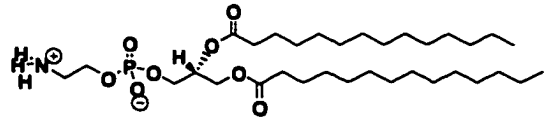

1,2-dilauroyl-sn-phosphatidylethanolamine (DLPE)

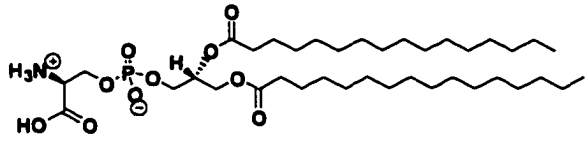

1,2-dipalmitoyl-sn-phosphatidylserine (DPPS)

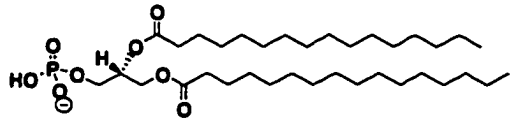

1,2-dipamitoyl-sn-phosphatidic acid (DPPA)

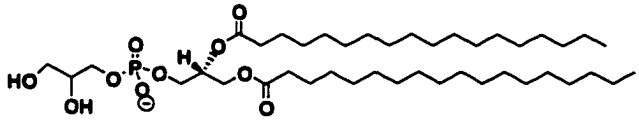

1,2-distearoyl-sn-phosphatidylglycerol (DSPG)

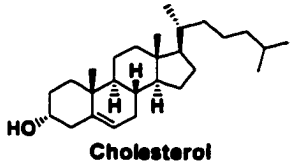

Cholesterol

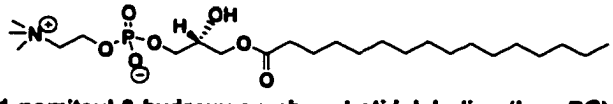

1-pamitoyl-2-hydroxy-sn-phosphatidylcholine (lyso PC)

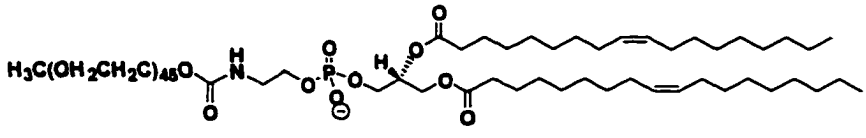

methoxy-PEG_{2000}-1,2-dioleoyl-sn-phosphatidylethanolamine (DOPE)

Figure 1.4. Structures of neutral and anionic phospholipids commonly used in liposomes for drug delivery.

1.3 Thermodynamic Properties of Lipids

1.3.1 Thermodynamic Properties of Pure Lipids

Liposome characteristics are determined by surface and membrane properties, including surface charge, steric interaction, and membrane rigidity. The most common lipids used for preparing liposomes for drug delivery are neutral or zwitterionic lipids, such as PCs and PEs. Therefore the thermal characteristics of these types of liposomes are determined by the thermodynamic properties of the lipids. Two of the most important thermodynamic parameters of chemically pure lipids is the phase transition temperature (T_m) and the associated enthalpy (ΔH). The low temperature phase for PC and PE is commonly referred to as the gel phase, where the acyl chains are packed tightly and lateral movement of lipid molecules is restricted (Fig. 1.5). For this reason, solute transport through lipid bilayers in the gel phase is limited. The high-temperature phase is called the liquid-crystalline, or fluid, phase, where the acyl chains become mobile and disordered, although the lipids are still arranged in a smooth bilayer structure. This phase transition between the ordered gel phase and the fluid phase is most commonly referred to as the main phase transition (T_m). Lipid phase transitions are cooperative events and can occur over a very narrow temperature range of less than one degree [6-8].

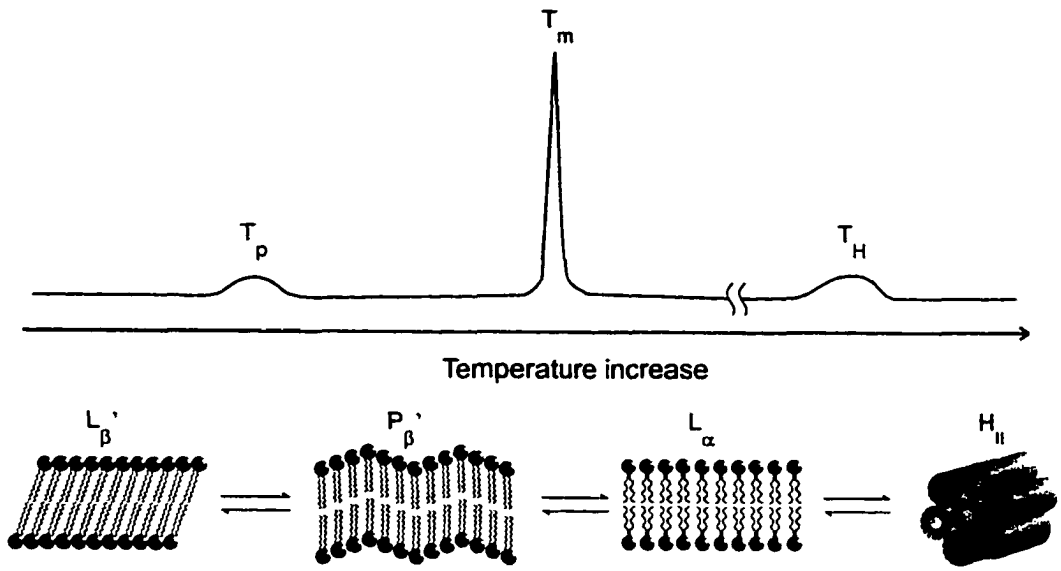

Figure 1.5. Representative DSC scan and phase diagram indicating a lipid bilayer when fully hydrated. The crystalline phase (L_{β}') transforms into a gel phase (P_{β}') at temperature T_p. The gel phase transforms into a liquid-crystalline phase (L_{α}) at temperature T_m. The liquid-crystalline phase transforms into the lamellar-hexagonal phase (H_{II}) at temperature T_H [2]. Typically, the T_p and T_m values are within several degrees, whereas the difference between the T_m and T_H values can be very large.

Factors affecting the phase transition properties are the type of polar head groups, and the length and degree of saturation of the acyl chains. For the same polar head groups, T_m increases with increasing acyl chain length [6, 8, 9]. Lipids with unsaturated acyl chains have much lower T_m values, due to the disorder introduced by the double bond. PEs usually have higher values of T_m than the corresponding PCs with identical acyl chains, because of the stronger interactions (intermolecular H-bonding) between PE head groups. The presence of charge on the polar heads (i.e., cationic and anionic lipids) tends to decrease the value of T_m, due to the repulsive interactions between molecules. It should be noted that some anionic lipids, such as

phosphatidic acid (PA) and phosphatidyl serine (PS), are known to exhibit strong intermolecular hydrogen bonding and therefore may have higher values of T_m [10, 11]. There are relatively few studies on the phase properties of the cationic lipids commonly used for delivery of DNA. These liposomes have DNA electrostatically bound to their surface and are typically called genosomes.

1.3.2 Thermodynamic Properties of Binary Lipid Mixtures

In most cases, liposomal formulations designed for drug delivery contain more than one type of lipid. An essential parameter to consider for formulation stability is the miscibility of the lipid matrix. Lipid mixtures that are poorly miscible will eventually phase separate (Fig. 1.6). For lipids with the same head groups, the degree of miscibility is mostly determined by the mismatch of the acyl chains as well as the degree of saturation of the acyl chain. PCs, for instance, with an acyl chain length differing by two carbons, have high miscibility, while a four-carbon difference results in poor miscibility. In contrast, di-18:1Δ^9 PC (two - 18 carbon length hydrophobic tails with a cis double bond in the nine position (DOPC) (Fig. 1.11)) has better miscibility with di-14:0 PC than with di-18:0 PC (two - (14 or 18) carbon length hydrophobic tails with zero double bonds (DMPC and DSPC respectively) (Fig. 1.11)) [12]. The binary phase behavior of PC with lipids having other types of head groups is rather complicated [8, 13]. PC and PE have medium or low miscibility unless the two have the same acyl chain length. It is interesting to note that PC and PG can be ideally miscible when the two have the same acyl chain length, because the thermodynamic properties of PGs are very similar to their corresponding PCs.

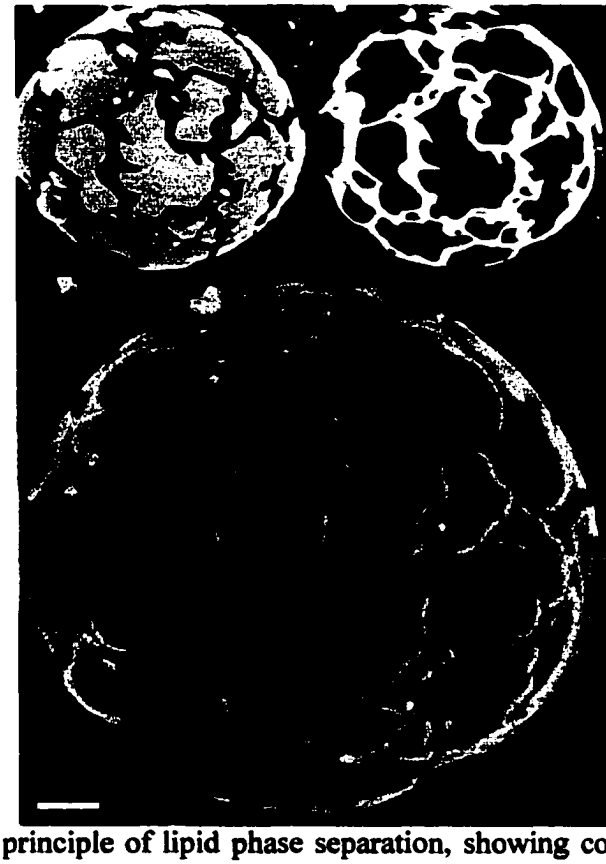

Figure 1.6. The principle of lipid phase separation, showing confocal fluorescence microscopy images of a GUV. The lipid composition of this GUV was DPPC/DLPC 5/1. The bar represents 5 μm [14].

Cholesterol is one of the most useful liposome components and can be readily incorporated into PC bilayers to a maximum of 50 mol%. Cholesterol itself does not exhibit a phase transition, but it does broaden significantly the main phase transition of the lipid bilayer into which it is incorporated. Cholesterol reduces the fluidity of membranes above the phase transition temperature, with a corresponding reduction in permeability to aqueous solutes. Consequently, inclusion of cholesterol into unsaturated membranes is often essential in order to achieve sufficient stability. That is to say that the liposomes are able maintain the encapsulation of compounds over

much longer periods of time without diffusion of those compounds through the membrane and into the external media. On the other hand, cholesterol increases the fluidity of membranes below the phase transition temperature, so that its inclusion in saturated membranes, which are usually in the lower, gel phase at ambient temperature, may result in a reduction in stability [15].

For maximum stability, therefore, the choice exists between saturated PC liposomes, composed of synthetic or hydrogenated lipid, and unsaturated PC liposomes incorporating cholesterol. Development work usually proceeds by evaluating these two approaches side by side.

1.3.3 Diffusion rates of lipids

Once the lipids are associated within a bilayer, there is free lateral movement, which can be described as similar to a milling crowd [16]. The lateral diffusion rate depends on the lamellar phase [17]. The vesicle lipid diffusion coefficient, D, is ca. 10^{-2} μm^2 s^{-1}, when the sample temperature is below the main phase transition temperature, T_m. The diffusion rate above the main transition temperature is ca. 1 μm^2 s^{-1}.

1.4 Polymerization of Hydrated Bilayers

The lamellar phase consists of extended bilayers of solvated amphiphiles with periodic smectic-like order (L_β' and P_β' structures in Fig. 1.5). However, for experimental convenience most polymerization studies have focused on lipid bilayer vesicles, i.e., liposomes. A lipid vesicle is a nearly spherical lipid bilayer shell that

encloses an aqueous volume as described earlier. The bilayer shell can be composed of hundreds of thousands of lipids with their hydrophilic headgroups exposed to water and their hydrophobic tails aggregated in a manner to reduce exposure to water. Typically, liposomes with a diameter of 100 nm have approximately 80,000 lipid molecules contained within the bilayer.

Polymerizable groups have been incorporated into bilayer-forming amphiphiles by chemical synthesis [16]. Subsequent formation of bilayer assemblies yields a two-dimensional array of the polymerizable groups. The lipid bilayer in the fast diffusion regime provides an organized structure for polymerization reactions that is sufficiently dynamic to permit monomers to diffuse to the growing polymer chain end. Electron microscopy and light scattering have been used to demonstrate that polymerization does not significantly alter the shape or diameter of vesicles [18]. However, polymerization of vesicles can dramatically alter their properties. In principle and practice the polymerizable moiety can be positioned anywhere along the lipid tails or linked (covalently or electrostatically) to the headgroup. Polymerization of the lipid tails usually leads to abolition of the bilayer T_m, whereas polymerization in the headgroup does not. Covalent linkage of the lipid tails inhibits formation of the gauche rotamers and the cooperativity typically observed as lipid bilayers undergo this phase transition. In some instances polymerizable amphiphiles clearly mimic natural lipids, e.g., phosphatidylcholine (PC) and phosphatidylethanolamine (PE), whereas others are more similar to synthetic surfactants, e.g., quaternary ammonium salts. Synthetic routes to polymerizable PCs and quaternary ammonium lipids were reported as early as 1980, due in part to the commercial availability of synthetic

intermediates. On the other hand the lack of corresponding intermediates for PE retarded the use of polymerizable PEs until a chemical synthesis was reported [19].

1.5 Liposomes as Drug Delivery Vehicles

Liposomes typically show excellent biocompatibility and their ability to encapsulate chemotherapeutic compounds recommends them as drug carriers. The advantages of liposomes as drug delivery vehicles are threefold: (1) compounds that are not water soluble may be encapsulated; (2) encapsulated therapeutic agents do not need to be altered by addition of a bulky group to mask it from the body's immune system; and (3) encapsulated chemotherapeutic compounds are kept from interacting at unintended sites. The disadvantages of conventional liposomes are their recognition by the immune system and their removal from the bloodstream by the reticuloendothelial system (RES) [20]. The disadvantages can be reduced through the use of covalently attached hydrophilic polymers, such as polyethylene glycol (PEG) [21, 22].

Hydrophilic polymers such as polyethylene glycol form a hydration sphere around the liposome [21]. This hydration sphere performs a dual role in the masking of liposomes from the RES and preventing the attachment of free floating antibodies within the bloodstream. Opsonins, a common antibody found within the bloodstream, are known to attach to the bilayer surface of conventional liposomes (CL - liposomes without an attached hydrophilic polymer). Liposomes that have undergone opsonization are now "marked" as foreign substances and are rapidly removed from the bloodstream. Sterically stabilized liposomes (SSL – so-called "Pegylated"

liposomes with an attached hydrophilic polymer), typically have an increase in retention time greater then 10 fold. An increase in the retention time of 11 fold, 3 hours to 33 hours, was seen in Theresa Allen's research, when a pegylated lipid in 5 mol % was added to the lipid formulation [21, 23-26]. The longer retention time of the liposomes can be directly attributed to their effectiveness for site-specific delivery.

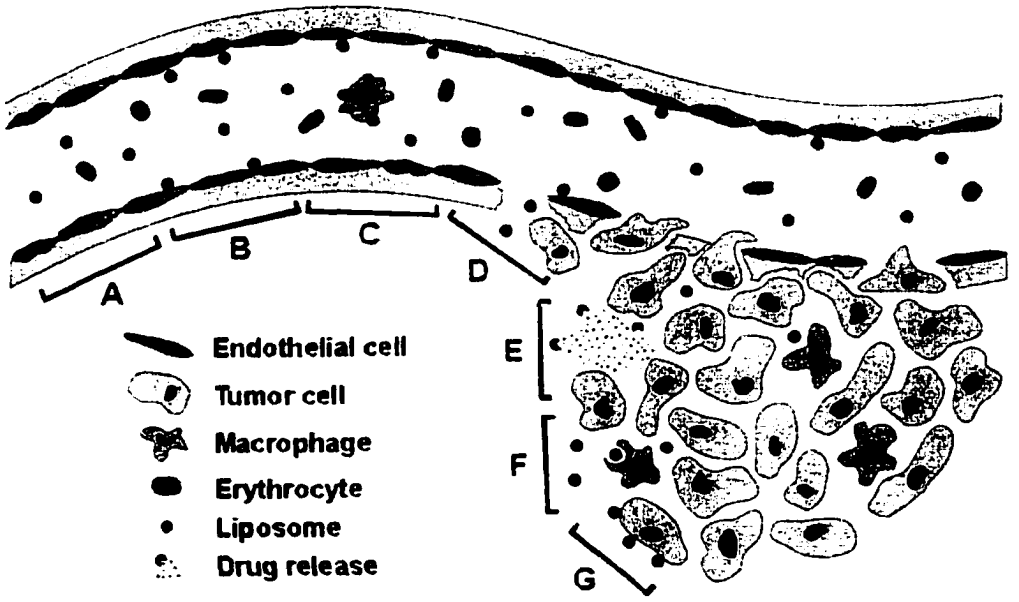

Figure 1.7. Liposomal drug delivery mechanism for improved therapeutic activity. (A) Liposomes circulating freely in the blood. (B) Liposomes interacting with endothelial cells. (C) Liposomes interacting with circulating macrophages. (D) Liposomes passively extravasating through the leaky vasculature of solid tumors. (E) Liposomes releasing entrapped drug in the tumor interstitum. (F) Liposomes being taken up by phagocytic cells in the solid tumor. (G) Liposomes associating with the surface in the solid tumor cells [27].

One of the greatest advantages of liposomes as drug delivery devices is their potential ability for site-specific delivery (Fig. 1.7). Liposomes which remain in the blood system for prolonged times tend to accumulate at tumor sites. Tumors

characteristically are supported by a leaky and disorganized vasculature. This permits long circulating liposomes to escape the vasculature and reach the interstitum, thereby increasing the concentration of the liposomes at the cancer site. The passive leakage of therapeutic agents from liposomes within the body can cause cancer cell death [28]. Preferentially, the transient time in the bloodstream would be very short, while the retention time at the cancer site would be long enough to allow for the complete release of the encapsulated compounds. Liposomes that are retained in the bloodstream are removed by the RES, thus preventing the encapsulated therapeutic agent from attacking other tissue.

Liposome applications in drug delivery depend, and are based on, physicochemical and colloidal characteristics such as composition, size, loading efficiency, and the stability of the carrier, as well as their biological interactions with the cells. There are four major interactions between liposomes and cells.

1) Lipid exchange. Lipid exchange is a long-range interaction that involves the exchange of liposomal lipids for the lipids of various cell membranes. Typically the lipid will diffuse from the lipid bilayer out to the external media and then come into contact with another liposome and diffuse into the bilayer. It depends on the mechanical stability of the bilayer and can be reduced by addition of cholesterol in liposomal formulation where the T_m is below room temperature. This can occur without the direct contact of the two liposomes.
2) Liposome adsorption to tumor cells. The second major interaction is adsorption onto cells, which occurs when there are attractive forces

(electrostatic, steric, hydration, undulation, protrusion, etc.) between the cell and the liposome membranes and can be nonspecific or specific [2]. This is reduced through the use of hydrophilic polymers as discussed above.

3) Liposome adsorption to phagocytic cells. Adsorption onto phagocytic cells is normally followed by endocytosis or, rarely, by fusion. Typically this occurs after opsonization of the liposomes and can be minimized through the incorporation of pegylated lipids into the liposomal formulation.

4) Liposome endocytosis. Endocytosis delivers the liposome and its contents into the cytoplasm indirectly via a lysosomal vacuole in which low pH and enzymes may inactivate an entrapped solute. If the liposomes fuses with the endosome, the liposome contents are delivered directly into the cell, and the liposomal lipids merge into the plasma membrane. Therefore a substantial effort to utilize this mode of drug entry is being undertaken. Efforts range from the incorporation of fusogenic proteins into the bilayer to the preparation of metastable bilayers and pH sensitive polymer coatings [29].

For drug delivery, liposomes can be formulated in a suspension, as an aerosol, or in a (semi) solid form such as a gel, cream, or dry powder; in vivo, they can be administered topically or systemically. After systemic (usually intravenous) administration, which seems to be the most promising route for this carrier system,

liposomes are typically recognized as foreign objects and consequently endocytosed by cells of the mononuclear phagocytic system (MPS), mostly fixed Kupffer cells in the liver and spleen. This fate is very useful for delivering drugs to these cells but, in general, excludes other application, including site specific drug delivery by using ligands expressed on the liposome surface in order to bind to the receptors (over) expressed on the diseased cell [2]. This is reduced through the use of hydrophilic polymers as discussed above.

Based on the liposome properties discussed above, several advantages of liposome drug delivery can be envisaged. The major advantages are; (1) enhanced drug solubilization (e.g., amphotericin B, minoxidil); (2) protection of sensitive drug molecules (e.g., cytosine arabinose, DNA, RNA, antisense oligonucleotides, ribozymes); and (3) altered pharmacokinetics and biodistribution of the encapsulated drug. The latter accounts for the decreased toxicity of liposomal formulations, because liposome-associated drug molecules cannot normally spill to organs such as the heart, brain, and kidneys as well as to increased targeting of the encapsulated drug to certain cells and tissues.

1.6 Vesicle Clearance Rates: The Role of Lipid Composition

The use of conventional liposomes as a carrier system for drug delivery has already shown promising results, but has been limited to specific applications because of their short circulation time in blood [30, 31]. The recognition of liposomes by the reticuloendothelial system (RES) is believed to occur primarily as a result of opsonization with blood opsonins [32]. The rapid clearance of conventional

liposomes with opsonins from blood is mediated primarily through the scavenging function of phagocytic cells located in the liver, spleen and to a lesser extent in other tissues known as the RES or as the MPS. The rapid uptake of liposomes by these cells has been the basis of a large portion of the biomedical uses through the last two decades, including efficacy against intracellular parasites, activation of macrophages, and antigen presentation. These cells may also act as a slow release system for liposomally encapsulated amphotericin B and doxorubicin, which are currently in the advanced phases of clinical evaluation [33].

In the course of work on liposomal stability, it was observed that solute retention by cholesterol-rich small unilamellar vesicles (SUVs), although always pronounced during relatively short (2 h) periods of exposure to blood plasma, was reduced significantly with some formulations (PC liposomes) on incubation for longer periods, whereas with others (SM liposomes) it remained unchanged [34]. It soon turned out that this phenomenon correlated with the residence time in the blood circulation of the corresponding (doubly labeled) vesicles: the greater the vesicle stability, the longer the half-life [35]. It was disappointing to note, however, that this relationship between vesicle stability and clearance observed for neutral SUVs (up to 80 nm) did not apply to very stable negatively charged SUVs or, more importantly, to larger neutral vesicles. In the latter case clearance rates were found to increase progressively with increasing size, even though bilayer stability remained high for prolonged periods of incubation with plasma [36]. It appears that vesicle size and surface charge both override bilayer stability in determining vesicle clearance from the circulation [37].

Because of their longer circulation times, and this increased ability to reach a variety of cells in tissues other than the liver and spleen, rigid, neutral SUVs have been studied intensively [38]. Unfortunately, such liposomes have serious disadvantages as delivery systems, including a small internal volume for drug encapsulation, size instability on prolonged storage, and strict limitations for liposome composition.

1.7 Sterically Stabilized Liposomes in Drug Delivery

The important breakthrough in the area of liposomal drug delivery was achieved with the discovery of so-called long circulating liposomes [39, 40]. Originally [24], such liposomes were prepared by the incorporation of ganglioside G_{M1} (Fig. 1.11) into the liposomal membrane. Another approach deals with liposome coating with poly(ethylene glycol) lipids or PEG-lipids [41-43]. The protective effect of G_{M1} on liposomes has already been clarified [23], whereas the molecular mechanism of PEG action remains obscure. The explanation of the phenomenon involves:

i) Participation of PEG in repulsive interactions between PEG-grafted membranes and other particles.

ii) Role of surface charge and hydrophilicity of PEG-coated liposomes.

iii) Decreased rate of opsonization (Fig. 8) on the hydrophilic surface of pegylated liposomes [44-46].

A key difference between G_{M1} and PEG lipids is the price of the compounds. Current prices from Avanti Polar Lipids are $220 for 10 mg of ganglioside G_{M1} and $220 for

500 mg of $mPEG_{2000}$ PE. While the molar effects of the compounds are similar, the 50-fold difference in price is an obvious advantage for PEG lipid use.

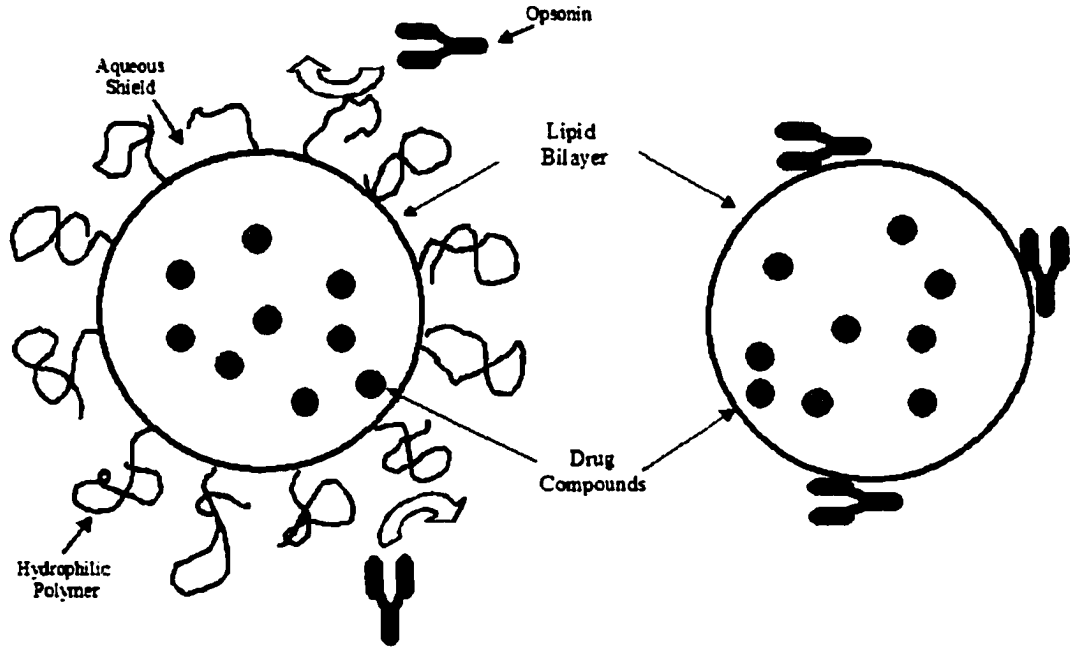

Figure 1.8. Representation of the effects of incorporating a large hydrophilic polymer on the surface of a liposome. The antibodies are less likely to attach to the liposome due to the presence of the polymer and the water associated with the polymer.

PEG, which is covalently attached to lipids within a lipid bilayer, is a highly hydrated, flexible polymer that associates to form a brush-barrier that strongly resists opsonization [47]. Because of the barrier formed by the PEG polymer, liposomes of this type are called 'sterically stabilized liposomes' (SSL) or 'PEG liposomes'.

1.8 Encapsulation of Therapeutic Agents

A wide variety of techniques are employed to encapsulate therapeutic compounds in liposomes suitable for drug delivery [48-51]. Primary considerations for choosing a suitable loading method are the physical and chemical properties of the

solutes. For water-soluble drugs that are weak bases, active or remote loading procedures are preferred, due to the high trapping efficiency and high drug-to-lipid ratio achievable. However, for most water-soluble solutes that do not respond to active loading processes, passive loading procedures have to be used.

Hydrophobic solutes can be incorporated into the hydrocarbon chain region, either by direct hydration of the solute-lipid mixtures or by the reverse-phase procedure. Detergent dialysis is very useful, especially for the reconstitution of membrane proteins. The most troublesome solutes to load are those having very low water solubility and at the same time cannot be solubilized in organic solvent due either to low solubility or to chemical instability. Examples of this type of drug are cisplatin and amphotericin.

The primary variables to consider in drug loading are encapsulation efficiency, drug-to-lipid ratio, and drug retention. The trapping efficiency is defined as the percentage of solute encapsulated, and the maximum encapsulation efficiency achievable depends on the loading technique. The drug-to-lipid ratio is determined after loading and is usually expressed as a weight ratio or a mole ratio.

1.8.1 Passive Loading of Water-Soluble Compounds

In passive loading, lipids and solute are codispersed in an aqueous medium, so solute entrapment is achieved while the liposomes are being formed. Typically lipid or lipid mixtures used in passive loading are in the form of thin films on glass walls, lyophilized powder, or simply dry cake in glass test tubes. The aqueous medium containing the water-soluble compounds is then added to the lipid. Liposomes are

generated by agitation at temperatures above the phase transition temperature. In order to achieve high encapsulation efficiency and drug-to-lipid ratio, a high concentration of solute is used whenever possible. Normally the encapsulation efficiency in a passive loading process is less than 10-20%. However, the trapping efficiency can be increased to 30-50% by the freeze-thaw technique [52, 53]. A high drug-to-lipid ratio is difficult to achieve unless the solute to be encapsulated is extremely water soluble.

1.8.2 Active Loading by Chemical Gradient

In active loading by chemical gradient, the solute is loaded after the liposomes have been formed, and the accumulation of solutes inside liposomes is mediated by certain active transportation mechanisms. For this reason it is often called remote loading. Lipophilic amino-containing solutes can be loaded with near 100% efficiency into liposomes exhibiting transmembrane pH and chemical gradients [54-56].

Many lipophilic amino agents can be actively driven into the interior of liposomes in response to a chemical gradient. LUVs are first prepared by extrusion in the presence of an ammonium salt (e.g., ammonium sulfate, ammonium citrate, or ammonium phosphate). The exterior ammonium salt is removed by means of dialysis or gel filtration column chromatography. The therapeutic compound is then added to the liposome solution, and the accumulation of the therapeutic compound inside the liposomes is achieved by incubation at a temperature above the T_m.

1.9 Triggered Release

Liposomes used for drug delivery in vivo must have very low permeability to the encapsulated compounds, so that most of the contents remain encapsulated after several hours in circulation. This both allows the delivery of the therapeutic agent to the desired site of action and prevents non-specific delivery, which can result in toxic side effects. Once liposomes reach the site of action, low permeability can reduce the effectiveness of the liposomal drug, as drugs that remain sequestered in liposomes are not available to be taken up by the cells. It has been suggested that slow release of therapeutic agents at the site of action is the major obstacle to further improvements in the therapeutic index of liposomal chemotherapeutic agents [57]. Several stimuli are potentially able to trigger the release of encapsulated drugs at the desired site of action. These include changes in pH, changes in temperature, light, and ionizing radiation.

1.9.1 pH Sensitive Liposomes

The frequently increased acidity of solid tumors, or (in the case that liposomes are endocytosed) inside the endosomal compartment can be used to trigger the release of encapsulated agents at these sites [26, 58-64]. This can be achieved either through increased permeability of the liposomal membrane or by fusion of the liposomal membrane with surrounding biomembranes (usually that of the endosome) (Fig. 1.9). It is well established that liposomes composed of high concentrations of unsaturated phosphatidylethanolamines (PE) (Fig. 1.4) fuse with other membranes at low to neutral pH. The low degree of hydration of the PE headgroup results in a small

effective headgroup volume. This gives the membrane a small positive spontaneous radius of curvature, and allows close contact of opposing bilayer leaflets. Both of these factors are necessary to promote the inverted structures of the fusion intermediates. At high pH, the PE headgroup has a net negative charge so that electrostatic forces will repel opposing bilayer leaflets and prevent fusion from occurring. Cholesterol hemisuccinate (Fig. 1.11) carries a negative charge at neutral pH, but at low pH (4 to 5) the free carboxyl is protonated, and the amphiphiles becomes neutral. If cholesterol hemisuccinate is combined with an unsaturated PE, liposomes can be formed that are stable at neutral pH but become fusogenic in mildly acidic conditions. This type of pH sensitive liposome, though useful in vitro, is not widely applicable in vivo, because the fluid membrane that is necessary for fusion is not stable to blood plasma. PEG-PE (Fig. 1.4) added to the lipid mixture will give the liposomes increased stability to plasma, and increased circulation time, however as little as 2 mole % PEG-PE can prevent liposome fusion [65]. In order for destabilization to occur, nearly all the PEG-lipid would need to be removed from large sections of the liposome surface. Reductive cleavage of a disulfide linked PEG_{2000}-1,2-distearoyl-*sn*-phosphatidylethanolamine (PEG-DSPE) completely restores fusogenicity of 1,2-dioleoyl-*sn*-phosphatidylethanolamine (DOPE) (Fig. 1.4) liposomes containing 3 to 6 mole % of the cleavable PEG-lipid. The pH sensitivity of pegylated DOPE/cholesterol hemisuccinate liposomes was also restored in this way [66].

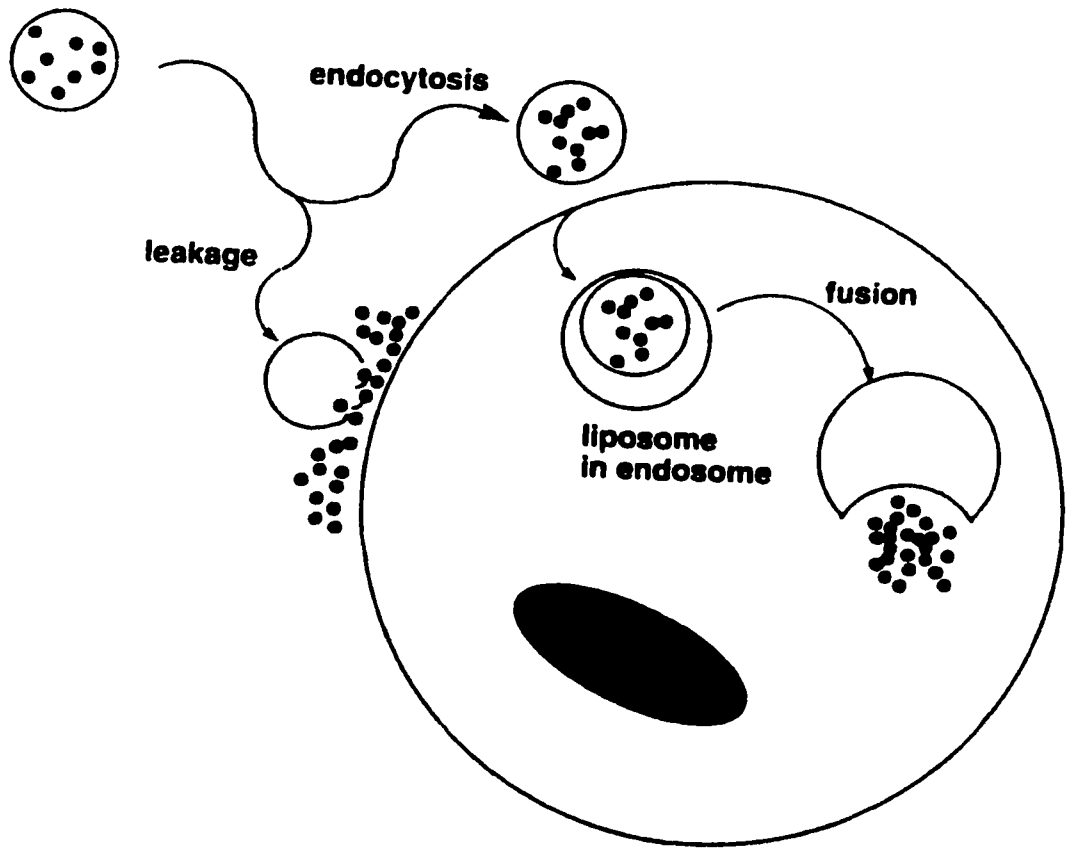

Figure 1.9. Schematic representation of potential drug delivery by a LUV to a cancer cell. The drug can be released outside the cell by leakage or by endocytosis of the LUV and fusion with the endosomal membrane releasing the therapeutic agent into the cytoplasm of the cell.

Anchored, hydrophilic polymers with pendant carboxyl functions can promote both liposome leakage and fusion at pH 5 and lower [67]. Poly(1-hydroxy-2-propylene oxide)(polyglicidol) (shown below) bearing a succinate ester at 56 % of the repeat units and a 1-decyl amide at 7 % of the repeat units, promotes fusion and leakage of egg PC liposomes at pH 4, while having relatively little effect at pH 7. EggPC liposomes bearing this polymer in PC/polymer ratio of 7/3 were found by Kono *et al.* to deliver encapsulated calcein to the cytoplasm of cultured green monkey

kidney cells, while unmodified egg yolk PC liposomes did not [68]. Though the capacity of the copolymer to prolong circulation time has not been reported, it could possibly confer some degree of steric stabilization.

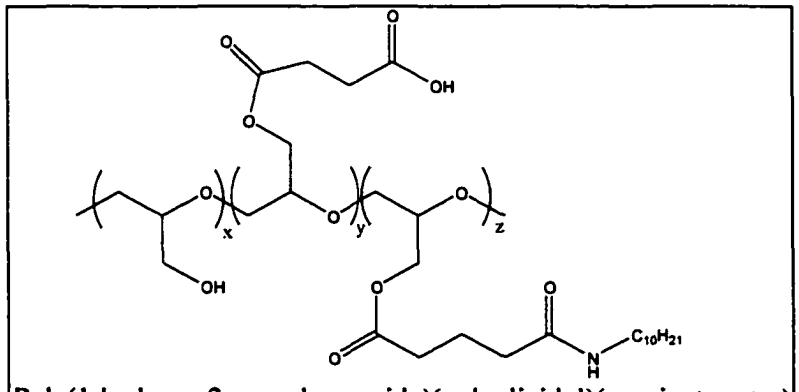

Poly(1-hydroxy-2-propylene oxide)(polyglicidol)(succinate ester)

Acid catalyzed hydrolysis of labile amphiphiles can be used in the design of pH sensitive liposomes. The naturally occurring diplasmenylcholine (DPPlsC) (Fig. 1.11), though stable at neutral pH, is degraded to produce a long chain aldehyde and glyceroPC at pH less than 4.5. Sterically stabilized liposomes targeted with folate and composed of DPPlsC/dihydrocholesterol (9/1) were shown to facilitate the cytoplasmic delivery of several different encapsulated compounds to KB cells in vitro [69]. Liposomes having this composition showed high plasma stability. Efficient synthetic routes to several diplasmenylcholine analogues, including a PEG derivative have been developed [70].

1.9.2 Thermally Sensitive Liposomes

A small increase in temperature above physiological temperature (37 °C) can be used to release contents from appropriately constituted liposomes with spatial and temporal control [71-77]. Localized heating (hyperthermia) can be achieved by direct

conduction or through the use of low intensity microwaves. Thermosensitive liposomes can be made from a 9 to 1 mixture of 1,2-dipalmitoyl-*sn*-phosphatidylcholine (DPPC) and 1,2-distearoyl-*sn*-phosphatidylcholine (DSPC) (Fig. 1.11). As DPPC crosses the main transition temperature (41.5 °C), the permeability of the liposomal membrane to small molecules increases sharply. This increase in permeability occurs even in the presence of 6 mole % G_{M1}, though higher concentrations reduce the thermosensitivity of the liposomes somewhat [78]. The liposomes displayed an increase of approximately an order of magnitude in the available Doxorubicin in implanted murine colon carcinoma tumors in mice after localized heating to 42 °C for 20 min., starting 5 min. after injection of doxorubicin containing liposomes composed of DPPC/DSPC (9/1) with 6 mole % G_{M1}. Other studies have shown that the thermosensitivity and plasma stability of quaternary mixtures of DPPC, hydrogenated soy phosphatidylcholine (HSPC), cholesterol, and PEG_{2000}-DSPE (100/50/30/6) gives the highest stability both in bovine serum and in human plasma with high thermosensitivity between 37 and 41 °C of all the mixtures that were studied [79]. Thermally induced release of large molecules from DPPC/DSPC liposomes is also possible [80]. Experiments indicated that formulations of DPPC/DSPC (9/1) that contained dextran (mw = 144,000) could be induced to release the contents by incubation at 40 to 42 °C. A hypo-osmotic buffer was used, giving the liposomes an internal osmotic pressure, which facilitated the release of the macromolecule.

Another technique by which thermosensitive liposomes can be made is through the use of a thermosensitive polymer. The solubility of a polymer is a

balance of enthalpic and entropic factors. Enthalpic considerations that favor solubility include the attractive forces such as hydrogen bonding between the polymer and the solvent. Those that disfavor solubility would include intramolecular attractive forces between repeat units of the polymer. Entropic factors favoring solubility include the increased freedom of motion of the repeat units in solution, while those disfavoring solubility would include the ordering of solvent molecules around the extended random coil polymer. If the entropy of solution is sufficiently negative then there will be a temperature above which $-T\Delta S > \Delta H$ and $\Delta G_{solution}$ is positive. This is the lower critical solution temperature (LCST) or the temperature at which the polymer starts to become insoluble. N-isopropyl acrylamide (NIPAM) and octadecylacrylate (ODA) combined with DOPE have been used to make temperature sensitive liposomes [81]. Poly-NIPAM-*co*-ODA has an LCST near 32 °C. Below this temperature the copolymer stabilizes the DOPE liposomal membrane by preventing close contact between bilayers. Above the LCST, the copolymer no longer stabilizes the liposomal membrane and allows formation of the inverse hexagonal phase. DOPE liposomes with 25 weight % of the copolymer showed complete release of encapsulated calcein within 2 min. at 35 °C, while less than 20 % leakage was observed over 5 min at 20 °C. This temperature range is below that which is useful for in vivo use (37 - 42 °C). Because the LCST varies greatly between polymers, a copolymer that has an LCST within the usable range can be made by making small changes in the copolymer composition [75]. The ability of copolymers of this type to prolong in vivo circulation time has not been reported. If a copolymer with the correct LCST and the ability to prevent RES uptake is found, this strategy could be

used for in vivo drug delivery. A significant advantage of this strategy is the delivery of labile drugs to the cytoplasm by liposome fusion with the endosomal membrane, because leakage occurs through the formation of inverted phases.

1.9.3 Photodestabilization of Liposomes

The use of light to stimulate the release of encapsulated compounds from liposomes is attractive because it is possible to control the spatial and temporal delivery of the radiation. Liposomes may be made photosensitive by the use of uniquely designed lipids that can alter the liposome properties via photoisomerization [82-85], photocleavage [86-90], or photopolymerization [50, 51, 91-96]. A particularly useful characteristic of the latter is the multiplicative nature of the polymerization process [93]. Ultraviolet light directly initiates the polymerization of phospholipids having the hexa-2,4-dienoyl (sorbyl) functionality at the chain ends. The photopolymerization reaction produces polymers with a low kinetic chain length of about 10 [97]. However, if lipids are substituted with polymerizable groups in both acyl chains, crosslinked polymer networks are formed [98]. Although UV initiated polymerization is not suitable for biological applications due to the high absorbance of UV light by many biomolecules, it does provide a convenient method to test lipid compositions which could, in a clinical setting, be polymerized by more biocompatible techniques such as photosensitization with longer wavelength light [95, 99], or by exposure to ionizing radiation.

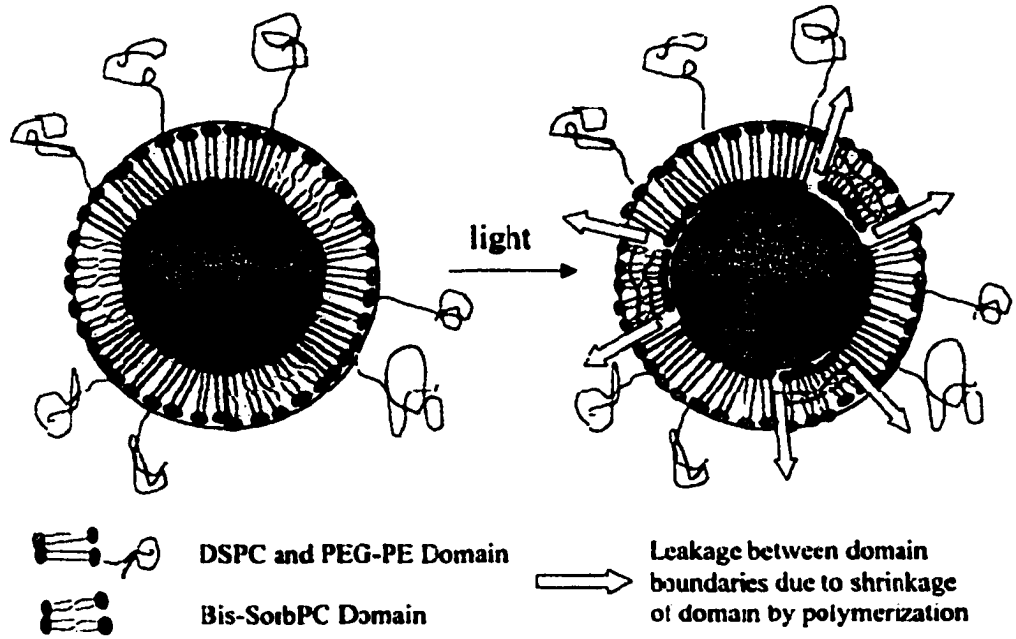

Figure 1.10. Schematic cross section of PEG-liposomes that represents the domains of bis-SorbPC and stearoyl lipids. The photopolymerization-induced reduction in the surface area of the polymerizable domains (black areas) during UV irradiation is shown on the right.

The destabilization and subsequent release of the encapsulated components may take place by the contraction of the polymerizable domain (Fig. 1.10) or distortion of the polymerized domain. The polymerizable lipids are drawn together by the covalent bonds that are formed in the hydrophobic tails upon irradiation. There may be a lag time between the contraction of the polymerized domain and the movement of the nonpolymerized domain to fill the vacated area. During this time, small fissures may exist between the domains until the nonpolymerized lipids are able to fill these spaces, or the fissures may not be filled if they appear in the interior of the polymerized domain.

Another possibility is that the shape of the polymerized domain cannot be incorporated into the lipid bilayer and therefore causes a distortion that leads to

micelle or disc formation. Micelle or disc formations would lead to unfavorable interactions between the hydrophilic head groups of the poly(lipid) domain and the hydrophobic tails of the lipid bilayer. Diffusion of the poly(lipid) domain would be favored which could lead to vacated areas and subsequent release of the encapsulated compounds.

Whatever the means of destabilization, it is important to be able to substantially increase the solute permeability of PEG-liposomes at the desired location. Obviously the liposome permeability must be low during the several minutes to hours the PEG-liposomes circulate in the bloodstream. Therefore if less than 1% of the encapsulated agent leaked during a circulation period of 10 h, it would then take more than a month for the rest of the drug to escape the liposome at the tumor site. In cases where it is desirable to release the drug in hours rather than weeks, the permeability must be increased by at least two orders of magnitude. Previously it was shown that this goal could be achieved through research within the O'Brien group [92].

In this dissertation the specific goals were to obtain a formulation that was thermally stable at body temperature, but could be induced to release the liposomal contents upon stimulation. Furthermore, the research involved the evaluation of several chemotherapeutic compounds as candidates for possible liposomal encapsulation, and their effect on the stability and reactivity of the photosensitive liposomes.

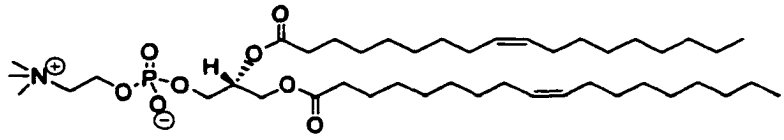

1,2-dioleoyl-sn-phosphatidylcholine (DOPC)

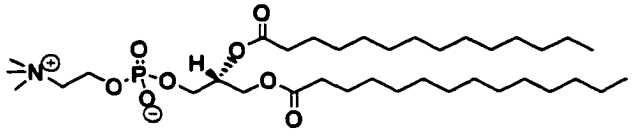

1,2-dilauroyl-sn-phosphatidylcholine (DLPC)

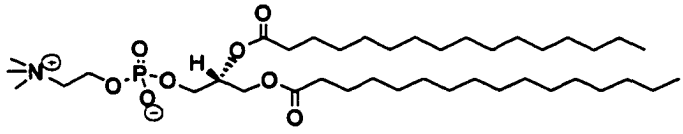

1,2-dipamitoyl-sn-phosphatidylcholine (DPPC)

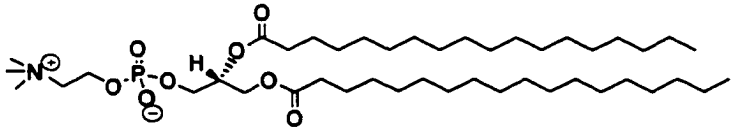

1,2-distearoyl-sn-phosphatidylcholine (DSPC)

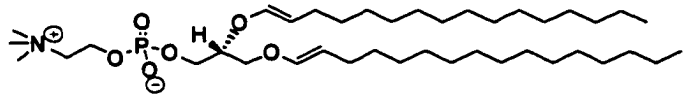

1,2-diplasmenyl-sn-phosphatidylcholine (DPPlsC)

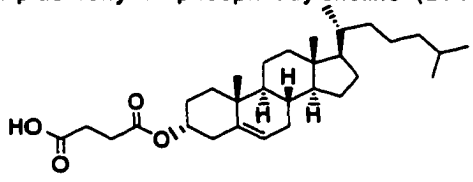

Cholesterol hemisuccinate

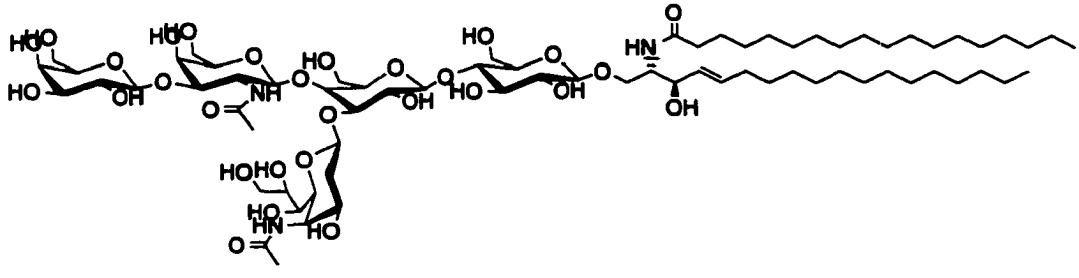

G_{M1}

Figure 1.11. Lipid structures. This is a composite list of the lipids discussed in chapter 1 and not included in Figure 1.4.

2 SYNTHESIS OF POLYMERIZABLE SORBYL LIPIDS

2.1 Introduction

Crosslinking polymerizations of phospholipids that have a polymerizable group attached to the ends of both acyl chains have been shown to dramatically alter the properties of multi-component bilayer membranes into which these lipids are incorporated [93, 100]. Several polymerizable groups have been studied, including the acryloyl, methacryloyl, and the 2,4-hexadienoyl (sorbyl) polymerizable esters [97, 101, 102]. Of these, the sorbyl and acryloyl polymerizable esters were used exclusively as the monomer in the photo-destabilization experiments presented in this dissertation. The acryloyl lipids will be discussed in the next chapter. The sorbyl group has the advantage of a UV λ_{max} of 244 to 258 (nm) and ε = 15,000 to 23,000 (L/mole cm) depending on solvent polarity. Irradiation with UV light in this range causes a photo-addition polymerization that is not inhibited by the presence of oxygen. Polymerization of sorbyl lipids can also be photo-sensitized by irradiation of specific dyes in the presence of molecular oxygen [99]. Additionally, in contrast to monomers such as diacetylene, polymerization of sorbyl-lipids can be carried out above or below the main phase transition temperature.

The synthesis of two types of sorbyl phosphatidylcholines is described in this chapter. These are bis-SorbPC$_{17,17}$, and bis-SorbPC$_{19,19}$, which have phase transition temperatures below and above physiological temperature, respectively. Though the general synthetic strategy presented here is identical to that previously described [103], some changes in reagents and purification procedures have been made.

Examples of these are the use of Jones reagent in acetone, rather than pyridinium dichromate in DMF, for oxidation of the hydroxy esters, and the use of a solvent gradient when purifying each of the products.

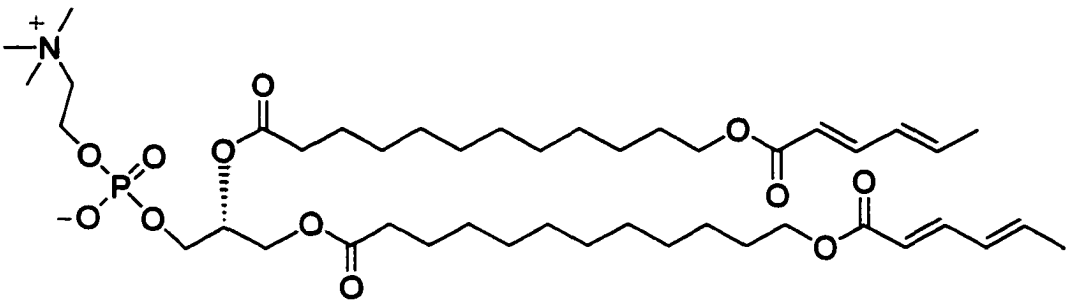

bis-SorbPC$_{19,19}$

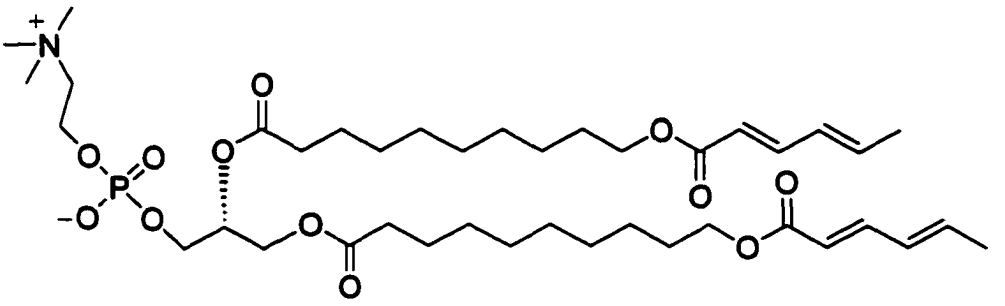

bis-SorbPC$_{17,17}$

Figure 2.1. Polymerizable sorbyl phosphatidylcholines

Synthetic scheme for bis-SorbPC$_{19,19}$

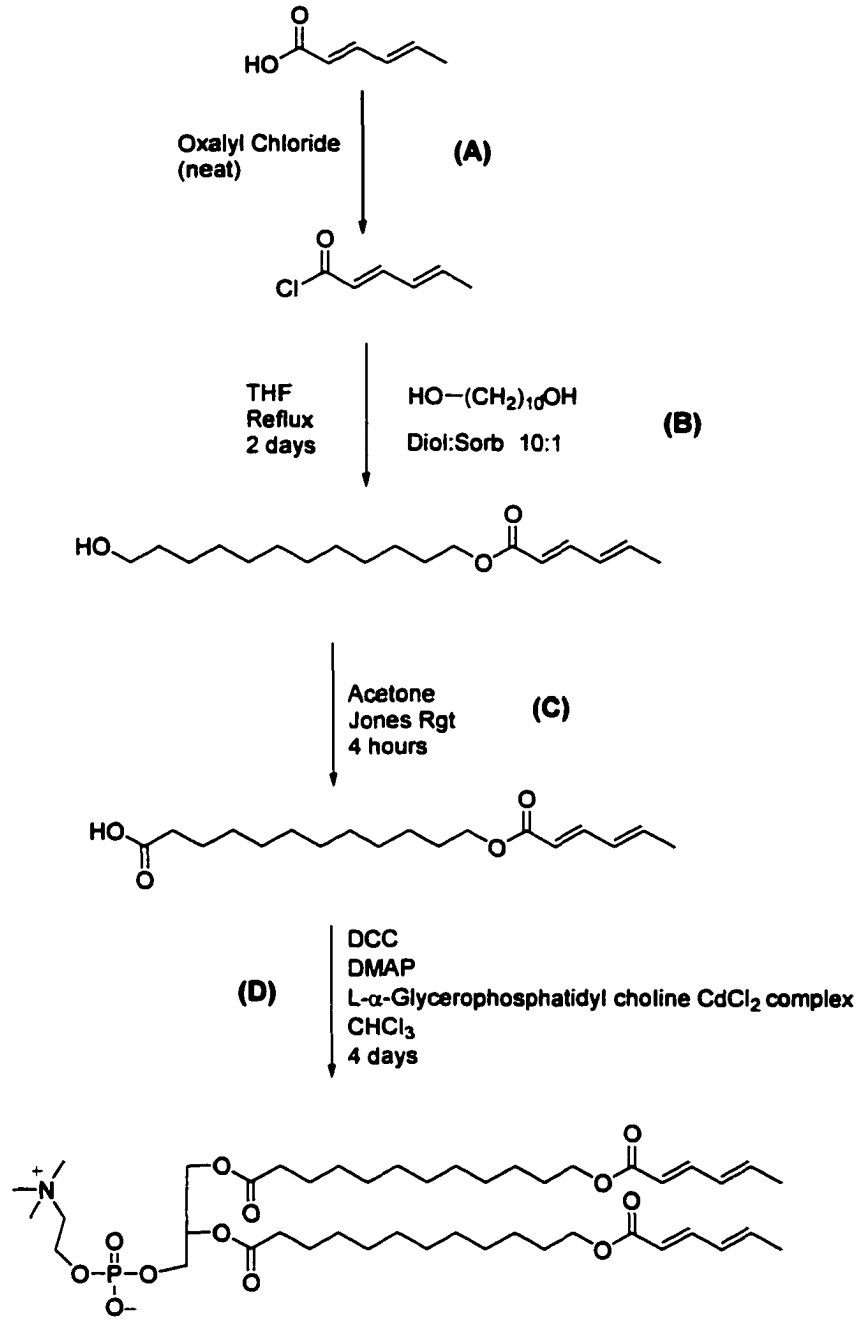

Scheme 2.1. Synthesis of polymerizable acid and PC; (A) RT, argon, 4hr, 90% yield; (B) 81% yield; (C) 0 °C to RT, 70% yield; (D) RT, 65% yield.

2.2 Experimental

2.2.1 Materials and Methods

Nuclear magnetic resonance (^{1}H NMR, ^{13}C NMR) spectra were recorded on a Bruker WM-250 spectrophotometer or a Varian Gemini 200 spectrophotometer. Samples were run with $CDCl_3$ as the solvent; chemical shifts are reported in parts per million downfield from the tetramethylsilane (TMS) peak. Ultraviolet spectra were recorded on a HP 8452 diode array spectrophotometer (Hewlett Packard). Samples were run in either buffer or methanol. Fluorescence spectra were measured on a Spex Fluorolog 2 Spectrophotometer (Spex Industries Inc.). Quasi elastic laser light scattering was performed with a Brookhaven BI-8000AT correlator (Brookhaven Instruments Corp.) with a 5 mW He-Ne laser as the light source. Samples were examined at 60°, 90°, and 120° and the following fitting methods were used to extract the set of exponential functions which make up the autocorrelation functions: cumulant analysis and non-negative least squares.

TLC analysis was performed to determine the purity of all the lipids received. Oxalyl chloride, 2,4-hexadienoic acid (97%), dicyclohexyl carbodiimide (DCC), and dimethyl-aminopyridine (DMAP) were purchased from Aldrich and used without further purification. 1,10-Decanediol, 1,12-dodecanediol, and 1,14-tetradecanediol were purchased from Fluka and the chain lengths were verified by GC mass spectroscopy. L-α-Glycerophosphocholine $CdCl_2$ complex was purchased from Sigma and placed under vacuum for 4 hours before use.

2.2.2 Hexa-2,4-dienoyl chloride

(sorbyl chloride)

Hexa-2,4-dienoic acid (50 g, 446 mmoles) was placed in a 3-neck round bottom flask equipped with an addition funnel and condensor. The flask was purged with argon and oxalyl chloride (58 mL, 665 mmole) was placed in the addition funnel under an argon positive pressure atmosphere. The oxalyl chloride was added dropwise over 30 minutes at room temperature. The reaction was allowed to continue for 4 hours. The resulting yellow solution was vacuum distilled at 0.2 mm Hg and 60 °C to produce 48 g (370 mmole, 84%) pure hexa-2,4-dienoyl chloride.

2.2.3 10-Hydroxydecyl-hexa-2,4-dienoate

($sorb_{17}$ alcohol)

1,10-Decandiol (10 g, 52.5 mmol) was placed into a 500 mL 3-neck round bottom flask and dissolved in 200 mL of THF at 65° C under an argon atmosphere with vigorous stirring. Sorbyl chloride (3.25 g, 24.9 mmol) was dissolved in 50 mL of THF and added via an addition funnel. The sorbyl chloride solution was added dropwise over 2 hours and stirred at reflux overnight or until completion. The reaction was monitored by TLC on silica plates with 3:1 hexane to ethyl acetate as the mobile phase. The product solution was concentrated and then purified using column chromatography with silica as the stationary phase and a gradient of hexane to ethyl acetate (H:E) as the mobile phase (1:0 H:E 400 mL, 3:1 H:E 400 mL, 2:1 H:E 400 mL, and 1:1 H:E 400 mL). Excess diol was recovered through recrystallization of the product mixture in methylene chloride. TLC indicated one spot. Yield 3.28 g (44

%). ^{1}H NMR ($CDCl_3$) δ 1.20-1.40 (m, 12H, C<u>H</u>$_2$), 1.45-1.65 (m, 2H, CH_2-C<u>H</u>$_2$-CH_2-O-CO), 1.70 (s, 1H, O<u>H</u>), 1.75-1.85 (d, 3H, CH=CH-C<u>H</u>$_3$), 3.50-3.65 (t, 2H, CH_2-C<u>H</u>$_2$-OH), 4.05-4.15 (t, 2H, CH_2-C<u>H</u>$_2$-O-CO), 5.65-5.80 (d, 1H, CH=C<u>H</u>-CO_2), 6.05-6.20 (m, 2H, CH=C<u>H</u>-CH=CH), 7.10-7.30 (m, 1H, CH=C<u>H</u>-CH_3).

2.2.4 <u>12-Hydroxydodecyl-hexa-2,4-dienoate</u>

(sorb$_{19}$ alcohol)

1,12-Dodecandiol (25 g, 110 mmol) was placed into a 500 mL 3-neck round bottom flask and dissolved in 200 mL of THF at 80° C under an argon atmosphere with vigorous stirring. Sorbyl chloride (3.25 g, 24.9 mmol) was dissolved in 50 mL of THF and added via an addition funnel. The sorbyl chloride solution was added dropwise over 1 hour and stirred at reflux for 24 hours or until completion. The reaction was monitored by TLC on silica plates with 3:1 hexane to ethyl acetate as the mobile phase. The product solution was concentrated and then purified using column chromatography with silica as the stationary phase and a gradient of hexane to ethyl acetate as the mobile phase (1:0 H:E 400 mL, 3:1 H:E 400 mL, 2:1 H:E 400 mL, and 1:1 H:E 400 mL). Excess diol was recovered through recrystallization of the product mixture in methylene chloride. TLC indicated one spot. Yield 6.28 g (81 %). ^{1}H NMR ($CDCl_3$) δ 1.20-1.40 (m, 16H, C<u>H</u>$_2$), 1.45-1.65 (m, 2H, CH_2-C<u>H</u>$_2$-CH_2-O-CO), 1.70 (s, 1H, O<u>H</u>), 1.75-1.85 (d, 3H, CH=CH-C<u>H</u>$_3$), 3.50-3.65 (t, 2H, CH_2-C<u>H</u>$_2$-OH), 4.05-4.15 (t, 2H, CH_2-C<u>H</u>$_2$-O-CO), 5.65-5.80 (d, 1H, CH=C<u>H</u>-CO_2), 6.05-6.20 (m, 2H, CH=C<u>H</u>-C<u>H</u>=CH), 7.10-7.30 (m, 1H, CH=C<u>H</u>-CH_3).

2.2.5 9-Carboxy-nonyl-hexa-2,4-dienoate

($sorb_{17}$ acid)

Jones reagent (2.67 M) was prepared by mixing chromium trioxide (26.7 g) with sulfuric acid (23 mL) and diluting to 100 mL with ice water. $Sorb_{17}$ alcohol (3.20 g, 11.5 mmol) was added with acetone (100 mL) to a 500 mL 3-neck round bottom flask and cooled to 0° C with an ice bath. Jones reagent (6 mL, 15.1 mmol) was then added dropwise to the solution over a 30-minute period. The reaction was allowed to warm to room temperature while stirring for an additional 30 minutes. Isopropanol (2 mL) was added to the mixture for quenching followed by addition of water (80 mL) and an additional 2 mL of isopropanol. The pH of the solution was raised to 5 with addition of potassium carbonate. The acetone was removed under vacuum by means of a rotary evaporator. Diethyl ether (100 mL) and 10% aqueous sulfuric acid (20 mL) were then added to the remaining solution. The organic phase was separated and the aqueous phase was washed with diethyl ether (4 x 50 mL). The combined organic extracts were washed with water (4 x 50 mL) and saturated brine (2 x 50 mL). The organic layer was dried with magnesium sulfate and the product was concentrated under vacuum with a rotary evaporator. The product was a green colored solid. The solid was dissolved in benzene (10 mL) and filtered through fine silica (2 g) to give a brownish solid. The product was then purified using column chromatography with silica as the stationary phase and 3:1 hexane to ethyl acetate as the mobile phase. The final product had a yellow tint. TLC indicated one spot. Yield 2.93 g (88%). ^1H NMR ($CDCl_3$) δ 1.20-1.40 (m, 10H, $C\underline{H}_2$), 1.45-1.65 (m, 4H, CH_2-$C\underline{H}_2$-CH_2-O-CO, CH_2-$C\underline{H}_2$-CH_2-CO_2H), 1.75-1.85 (d, 3H, CH=CH-$C\underline{H}_3$), 2.10-2.25

(t, 2H, CH_2-C<u>H</u>$_2$-CO_2H), 4.05-4.15 (t, 2H, CH_2-CH_2-O-CO), 5.65-5.80 (d, 1H, CH=CH-CO_2), 6.05-6.20 (m, 2H, CH=C<u>H</u>-C<u>H</u>=CH), 7.10-7.30 (m, 1H, CH=C<u>H</u>-CH_3).

2.2.6 <u>11-Carboxy-undecyl-hexa-2,4-dienoate</u>

(sorb$_{19}$ acid)

Jones reagent (2.67 M) was prepared by mixing chromium trioxide (26.7 g) with sulfuric acid (23 mL) and diluting to 100 mL with ice water. 12-(Sorbyloxy)dodecan-1-ol (3.20 g, 10.3 mmol) was added with acetone (100 mL) to a 500 mL 3-neck round bottom flask and cooled to 0° C with an ice bath. Jones reagent (6 mL, 15.1 mmol) was then added dropwise to the solution over a 30-minute period. The reaction was allowed to warm to room temperature while stirring for an additional 30 minutes. Isopropanol (2 mL) was added to the mixture for quenching followed by addition of water (80 mL) and an additional 2 mL of isopropanol. The pH of the solution was raised to 5 with addition of potassium carbonate. The acetone was removed under vacuum by a rotary evaporator. Diethyl ether (100 mL) and 10% aqueous sulfuric acid (20 mL) were then added to the remaining solution. The organic phase was separated and the aqueous phase was washed with diethyl ether (4 x 50 mL). The combined organic extracts were washed with water (4 x 50 mL) and saturated brine (2 x 50 mL). The organic layer was dried with magnesium sulfate and the product was concentrated under vacuum with a rotary evaporator. The product was a green colored solid. The solid was dissolved in benzene (10 mL) and filtered through fine silica (2 g) to give a brownish solid. The product was then purified using

column chromatography with silica as the stationary phase and 3:1 hexane to ethyl acetate as the mobile phase. The final product had a yellow tint. TLC indicated one spot. Yield 2.71 g (84%). ^{1}H NMR ($CDCl_3$) δ 1.20-1.40 (m, 14H, $C\underline{H}_2$), 1.45-1.65 (m, 4H, CH_2-$C\underline{H}_2$-CH_2-O-CO, CH_2-$C\underline{H}_2$-CH_2-CO_2H), 1.75-1.85 (d, 3H, CH=CH-$C\underline{H}_3$), 2.10-2.25 (t, 2H, CH_2-$C\underline{H}_2$-CO_2H), 4.05-4.15 (t, 2H, CH_2-$C\underline{H}_2$-O-CO), 5.65-5.80 (d, 1H, CH=C<u>H</u>-CO_2), 6.05-6.20 (m, 2H, CH=C<u>H</u>-C<u>H</u>=CH), 7.10-7.30 (m, 1H, CH=C<u>H</u>-CH_3).

2.2.7 1,2-Bis[10-(sorbyloxy)decanoyl)]-*sn*-glycero-3-phosphatidylcholine (bis-SorbPC$_{17,17}$)

L-α-Glycerophosphocholine $CdCl_2$ complex (GPC; 1g, 2.3 mmole) was placed under vacuum for a minimum of 4 hours prior to the reaction to remove any water. $Sorb_{17}$ acid (2.2 g, 6.8 mmole), DCC (1.87 g, 9.07 mmole), DMAP (0.7 g, 6 mmole), $CHCl_3$ (20 mL), and the GPC were combined in a 100 mL round bottom flask that had been purged with argon. The reaction was vigorously stirred at room temperature and allowed to continue for 4 days. TLC was used to monitor the reaction. The reaction mixture was filtered and the precipitate was washed with 2 x 10 mL of chloroform. Methanol (40 mL) was added to the combined filtrates and the solution was reduced to approximately ½ of the initial volume with a rotary evaporator. The resulting solution was placed in an ice bath and Bio-Rad AG ® 501-x8 (D) ion exchange resin (17 g) was added to remove the DMAP and $CdCl_2$. The suspension was stirred vigorously for 1 hour. TLC was used to indicate the removal of the DMAP. The suspension was filtered and concentrated. The product was

purified with column chromatography using silica gel as the stationary phase and $CHCl_3$ (200 mL), 9:1 $CHCl_3$:methanol (200 mL), 8:2 $CHCl_3$:methanol (200 mL), 7:3 $CHCl_3$:methanol (200 mL), 65:25:1 $CHCl_3$:methanol:water (100 mL), and 65:25:3 $CHCl_3$:methanol:water (100 mL) were used as the mobile phase. Only those fractions where water was added to the mobile phase were collected in test tubes. Pure bis-Sorb$PC_{17,17}$ (800 mg, 1 mmole, 44% yield) was recovered. TLC indicated one spot. ^1H NMR ($CDCl_3$): δ 7.28 – 7.20 (m, 3 H, $CH_2O(O)CCHC\underline{H}CHCHCH_3$ and $CHCl_3$), 6.24 – 6.09 (m, 4 H, $CH_2O(O)CCHCHC\underline{H}C\underline{H}CH_3$), 5.80 – 5.74 (d, J = 16 Hz, 2 H, $CH_2O(O)CC\underline{H}CHCHCHCH_3$), 5.22 – 5.19 (m, 1 H, $CH_2C(O)OC\underline{H}CH_2$), 4.43 – 4.38 (dd, J_1 = 3.0 Hz, J_2 = 12 Hz, 1H, $C(O)OC\underline{H}_2CH$), 4.32 (S, 2 H, $C(O)OCH_2CHC\underline{H}_2OP$), 4.14 – 4.10 (t, J = 6.75 Hz, 5 H, $C\underline{H}_2O(O)CCHCHCHCHCH_3$ and $C(O)OC\underline{H}_2CH$), 3.99 – 3.93 (q, J = 5.9 Hz, 2 H, $OP(O)_2OC\underline{H}_2CH_2N$), 3.84 – 3.83 (m, 2 H, $OP(O)_2CH_2C\underline{H}_2N$), 3.39 (s, 10 H, $CH_2N^+(CH_3)_3$) 2.32 – 2.25 (d t, J_1 = 2.4 Hz, J_2 = 5.4 Hz, 4 H, $C\underline{H}_2C(O)OCH_2$ and $C\underline{H}_2C(O)OCH$), 1.86 – 1.84 (d, J = 5.4 Hz, 6 H, $CH_2O(O)CCHCHCHCHC\underline{H}_3$), 1.67 – 1.56 (m, 8 H, $C\underline{H}_2CH_2C(O)OCH_2$, $C\underline{H}_2CH_2C(O)OCH$ and $C\underline{H}_2CH_2O(O)CCH$), 1.34 – 1.28 (s, 20 H, $(CH_2)_5$) ppm. High resolution FAB mass spectrum: calculated mw $(C_{40}H_{60}NO_{12}P)^+$; 786.4557 (100%), 787.4591 (46.35%), measured m/z; 786.4564 (100%), 787.4602 (49.3%).

2.2.8 1,2-Bis[12-(sorbyloxy)dodecanoyl)]-*sn*-glycero-3-phosphatidylcholine (bis-SorbPC$_{19,19}$)

L-α-Glycerophosphocholine $CdCl_2$ complex (GPC; 0.5g, 1.2 mmole) was placed under vacuum for a minimum of 4 hours prior to the reaction to remove any water. $Sorb_{19}$ acid (1.0 g, 2.6 mmole), DCC (0.2 g, 0.8 mmole), DMAP (0.35 g, 3 mmole), $CHCl_3$ (20 mL), and the GPC were combined in a 100 mL round bottom flask that had been purged with argon. The reaction was vigorously stirred at room temperature and allowed to continue for 4 days. Additional amounts of DCC were added to the solution over the 4 days (0.2 g every 8 to 12 hours). TLC was used to monitor the reaction. The reaction mixture was filtered and the precipitate was washed with 2 x 10 mL of chloroform. Methanol (40 mL) was added to the combined filtrates and the solution was reduced to approximately ½ of the initial volume with a rotary evaporator. The resulting solution was placed in an ice bath and Bio-Rad AG ® 501-x8 (D) ion exchange resin (10 g) was added to remove the DMAP and $CdCl_2$. The suspension was stirred vigorously for 1 hour. TLC was used to indicate the removal of the DMAP. The suspension was filtered and concentrated. The product was purified with column chromatography using silica gel as the stationary phase and $CHCl_3$ (200 mL), 9:1 $CHCl_3$:methanol (200 mL), 8:2 $CHCl_3$:methanol (200 mL), 7:3 $CHCl_3$:methanol (200 mL), 65:25:1 $CHCl_3$:methanol:water (100 mL), and 65:25:3 $CHCl_3$:methanol:water (100 mL) were used as the mobile phase. Only those fractions where water was added to the mobile phase were collected in test tubes. Pure bis-SorbPC$_{19,19}$ (356 mg, 0.54 mmole, 48% yield) was recovered. TLC indicated one spot. ^{1}H NMR ($CDCl_3$): δ 7.28 – 7.20 (m, 3 H, $CH_2O(O)CCHCHCHCH_3$ and

$CHCl_3$), 6.24 – 6.09 (m, 4 H, $CH_2O(O)CCHCHC\underline{H}C\underline{H}CH_3$), 5.80 – 5.74 (d, J = 16 Hz, 2 H, $CH_2O(O)CC\underline{H}CHCHCHCH_3$), 5.22 – 5.19 (m, 1 H, $CH_2C(O)OC\underline{H}CH_2$), 4.43 – 4.38 (dd, J_1 = 3.0 Hz, J_2 = 12 Hz, 1H, $C(O)OC\underline{H_2}CH$), 4.32 (S, 2 H, $C(O)OCH_2CHC\underline{H_2}OP$), 4.14 – 4.10 (t, J = 6.75 Hz, 5 H, $C\underline{H_2}O(O)CCHCHCHCHCH_3$ and $C(O)OC\underline{H_2}CH$), 3.99 – 3.93 (q, J = 5.9 Hz, 2 H, $OP(O)_2OC\underline{H_2}CH_2N$), 3.84 – 3.83 (m, 2 H, $OP(O)_2CH_2C\underline{H_2}N$), 3.39 (s, 10 H, $CH_2N^+(CH_3)_3$) 2.32 – 2.25 (d t, J_1 = 2.4 Hz, J_2 = 5.4 Hz, 4 H, $C\underline{H_2}C(O)OCH_2$ and $C\underline{H_2}C(O)OCH$), 1.86 – 1.84 (d, J = 5.4 Hz, 6 H, $CH_2O(O)CCHCHCHCHC\underline{H_3}$), 1.67 – 1.56 (m, 8 H, $C\underline{H_2}CH_2C(O)OCH_2$, $C\underline{H_2}CH_2C(O)OCH$ and $C\underline{H_2}CH_2O(O)CCH$), 1.34 – 1.28 (s, 24 H, $(CH_2)_5$) ppm. High resolution FAB mass spectrum: calculated mw $(C_{40}H_{60}NO_{12}P)^+$; 842.2651 (100%), 843.2685 (46.35%), measured m/z; 842.2655 (100%), 843.2736 (47.2%).

2.3 Results and Discussion

2.3.1 Sorb Acid Synthesis

The polymerizable acids, hexa-2,4-dienoic acid 9-carboxynonyl ester and hexa-2,4-dienoic acid 11-carboxyundecyl ester, are potentially common intermediates for a variety of polymerizable lipids, simply by acylation of the desired headgroup, or headgroup precursor. This makes it important to be able to efficiently synthesize large amounts of these compounds in high purity. Initial purity of the starting materials, 1,10-decanediol and 1,12-dodecanediol, is critical, as contamination with shorter or longer chainlength diols would result in a mixture of polymerizable acids that may be inseparable by chromatography or recrystallization. Incorporation of

such a mixture of acyl chains into lipids would result in an even larger number of products. For example, reaction of two different chain length acids with L-α-glycerophosphocholine would result in a statistical mixture of 4 different diacyl PC's. This type of mixture may have altered thermotropic properties, and it would become impossible to achieve consistency and reproducibility of experiments from one batch of lipid to another. A high resolution FAB mass spectrum of bis-SorbPC$_{17,17}$ made from this starting material showed it to be only one product. Differential scanning calorimetry of a aqueous suspension of this compound showed a correspondingly sharp peak at 28.7 °C and high (120 to 220) cooperativity units.

The first reaction of the diol is a statistical mono-acylation with sorbyl chloride. Though a large excess of the diol is used in the reaction to prevent bis-acylation, this reaction is not wasteful, because the unreacted starting material can be recycled by recrystallization from methylene chloride as described in the experimental. The bis-acylated product, on the other hand cannot be easily recycled, and must be discarded. The yield of the mono-acylated product relative to the limiting reagent, sorbyl chloride, is an approximate inverse measure of the amount of bis-substituted product. It can be seen from this that the reaction of 10 equivalents of 1,12-dodecanediol with 1 equivalent of sorbyl chloride (81% yield) is more efficient than the reaction of 2 equivalents of the 1,10-decanediol with 1 equivalent of sorbyl chloride (44% yield). In order to benefit from excess diol, it is also necessary that all diol be soluble in the reaction mixture, even if this requires heating the reaction to reflux, as was described in the experimental.

The Jones oxidation of the mono-acyl diol to the acid presents two problems. The newly formed acid, which is probably in the form of a hemi-acetal, can react with the starting material to form an ester with sorbyl groups on each end. This is a minor side product of the reaction. Even though Jones reagent is added to a fairly concentrated solution of alcohol, only a small amount of ester byproduct is produced. Attempts to add the alcohol to Jones reagent in acetone failed because the acetone polymerized and deactivated the Jones reagent. Because the reaction is done in acetone/water, all organic solvents can be removed by evaporation after workup and extraction. Successive recrystallization from hexanes or petroleum ether is an effective method for purification of large amounts of polymerizable acids and their alcohol. However, small quantities (less than ten grams) should be purified by chromatography with a hexanes/ethyl acetate gradient system, as this is faster and less wasteful.

2.3.2 Bis-SorbPC

Bis-SorbPC$_{17,17}$ and bis-SorbPC$_{19,19}$ were synthesized from L-a-glycerophosphocholine (GPC) and the corresponding polymerizable acid in 65% yields. The acylation takes place through the formation of an activated complex of DCC with the acid. The DCC is then displaced by DMAP to form dicyclohexyl urea (DCU) and an activated amide, which can then be attacked by the glycerol hydroxyls to form the ester. GPC is present at low concentrations because it is only sparingly soluble in chloroform. If DCC is added slowly, the activated complex will react as quickly as it is formed because of the higher concentration of the other reactants, and

side reactions can be minimized. This strategy was used in the synthesis of bis-SorbPC$_{19,19}$, in which only 2.2 equivalents of polymerizable acid was used, and DCC was added 0.3 equivalents at a time. Though the yield relative to GPC was lower in this reaction, the yield relative to polymerizable acid was slightly greater. It is possible that the modification of this strategy, such as gradual addition of DCC with a syringe pump, the overall yield may be improved. Another important factor that can increase the yield is the rigorous removal of ethanol from the chloroform, because ethanol is a better substrate for acylation than GPC.

The initial workup of the acylation reaction involves treatment with ion exchange resin to remove basic compounds and salts such as DMAP and cadmium chloride. The previous procedure of stirring at room temperature for 2 hr has occasionally resulted in hydrolysis of the ester. The procedure of stirring for 30 min at 0 °C takes advantage of the higher activation energy for hydrolysis than for ion exchange to prevent lipid decomposition.

3 SYNTHESIS OF POLYMERIZABLE ACRYL LIPIDS

3.1 Introduction

While the sorbyl groups in the previous chapter have been shown to give the desired effects of destabilization of lipid membrane upon polymerization [50, 51, 91-96, 100, 104], an attempt was undertaken to find a more efficient polymerizable lipid that would have a higher rate of propagation. The acryloyl group has been shown to have a higher rate of propagation because of the lesser amount of stabilization [105]. While there is a strong sensitivity to the presence of molecular oxygen, this may prove to be an advantage as well. The area surrounding tumor sites is typically lacking oxygen because of the constant demand by the tumor tissue, whereas normal tissue would contain molecular oxygen. This suggests that the destabilizing polymerizations could only proceed near hypoxic tumor sites, while being inhibited in the normal tissue. The side effects of encapsulated therapeutic agents could further be minimized through this strategy.

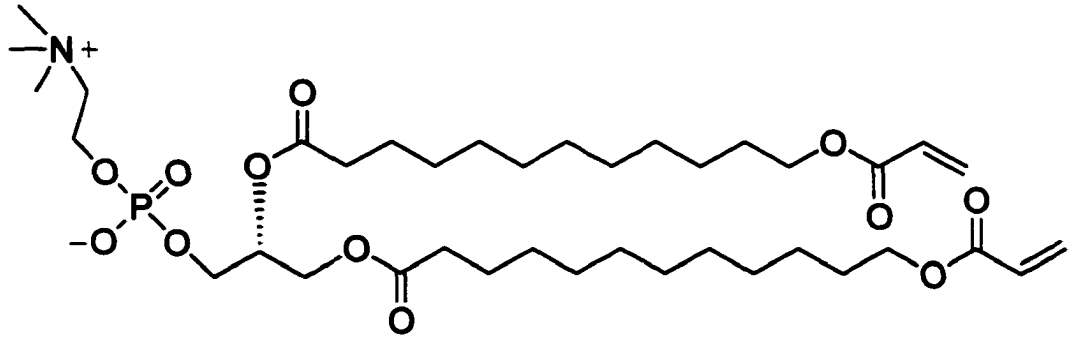

bis-AcrylPC$_{18,18}$

Synthetic scheme for bis-AcrylPC$_{19,19}$

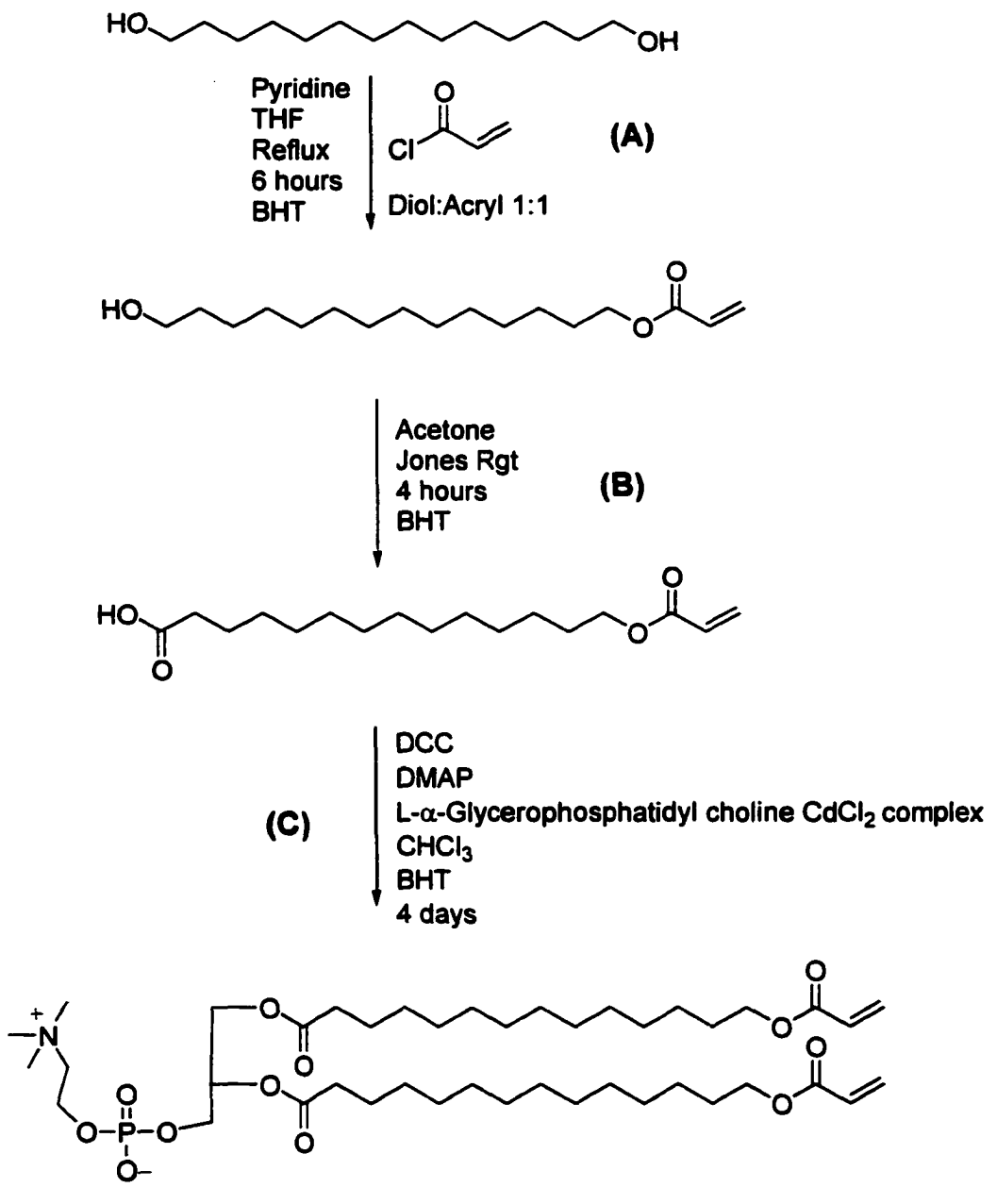

Scheme 3.1. Synthesis of polymerizable acid and PC; (A) 48% yield (acryl); (B) 0 °C to RT, 84% yield; (C) RT, 68% yield.

3.2 Experimental

3.2.1 14-Hydroxytetradecyl-propenoate

($acryl_{18}$ alcohol)

1,14-Tetradecandiol (5 g, 22 mmol) was placed into a 500 mL 3-neck round bottom flask and dissolved in 200 mL of THF at reflux under an argon atmosphere with vigorous stirring. Several crystals of 2,6-di-*t*-butyl-4-methylphenol (BHT) were added to the solution as a radical scavenger to prevent polymerization of the acryl moiety. Acryl chloride (0.65 g, 7.22 mmol) was dissolved in 10 mL of THF and added via an addition funnel. The acryl chloride solution was added dropwise over 1 hour and stirred at 60 °C for 24 hours. The reaction was monitored by TLC on silica plates with 3:1 hexane to ethyl acetate as the mobile phase. The product was concentrated and then purified using column chromatography with silica as the stationary phase and a gradient of hexane to ethyl acetate as the mobile phase (1:0 H:E 400 mL, 3:1 H:E 400 mL, 2:1 H:E 400 mL, and 1:1 H:E 400 mL). TLC indicated one spot. Yield 1.1 g (48 %). ^{1}H NMR ($CDCl_3$) δ 1.20-1.40 (m, 20H, $C\underline{H}_2$), 1.45-1.65 (m, 2H, CH_2-$C\underline{H}_2$-CH_2-O-CO), 3.50-3.65 (t, 2H, CH_2-$C\underline{H}_2$-OH), 4.05-4.15 (t, 2H, CH_2-$C\underline{H}_2$-O-CO), 5.70-5.85 (dd, CH_2=$C\underline{H}$-COO), 5.90-6.15 (dd, $C\underline{H}_2$=CH-COO), 6.20-6.40 (dd, $C\underline{H}_2$=CH-COO).

3.2.2 13-Carboxy-tridecyl-propenoate

(acryl$_{18}$ acid):

Jones reagent (2.67 M) was prepared by mixing chromium trioxide (26.7 g) with sulfuric acid (23 mL) and diluting to 100 mL with ice water. Several crystals of BHT were added to the solution as a radical scavenger to prevent polymerization of the acryl moiety. 14-(Acryloxy)tetradecan-1-ol (1.10 g, 3.47 mmol) was added with acetone (100 mL) to a 500 mL 3-neck round bottom flask and cooled to 0° C with an ice bath. Jones reagent (1.5 mL, 3.75 mmol) was then added dropwise to the solution over a 30-minute period. The reaction was allowed to warm to room temperature while stirring for an additional 30 minutes. Isopropanol (2 mL) was added to the mixture for quenching followed by addition of water (80 mL) and an additional 2 mL of isopropanol. The pH of the solution was raised to 5 with addition of potassium carbonate. The acetone was removed under vacuum by a rotary evaporator. Diethyl ether (100 mL) and 10% aqueous sulfuric acid (20 mL) were then added to the remaining solution. The organic phase was separated and the aqueous phase was washed with diethyl ether (4 x 50 mL). The combined organic extracts were washed with water (4 x 50 mL) and saturated brine (2 x 50 mL). The organic layer was dried with magnesium sulfate and the product was concentrated under vacuum with a rotary evaporator. The product was a green colored solid. The solid was dissolved in benzene (10 mL) and filtered through fine silica (2 g) to give a brownish solid. The product was then purified using column chromatography with silica as the stationary phase and 3:1 hexane to ethyl acetate as the mobile phase. TLC indicated one spot. Yield 0.93 g (84%). ^{1}H NMR ($CDCl_3$) δ 1.20-1.40 (m, 18H, $C\underline{H}_2$), 1.45-1.65 (m,

4H, CH_2-C<u>H_2</u>-CH_2-O-CO, CH_2-C<u>H_2</u>-CH_2-CO_2H), 2.10-2.25 (t, 2H, CH_2-C<u>H_2</u>-CO_2H), 4.05-4.15 (t, 2H, CH_2-C<u>H_2</u>-O-CO), 5.70-5.85 (dd, 1H, CH_2=C<u>H</u>-COO), 5.90-6.15 (dd, 1H, C<u>H_2</u>=CH-COO), 6.20-6.40 (dd, 1H, C<u>H_2</u>=CH-COO).

3.2.3 <u>1,2-Bis[14-(acryloxy)tetradecanoyl)]-*sn*-glycero-3-phosphatidylcholine</u>

(bis-AcrylPC$_{18,18}$)

L-α-Glycerophosphocholine $CdCl_2$ complex (GPC; 0.5g, 1.2 mmole) was placed under vacuum for a minimum of 4 hours prior to the reaction to remove any water. Acryl$_{18}$ acid (0.93 g, 1.5 mmole), DCC (1.0 g, 4.5 mmole), DMAP (0.35 g, 3 mmole), $CHCl_3$ (20 mL), and the GPC were combined in a 100 mL round bottom flask that had been purged with argon. Several crystals of BHT were added to the solution as a radical scavenger to prevent polymerization of the acryl moiety. The reaction was vigorously stirred at room temperature and allowed to continue for 4 days. TLC was used to monitor the reaction. The reaction mixture was filtered and the precipitate was washed with 2 x 10 mL of chloroform. Methanol (40 mL) was added to the combined filtrates and the solution was reduced to approximately ½ of the initial volume with a rotary evaporator. The resulting solution was placed in an ice bath and Bio-Rad AG ® 501-x8 (D) ion exchange resin (10 g) was added to remove the DMAP and $CdCl_2$. The suspension was stirred vigorously for 1 hour. TLC was used to indicate the removal of the DMAP. The suspension was filtered and concentrated. The product was purified with column chromatography using silica gel as the stationary phase and $CHCl_3$ (200 mL), 9:1 $CHCl_3$:methanol (200 mL), 8:2

$CHCl_3$:methanol (200 mL), 7:3 $CHCl_3$:methanol (200 mL), 65:25:1 $CHCl_3$:methanol:water (100 mL), and 65:25:3 $CHCl_3$:methanol:water (100 mL) were used as the mobile phase. Only those fractions where water was added to the mobile phase were collected in test tubes. Pure bis-AcrylPC$_{18,18}$ (600 mg, 0.88 mmole, 68% yield) was recovered. TLC indicated one spot. ^{1}H NMR ($CDCl_3$): δ 6.20 - 6.40 (dd, J_1 = 2.0 Hz, J_2 = 18 Hz, 1H, C$\underline{H_2}$=CH-COO), 5.90-6.15 (dd, J_1 = 10 Hz, J_2 = 10 Hz, 1H, C$\underline{H_2}$=CH-COO), 5.70-5.85 (dd, J_1 = 0.8 Hz, J_2 = 8.0 Hz, 1H, CH_2=C$\underline{H}$-COO), 5.22 – 5.19 (m, 1 H, C$\underline{H_2}$C(O)OCHCH_2), 4.43 – 4.38 (dd, J_1 = 3.0 Hz, J_2 = 12 Hz, 1H, C(O)OC$\underline{H_2}$CH), 4.32 (S, 2 H, C(O)OCH_2CHC$\underline{H_2}$OP), 4.14 – 4.10 (t, J = 6.75 Hz, 5 H, C$\underline{H_2}$O(O)CCHCHCHCHCH_3 and C(O)OC$\underline{H_2}$CH), 3.99 – 3.93 (q, J = 5.9 Hz, 2 H, OP(O)$_2$OC$\underline{H_2}$CH_2N), 3.84 – 3.83 (m, 2 H, OP(O)$_2$CH_2C$\underline{H_2}$N), 3.39 (s, 10 H, CH_2N^+(C$\underline{H_3}$)$_3$) 2.32 – 2.25 (d t, J_1 = 2.4 Hz, J_2 = 5.4 Hz, 4 H, C$\underline{H_2}$C(O)OCH_2 and C$\underline{H_2}$C(O)OCH), 1.67 – 1.56 (m, 8 H, C$\underline{H_2}$CH_2C(O)OCH_2, C$\underline{H_2}$CH_2C(O)OCH and C$\underline{H_2}$CH_2O(O)CCH), 1.34 – 1.28 (s, 32 H, $(CH_2)_8$) ppm. High resolution FAB mass spectrum: calculated mw $(C_{42}H_{76}NO_{12}P)^+$; 817.5105 (100%), measured m/z; 817.5113 (100%).

3.3 Results and Discussion

3.3.1 1,14-tetradecanediol

The 14-diol used for the initial ester formation of the acryl alcohol proposed a significant problem. The compound is commercially available, but the cost is $354.00 per gram, while the 12 and 16 diols are much cheaper, $1.04 and $67.10 respectively. Numerous coupling reactions were attempted with shorter chain

precursors to form the 14-diol, but the processes proved troublesome because of solubility problems. The 14-diol is only mildly soluble in refluxing solvents such as THF, chloroform, methylene chloride, and benzene. Eventually, because of the difficulties in obtaining an efficient synthetic route to the 14-diol, the 1,14-tetradecanediol was purchased and used in the synthesis of the 1,2-bis[14-(acryloxy)tetradecanoyl)]-*sn*-glycero-3-phosphatidylcholine (bis-Acryl$PC_{18,18}$).

3.3.2 Acryl$_{18}$ Alcohol Synthesis

In the Sorb alcohol synthesis, chapter 2.3.1, a large excess of the diol was used to maximize the amount of monoester product formed and minimize the diester product. Because of the expense of the 14-diol, a ratio of only 2 to 1 (diol:acryl chloride) was used to maximize the weight yield. The unreacted 14-diol was recovered through recrystallization of the crude product in ethyl acetate. The diester product was separated via column chromatography and then cleaved through a base hydrolysis reaction. The 14-diol was recovered through column chromatography with 2:1 hexanes:ethyl acetate as the mobile phase. A lower yield of 48% was obtained using this methodology, as compared to the 81% yield obtained with a 10:1 diol:sorbyl chloride ratio that was used in chapter 2.3.1. The recovered 14-diol was then reused without further purification.

3.3.3 Acryl$_{18}$ Acid Synthesis

The polymerizable acid, 13-carboxy-tridecyl-propenoate, is a potential intermediate for a variety of polymerizable phospholipids similar to the Sorb acid

compounds. A special consideration must be given to the high reactivity of the acryl moiety and its potential for immediate polymerization under mild initiation conditions, such as ambient light. An inhibitor, 2,6-di-*t*-butyl-4-methylphenol (BHT), was used to prevent polymerization from the use of the Jones reagent. BHT is easily separated from the resulting $Acryl_{18}$ acid during column chromatography.

The chromatography must be done in a timely manner and was performed under pressure. Polymerization of the $acryl_{18}$ acid occurred during the initial purification on the column without pressure that increases the flow rate of the mobile phase. Polymerization of the $acryl_{18}$ acid may have occurred due to the ambient light present or the slightly acidic conditions that typically occur on a silica gel column.

3.3.4 Bis-Acryl$PC_{18,18}$ Synthesis

Bis-Acryl$PC_{18,18}$ was synthesized from L-a-glycerophosphocholine and the corresponding polymerizable acid in 68% yields. The acylation takes place through the formation of an activated complex of DCC with the acid. The DCC is then displaced by DMAP to form DCU and an activated amide, which can then be attacked by the glycerol hydroxyls to form the ester. GPC is present at low concentrations because it is only sparingly soluble in chloroform. If DCC is added slowly, the activated complex will react as quickly as it is formed because of the higher concentration of the other reactants, and side reactions can be minimized. In chapter 2.3.2, the importance of rigorous ethanol removal from chloroform was stated; ethanol free chloroform is available and was purchased from Aldrich to remove this possibility.

The initial workup of the acylation reaction involves treatment with ion exchange resin to remove basic compounds and salts such as DMAP and cadmium chloride. The procedure of stirring for 30 min at 0 °C takes advantage of the higher activation energy for hydrolysis than for ion exchange to prevent lipid decomposition. The column chromatography purification was performed under pressure to increase the flow of the mobile phase and minimize the chance for polymerization of bis-Acryl$PC_{18,18}$ product.

4 CHARACTERIZATION AND γ-IRRADIATION INITIATED POLYMERIZATION OF ACRYL PC-BASED LIPOSOMES

4.1 Introduction

The need for more effective approaches to the controlled delivery of therapeutic agents continues to be of utmost importance. Passive or active targeting of anticancer agents to tumors is a traditional approach to minimizing side effects. An alternative strategy relies on the activation or release of therapeutic agents only in the vicinity of the diseased tissue. The O'Brien group has previously proposed that the attractive features of photodynamic therapy, i.e. spatial and temporal selectivity, could be significantly broadened if radiant energy were used to release drugs [51, 96, 104, 106]. Indeed the selective photolysis of appropriately designed liposomes can trigger the release of their contents upon UV exposure [50, 51, 91-93, 95, 96, 100]. These previous studies now permit the design of sterically stabilized liposomes (PEG-LUV) that are sensitive to ionizing radiation. The selective destabilization of PEG-LUV and release of therapeutic agents upon exposure to clinical doses of radiation holds new promise for controlled drug delivery.

Polymerization in organized assemblies can be initiated by gamma irradiation [107-109]. Unlike photodynamic therapies, ionizing radiation is readily available in most medical centers since it is a principle component of many cancer treatments. The total dose of irradiation can be controlled by regulating the distance from the source and the duration of irradiation. Therapeutic gamma irradiation treatments are generally fractionated over time. In a typical radiation treatment regimen, patients receive a total dose of 200 Rad per day five or six times a week. Typical treatments

last 5-7 weeks and the cumulative total dose is 5 – 8.4 Krad [104]. The premise of fractionating the total dose is that cells with a large proliferative capacity, e.g. tumor cells, generally have a high intrinsic radiative sensitivity [107]. Fractionating the dose reduces damage to the surrounding normal tissue since it probably has a lower radiation sensitivity. Gamma initiation may be especially important in drug delivery systems that require polymerization *in vivo*. UV and visible light do not penetrate deeply beyond the epidermal layer of the body. Red light of 632 nm penetrates the tissue to a maximum of 1 cm. Fiber optic cables must be surgically implanted into the body to deliver light to most targeted areas. The enhanced depth of penetration that gamma rays exhibit is one advantage over UV and visible light initiation. The actual initiating species in gamma polymerizations of hydrated amphiphiles is a hydroxy radical [108, 109]. The mechanism which the production of hydroxyl radicals is shown in Figure 4.1.

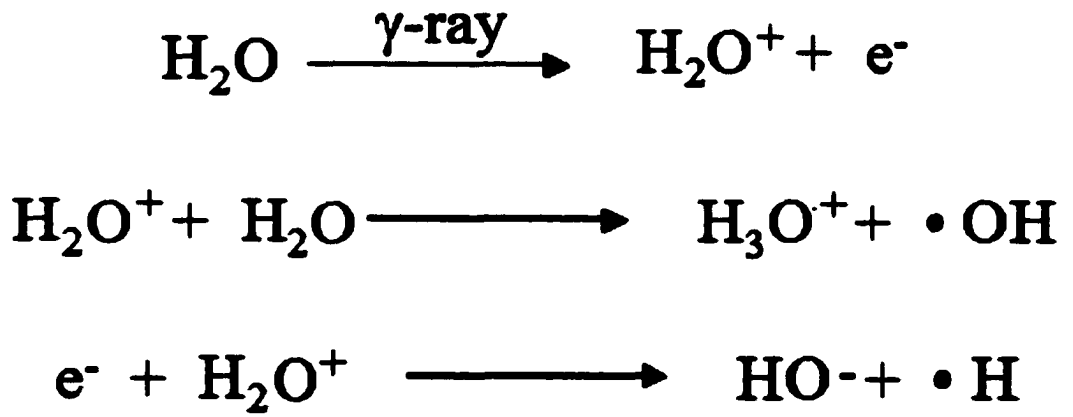

Figure 4.1. Proposed pathway for generation of hydroxyl radicals by gamma irradiation of water.

Further consideration was given to the use of acryl lipids in γ-initiated polymerizations. Sorbyl moieties have been shown to polymerize with γ-irradiation, but the dosages necessary to induce release of the encapsulated compounds were well in excess of therapeutic doses [103]. Since the reactivity of the acryl moiety is enhanced compared to the sorbyl moieties, then an advantage could be obtained by an increase in the amount of polymerization and liposomal destabilization with the same amount of therapeutic dosage of radiation. Additionally, acryl moieties have indicated an extreme dependence on the presence of molecular oxygen. As discussed in chapter 3, tissue areas near tumors have very low concentrations of oxygen because of the high metabolism of the tumors and their excess need of nutrients, while healthy tissue contains molecular oxygen that would inhibit polymerization. Theoretically, liposomes in healthy tissue would not undergo polymerization and the subsequent release of the liposomal contents.

In radical polymerizations the acryl functionality is a more reactive group than sorbyl because the propagating radical species is less stabilized (Fig. 4.2). The increased reactivity of the acryl group results in an increase in the rate and degree of polymerization observed in radical polymerization of phospholipids [110, 111]. Differential scanning calorimetry and UV data were obtained to determine the feasibility of incorporating the bis-AcrylPC$_{18,18}$ in liposomal formulations. While bis-AcrylPC$_{16,16}$ had been previously synthesized within the O'Brien Group [18, 102, 105], the 18 atom chain was considered a better candidate for thermally stable liposomes. The bis-AcrylPC$_{16,16}$ has a phase transition temperature of 31 °C and liposomal formulations containing lipids with T_m values below 37 °C indicated poor

encapsulation efficiency and high permeability as discussed in chapter 5. The T_m value of bis-AcrylPC$_{18,18}$ is expected to be well above 37 °C based upon the increase in T_m values observed in sorbyl lipids when increasing the length of the chains (bis-SorbPC$_{17,17}$ = 29 °C vs. bis-SorbPC$_{19,19}$ = 42.5 °C).

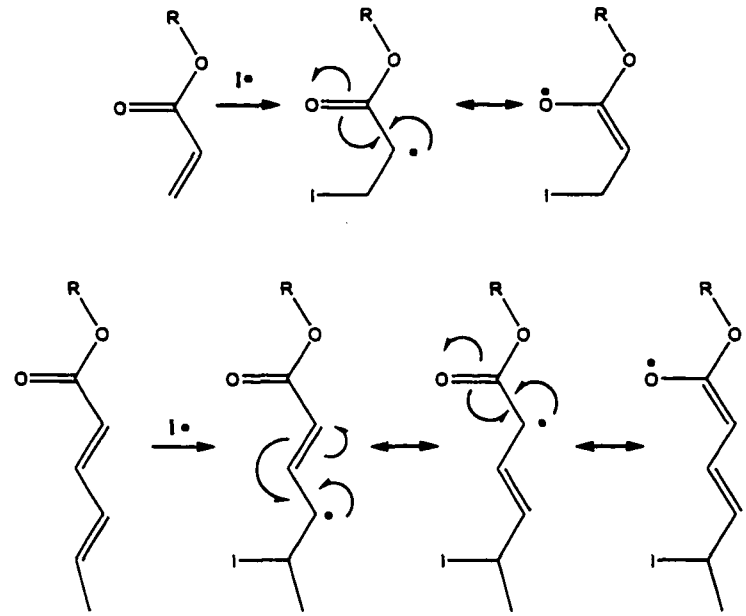

Figure 4.2. Resonance structures that stabilize the radicals after initiation by a radical (I •). The sorbyl moiety has three resonance structures while the acryl moiety has only two resonance structures. Obviously the initiation can occur at any point of the dienoyl moiety, but the terminal attachment is shown to demonstrate the largest number of resonance structures.

Previously bis-AcrylPC$_{16,16}$ (T_m = 31 °C) was investigated for the rate of polymerization with γ-irradiation by Tom Sisson within the O'Brien group [111]. Results indicated the rate of polymerization was observed in the absence of oxygen to be 8.8 x 10^{-8} M/Rad and complete inhibition of polymerization in the presence of

molecular oxygen. Because the experiments were done at body temperature (37 °C), the liposomes would be expected to be in the liquid crystalline phase. This data indicated a greater than 20 fold increase in the rate of polymerization when compared to liposomes formed from bis-SorbPC$_{17,17}$ (T_m 29.5 °C) in the liquid crystalline phase (3.8×10^{-9}). These values obtained by Tom Sisson are the basis of this research and an attempt to translate these results to lipids with higher T_m values was made. Liposomal formulations with lipids that have a Tm value above 37 °C have been shown to form more thermally stable liposomes and have indicated higher encapsulation efficiencies as discussed in chapter 5.

4.2 Methods and Materials

Bis-AcrylPC$_{18,18}$ was synthesized as described in chapter 3. Compounds containing UV-sensitive groups were handled under yellow lights. UV-Vis absorption spectra were recorded on a Varian DMS 200 spectrophotometer. Lipid purity was evaluated by thin-layer chromatography (TLC) with chloroform/methanol/water (65:25:4 by volume) and visualized by a UV lamp and charred with phosphomolybdic acid (PMA) stain. The lipids were hydrated in MilliQ water, Millipore Inc. Benzene was distilled from sodium benzophenone ketyl.

Liposomes used in γ-irradiated polymerization studies were unilamellar with a diameter of about 100 nm. Lipids were measured volumetrically into a weighed 10 mL round bottom flask from a stock solution of known concentration in benzene. An argon stream was passed over the solution to remove the solvent and the flasks were then placed under high vacuum for a minimum of eight hours to complete the drying.

The flask was weighed to obtain the amount of lipid in the flask. The lipids were then suspended in MilliQ water. The lipid suspension was then subjected to ten freeze thaw cycles and then extruded three times through two stacked 600 nm Nuclepore membranes followed by extrusion three times through two stacked 200 nm Nuclepore membranes and finally extrusion four times through two stacked 100 nm Nuclepore membranes. The concentration of the resulting liposome suspensions was determined by UV absorbance at 194 nm (acryl $\lambda_{max} = 194_{water}$, $\varepsilon = 12{,}000$) of a 30 µl aliquot in 0.97 mL of MilliQ water. The total lipid concentrations of resulting liposomes were typically between 1 and 10 mM.

Liposomes used in DSC measurements were formed through the same methodology as above, except the procedure was halted before extrusion. This produced multilamellar liposomes. Multilamellar liposomes are used because the soluble concentrations are typically higher. High concentrations of unilamellar liposomes can form a gel. Additionally, multilamellar liposomes give identical experimental results, but require fewer steps that can lead to errors. The concentration of the multilamellar liposomes for DSC measurements was maintained at 9 mM.

Monomer conversion was calculated as

$$\% \text{ conversion} = (A_0^{194} - A_t^{194}) / (A_0^{194}) \times 100$$

where A_0 is the initial absorbance of the standard sample, A_t is the absorbance of the sample after time (t) of irradiation.

4.3 Results

4.3.1 DSC and UV Characterization

The bis-AcrylPC$_{18,18}$ was characterized to determine its absorbance wavelength (λ_{max}), extinction coefficient (ε), and transition temperature (T_m). Each of these factors is extremely important in deciding the usefulness of this bis-Acryl lipid as a polymerizable lipid, which could then be incorporated within the liposomal membrane. The λ_{max} and ε can be used to follow the quantitative loss of monomer during the irradiation and to determine the initial concentration of the acryl lipid present in the sample.

Bis-AcrylPC$_{18,18}$ liposomes were shown to have a UV λ_{max} of 194 nm and an extinction coefficient of 12,000 M^{-1} cm^{-1} in MilliQ water. Figure 4.3 represents the UV absorbance plot of liposomes formed from bis-AcrylPC$_{18,18}$ in MilliQ water at varying concentrations from a single stock solution. The concentrations were varied to obtain a plot of the λ_{max} absorbance value versus the concentration where the slope of the resulting line is equal to the extinction coefficient (Fig. 4.4). The absorbance maxima and extinction coefficient were consistent with previous results for bis-AcrylPC$_{16,16}$ [111].

Differential Scanning Calorimetry (DSC) was used to determine the transition temperature of bis-AcrylPC$_{18,18}$. The resulting graph (Fig. 4.5) indicated a T_m value of 48 °C. As the temperature increases, the transition is from the L'_β phase to the L_α phase as described in chapter 1. The transition is reversible and can be observed when proceeding from higher to lower temperatures as well. This value is near the

value of bis-SorbPC$_{19,19}$ (44 °C), and should permit thermally stable domains at body temperature.

The DSC displayed a broad peak for the transition temperature, indicating very low cooperativity units. The cooperativity units are a measure describing the amount of lipids that undergo a phase change simultaneously. A high cooperativity unit suggests that the lipids are tightly packed and as one lipid undergoes the phase transition, other surrounding lipids must undergo the phase transition as well. A low cooperativity unit suggests that the lipids are loosely packed. This could also be explained if there were impurities within the lipids, such as mixed chain lengths, but TLC, ^{1}H NMR, ^{13}C NMR, and mass spectrometry indicated only one product. Bis-SorbylPC lipids have indicated a much higher cooperativity in DSC investigations and suggest that the structure and/or polarity of the acryl moiety may have a distinct effect on the packing efficiency of the lipids. The acryl ester lies at the terminal portion of the hydrophobic chains and may make it difficult for the terminal portions of these chains to closely associate because of the structure, which could be considered similar to an isobutyl chain. The carbonyl may disrupt the packing, much like a methyl group, and the shorter polymerizable chain (3-carbons) may be unable to compensate for the disruption. A simple example of this is the difference in the melting points and densities of 3-undecanone (12 °C, 0.825 g/mL) and 6-undecanone (14.6 °C, 0.831 g/mL).

The polarity of the sorbyl and acryl moieties may also play an important role in distinguishing between the cooperativity units of the compounds. Because of the extended conjugation of the sorbyl moiety, there may be π-bond interaction between

the independent lipids. In the acryl lipids, the loss of the second double bond may disallow this interaction because of the sterics imposed by the carbonyl group. Another possibility is that the acryl liposomes may have water associated within the typically hydrophobic tails because of the increased polarity of the acryl moiety. There are no known studies to show this, but I strongly believe that each of these possibilities play a part in the overall packing efficiency and cooperativity of the bis-AcrylPC$_{18,18}$ liposomes.

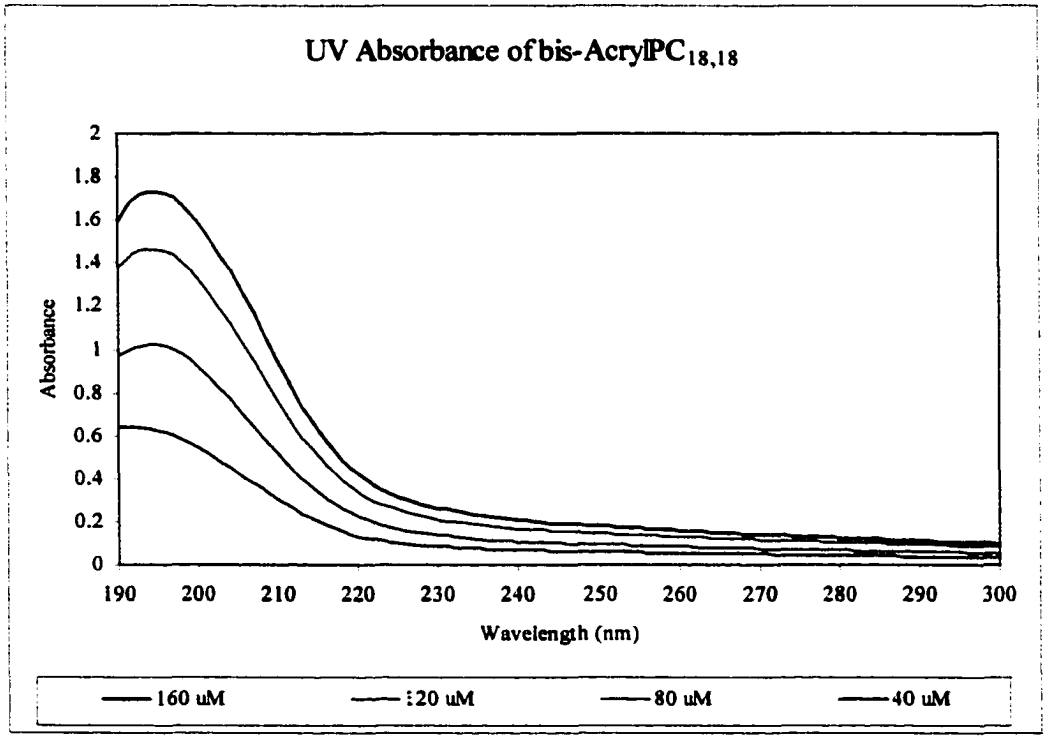

Figure 4.3. UV absorbance spectra of bis-AcrylPC$_{18,18}$ in PBS buffer at room temperature at varying concentrations.

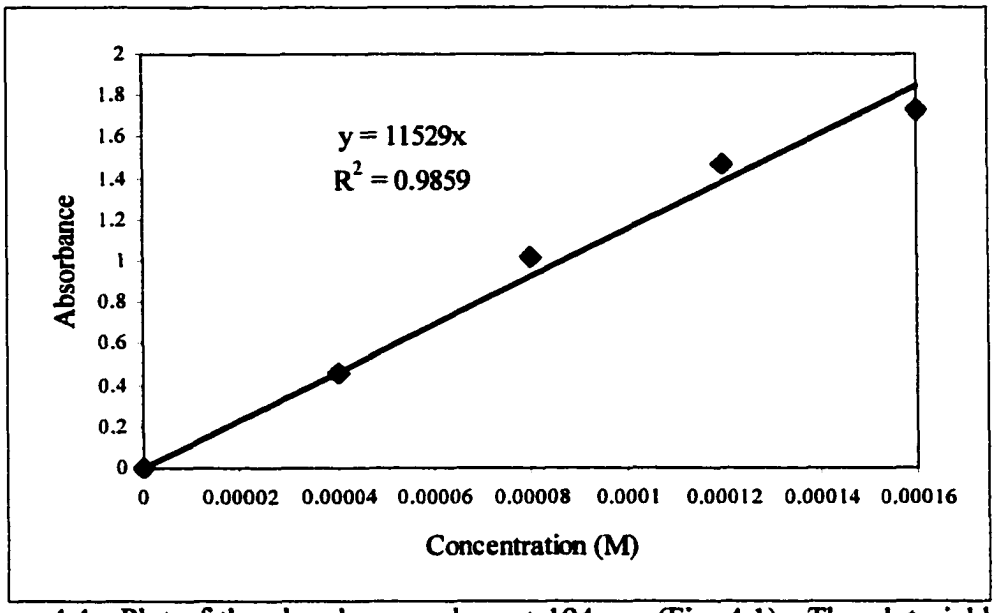

Figure 4.4. Plot of the absorbance values at 194 nm (Fig. 4.1). The plot yields an extinction coefficient of 12,000 M^{-1} cm^{-1}.

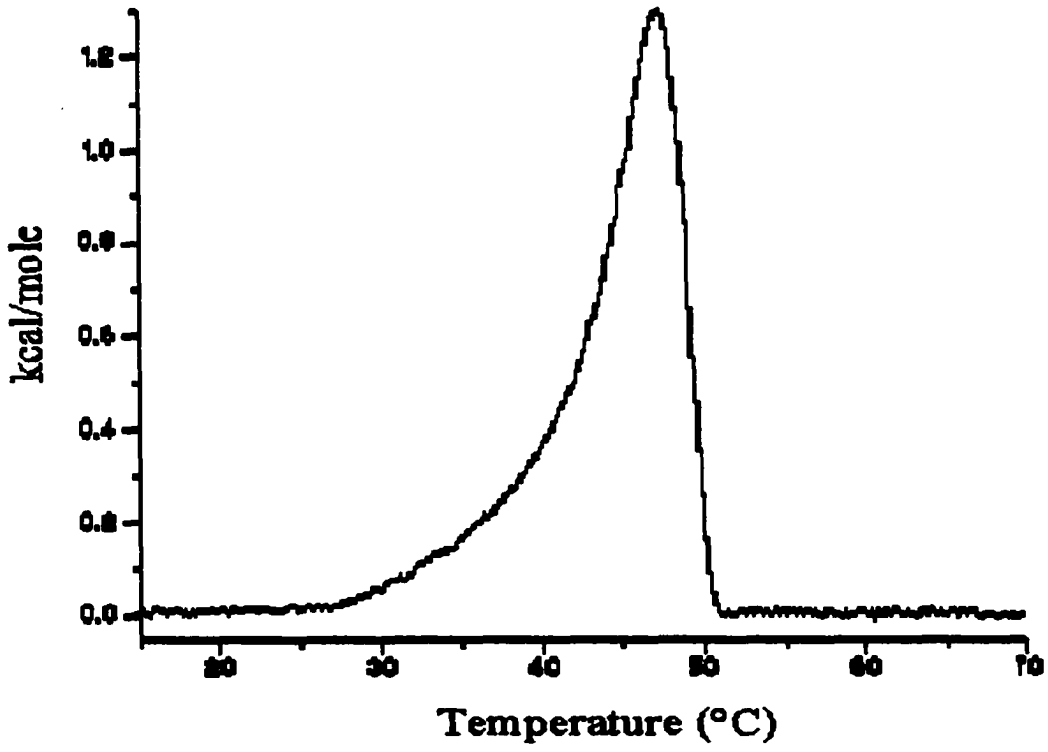

Figure 4.5. Differential Scanning Calorimetry plot of multilamellar liposomes composed of bis-AcrylPC$_{18,18}$ in MilliQ water.

4.3.2 Rates of Polymerization

Results of the γ-irradiated polymerization are shown below. The bis-AcrylPC$_{18,18}$ indicated a significantly lower rate of polymerization at 37 °C as compared to bis-AcrylPC$_{16,16}$.

Lipid Monomer	R_p (M/Rad)
bis-SorbPC$_{17,17}$	3.8×10^{-9}
bis-AcrylPC$_{16,16}$	8.8×10^{-8}
bis-AcrylPC$_{18,18}$	1.0×10^{-8}

Table 4.1. Rates of polymerization in moles per Rad. Bis-SorbPC$_{17,17}$ and bis-AcrylPC$_{16,16}$ were previously investigated [110, 111] at room temperature and used as a comparison for the bis-AcrylPC$_{18,18}$, which was tested at 37 °C.

The bis-AcrylPC$_{16,16}$ indicated an increase in the rate of polymerization, compared to bis-SorbPC$_{17,17}$, and appeared to be an excellent candidate for in vivo γ-initiated polymerizations for the development of triggered catastrophic release in cancer treatments. Unfortunately, liposomal formulations containing bis-AcrylPC$_{16,16}$ indicated a high rate of leakage for the encapsulated compounds [112]. In the attempt to form more thermally stable formulations, the bis-AcrylPC$_{18,18}$ was synthesized, but the increase in phase transition temperature (31 to 48 °C) appears to have a negative effect on the rate of polymerization, which decreases approximately 9-fold relative to bis-AcrylPC$_{16,16}$ (Table 4.1). This is probably due to the lipids being in the solid phase, which may slow the diffusion rate of the hydroxyl radicals from the aqueous

media to the inner portions of the bilayer when formed by γ-irradiation. This effect is also seen in the γ-irradiated polymerization of bis-SorbPC$_{19,19}$ liposomes, which are in the solid phase at 37 °C, discussed in chapter 6.

4.4 Discussion

Bis-AcrylPC$_{18,18}$ was extremely sensitive to molecular oxygen in γ-irradiated polymerizations. The aqueous samples were purged with an argon stream for several hours before transfer to 2 mL vials for irradiation. Samples that were not completely full (Fig. 4.6) indicated no polymerization, even when the vials were placed in a glove bag under an argon atmosphere. Teflon tape was used to seal the sample vials and every caution was taken to ensure the exclusion of molecular oxygen. Similar samples that were prepared from the same stock solution, but were filled completely, indicated a rate of polymerization consistent with sorbyl lipids.

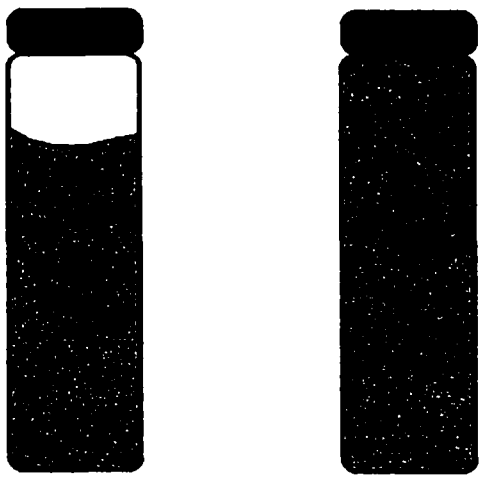

Figure 4.6. Illustration of the 2 mL vial samples used in the γ-initiated polymerization studies of bis-AcrylPC$_{18,18}$. Sample vials that were not completely full (left) indicated no polymerization even at very high dosages of irradiation (50,000 Rads), whereas samples that were full indicated a rate of polymerization consistent with sorbyl samples.

The addition of cholesterol into the bis-Acryl$PC_{18,18}$ formulations may increase the rate of polymerization in ionizing radiation experiments for reasons discussed in chapter 5. Currently, there appears to be little or no advantage in using acryl lipids in the formulations to be tested for liposomal destabilization in ionizing radiation experiments. Once the experiments progress to the advance stages of animal studies, the advantages of the acryl lipids may again become prominent because of their sensitivity to molecular oxygen as discussed in the introduction.

5 UV INITIATED DESTABILIZATION OF LIPOSOMES

5.1 Introduction

Liposomes typically show excellent biocompatibility and their ability to encapsulate chemotherapeutic compounds recommends them as drug carriers. The advantages of liposomes include (i) the ability to incorporate compounds that are not water soluble, (ii) therapeutic agents do not need to be altered by addition of a bulky group to mask it from the body's immune system, and (iii) chemotherapeutic compounds are kept from interacting at unintended sites. The disadvantages of the liposomes are their recognition by the immune system and their removal from the bloodstream by the reticuloendothelial system (RES). The disadvantages can be reduced through the use of covalently attached hydrophilic polymers, such as polyethylene glycol (PEG), which effectively coat the surface of the liposome and minimize the clearance. The ability of Pegylated liposomes to remain within the bloodstream for prolonged periods of time is the potential ability for site-specific attack.

Liposomes which remain in the blood system for prolonged times tend to accumulate at the cancer sites. Tumors have a greater need for nutrients due to their rapid growth, and one of the ways in which they obtain the nutrients is to increase the permeability of the surrounding blood vessels. This permits long circulating liposomes to escape the vasculature and reach the interstitum, thereby increasing the concentration of the liposomes at the cancer site. The passive leakage of therapeutic agents from liposomes in the interstitum can cause cancer cell death. Liposomes that

are retained in the bloodstream are removed by the RES, thus preventing the encapsulated therapeutic agent from attacking other tissue.

The use of light to stimulate the release of encapsulated compounds from liposomes is attractive because it is possible to control the spatial and temporal delivery of the radiation. Liposomes may be made photosensitive by the use of uniquely designed lipids that can alter the liposome properties via photoisomerization, photocleavage, or photopolymerization. A particularly useful characteristic of the latter is the multiplicative nature of the polymerization process. Ultraviolet light directly initiates the polymerization of phospholipids having the hexa-2,3-dienoyl (sorbyl) functionality at the chain ends. The photopolymerization reaction produces polymers with a low kinetic chain length of about 10 [97]. However, if lipids are substituted with polymerizable groups in both acyl chains, crosslinked polymer networks are formed [98]. Although UV initiated polymerization is not suitable for biological applications due to the high absorbance of UV light by many biomolecules, it does provide a convenient method to test lipid compositions which could, in a clinical setting, be polymerized by more biocompatible techniques such as photosensitization with longer wavelength light, or by exposure to therapeutic doses of ionizing radiation.

The liposomes tested in this section are designed to release their contents to the surrounding solution through a photoinduced increase in membrane permeability, rather than by photoinduced membrane fusion, which has been demonstrated previously for conventional liposomes [100]. The mechanism by which this was initially thought to occur is through domain formation due to the polymerization of

Sorb-lipid and the partitioning of pegylated lipids into the non-polymerized domains (Fig. 5.1). The resulting lipid domains with high PEG concentration would be thermodynamically unstable and should form mixed micelles (chapter 1.1), leaving holes or areas of disrupted, permeablized membrane. The liposome formulation necessary for this mechanism to work needs to have a pegylated lipid concentration after polymerization of greater than 20 mol % within the non-polymerized domain [96].

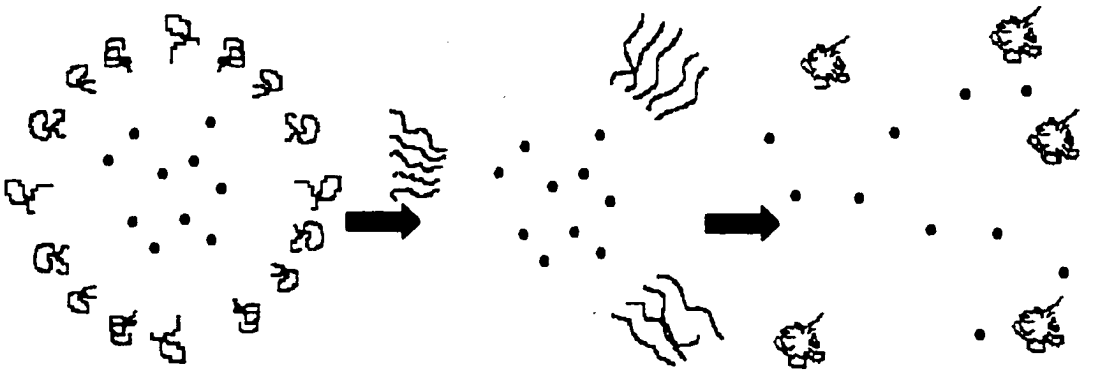

Figure 5.1. Schematic cross section of PEG-liposomes that represents the Pegylated and non-Pegylated lipids. The photopolymerization-induced concentration of the Pegylated lipids is shown in the middle, while the diffusion of the Pegylated lipids and resulting holes are shown on the right.

A second, and more effective mechanism for photoinduced leakage became apparent as the leakage assays were being carried out (Fig. 5.2). In this case, the bilayer has phase separated monomer domains before polymerization, and these are disrupted by the polymerization. Either leaky fissures between polymerized and non-polymerized domains or pores inside the polymerized domain are formed. Evidence

for such phase separated domains has been observed by differential scanning calorimetry, thermally induced leakage, and confocal microscopy [14]. The onset of photoinduced leakage in liposomes with these lipid compositions occurs at as little as 20 % loss of monomer, compared to greater than 90 % loss of monomer that is required for photoinduced leakage to occur in liposomes in which phase separation is not observed prior to polymerization.

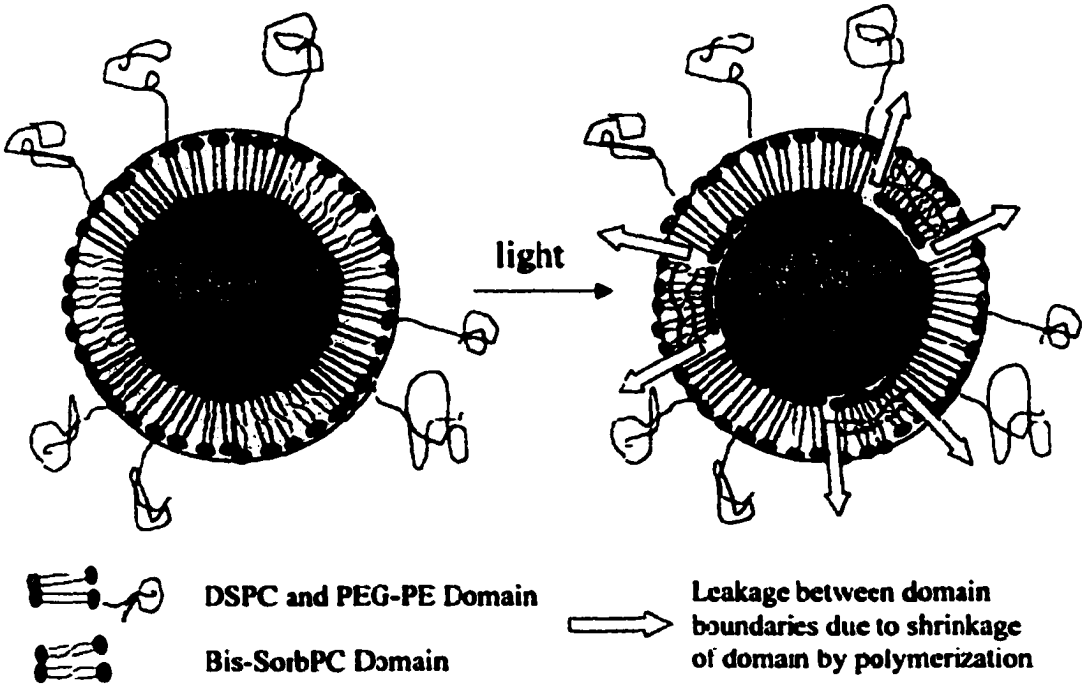

Figure 5.2. Schematic cross section of PEG-liposomes that represents the domains of bis-SorbPC and stearoyl lipids. The photopolymerization-induced reduction in the surface area of the polymerizable domains (black areas) during UV irradiation is shown on the right.

5.2 Methods and Materials

5.2.1 Materials

The collisional quencher, α,α'-bis-pyridinium-1,4-xylene dibromide (DPX) (Fig. 5.3) was prepared as follows: α,α'-dibromo-1,4-xylene (20.0 g, 75.7 mmole) was suspended in chloroform (1.0 L) in a 2 L, 3 neck, round bottom flask fitted with a mechanical stirrer and a reflux condenser. Pyridine (18.0 g, 227 mmole) was added and the reaction mixture was heated to reflux for 3 hr. The resulting white precipitate was collected by vacuum filtration, washed twice with chloroform (200 mL), and recrystallized from methanol/isopropanol. The colorless needle crystals were dissolved in nanopure water (200 mL) and filtered through a 0.45 micron membrane filter. The water was removed under reduced pressure. Dry benzene (200 mL) was added and evaporated under reduced pressure to remove any residual water. The resulting solid (23.4 g, 90 % theoretical yield) was dried at 25 °C under 0.1 torr pressure for 24 hr. ^{1}H NMR (D_2O): 8.83 – 8.78 (dd, J = 10.2 Hz, 2.0 Hz, 4H, $CH_2N^+C\underline{H}$), 8.51 – 8.42 (tt, J = 11.9 Hz, 2.0 Hz, 2H, $CH_2N^+CHCHC\underline{H}$), 8.0 – 7.93 (dd, J = 11.9 Hz, 10.6 Hz, 4H, $CH_2N^+CHC\underline{H}$), 7.44 (s, 4H, $CH_2CC\underline{H}C\underline{H}$), 5.76 (s 4H, CH_2) ppm. ANTS was purchased from Molecular Probes Inc. (Eugene, Oregon) and used without further purification. Bis-SorbPC$_{17,17}$ and bis-SorbPC$_{19,19}$ were prepared as described in chapter 2. 1,2-Dipalmitoyl-*sn*-phosphatidylcholine (DPPC), 1,2-dioleoyl-*sn*-phosphatidylcholine (DOPC), 1,2-distearoyl-*sn*-phosphatidylcholine (DSPC), 1,2-diarachidoyl-*sn*-phosphatidyl-choline (DAPC), PEG$_{2000}$-1,2-dioleoyl-*sn*-phosphatidylethanolamine (PEG-DOPE), and PEG$_{2000}$-1,2-distearoyl-*sn*-phosphatidylethanolamine (PEG-DSPE) were obtained from Avanti Polar Lipids.

Cholesterol was purchased from Sigma and used without further purification. Octylphenoxy polyethoxyethanol (Triton X-100) (Sigma) was used in a 5% (wt/wt) solution with Millipore water.

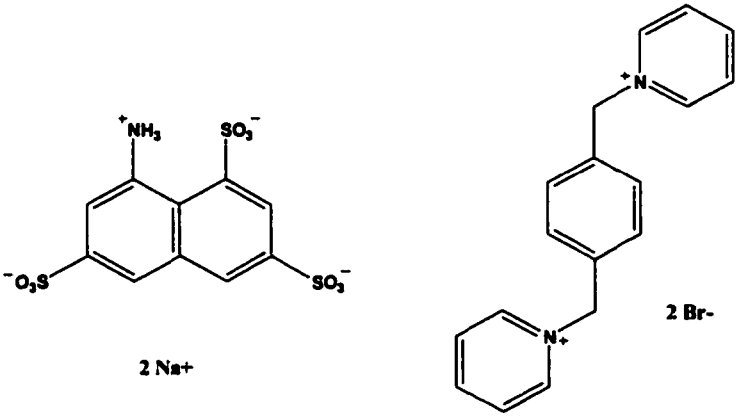

Figure 5.3. Probes used in leakage assays; (Left) Fluorescent marker, 8-aminonapthalene-1,3,6-trisulfonic acid (ANTS); (Right) Collisional quencher, α,α'-bis-pyridinium-1,4-xylene dibromide (DPX)

5.2.2 Liposome Formation

Lipids were measured volumetrically into separate weighed 10 mL round bottom flasks from stock solutions of known concentrations. An argon stream was passed over each solution to remove the solvent and the flasks were then placed under high vacuum for a minimum of four hours to complete the drying. The flasks were weighed to obtain the amount of lipid in each flask. Approximately 2 mL of chloroform were then added to all but one of the flasks and the contents were combined and dried as above. A final weight was taken to ensure the complete transfer of lipids. The lipids were then suspended in a sufficient amount of dye containing pH 7 phosphate buffer to make a 10 mM total lipid concentration. The

buffer used for the hydration of the lipids contained ANTS (25 mM), DPX (90 mM) and sodium phosphate (10 mM). The osmolarity of the buffer solution was found to be 277 mosmol. The lipid suspension was then subjected to ten freeze thaw cycles and then extruded three times through two stacked 600 nm Nuclepore membranes followed by extrusion three times through two stacked 200 nm Nuclepore membranes and finally extrusion four times through two stacked 100 nm Nuclepore membranes. The resulting ANTS/DPX containing liposomes were eluted through a Sephadex G-75 column with pH 7 buffer solution containing sodium phosphate (10 mM), sodium chloride (139 mM), and having an osmolarity of 277 mosmol. The concentration of the resulting liposome suspensions were determined by UV absorbance at 260 nm (sorbyl $\lambda_{max} = 258_{MeOH}$, $\varepsilon = 47{,}100$) of a 30 μl aliquot in 0.97 mL of HPLC grade methanol. The total lipid concentrations of the resulting liposomes were between 1 and 3 mM.

5.2.3 Fluorescence measurements

Fluorescence time based scans were done on 3 mL, 0.15 mM dilutions of the liposome suspensions in pH 7.0 PBS, with 360 nm excitation and 520 nm emission on a Spex Fluorolog 2 fluorometer. The slit width for both excitation and emission monochrometers was 4 mm. Complete leakage was determined after lysis of the liposome by addition of 0.3 mL of 5% (v/v) aqueous Triton X-100 to a 3 mL sample. Photopolymerization was carried to between 20 and 99% by exposures of 1 s up to 8 min to light from a low pressure Hg pen lamp at 0.02 to 0.04 W/cm^2. The percent conversion was determined by the change in UV absorbance at 258 nm. A Corning

CS-9-54 filter (> 230 nm) was used to prevent photolysis of the polymerization product. Monomer conversion was calculated as

$$\% \text{ conversion} = (A_0^{254} - A_t^{254}) / (A'_0{}^{254} - A'_{20}{}^{254})(A_0^{254}) \times 100\%$$

where A_0 is the initial absorbance of the sample, A'_0 is the initial absorbance of the standard sample, A_t is the absorbance of the sample after time (t) of irradiation, and A'_{20} is the absorbance of the standard sample after 20 min of irradiation.

5.2.4 Determination of Encapsulated ANTS

The total amount of ANTS encapsulated in the liposomes was determined shortly (within 1-2 h) after chromatographic separation of the unencapsulated dye. A 3 mL sample of liposomes having a total lipid concentration of 150 μM was prepared at room temperature, and the fluorescence at 520 nm with excitation of 360 nm was measured for 45 s. Triton X-100 (0.3 mL at 5% aq. v/v) was added, and the fluorescence measurement was continued for an additional 45 s. The emission intensity of the sample after addition of Triton X-100 was multiplied by 1.1 to adjust for the dilution by the detergent solution and the difference between this and the initial measurement was compared to the emission intensity of standard solutions of ANTS/DPX (5:18 ratio).

5.2.5 Determination of Liposome Leakage

In order to determine the percent leakage of liposome encapsulated ANTS/DPX, the fluorescence of each sample was measured over 30 s prior to photolysis. Immediately after photolysis, the percent conversion was determined

from the sample absorbance with a diode array spectrophotometer, and the fluorescence was measured continuously over several minutes. After the leakage measurement, a 90 s time scan was performed during which a 5% solution of Triton X-100 was added at 45 s. The fluorescence due to 100% leakage was determined from this measurement after correcting for the bleaching of ANTS during photolysis and the dilution factor due to the Triton X-100 solution.

The fluorescent marker, ANTS, has a minor absorption at 258 nm at the sample concentration. For this reason, irradiation of the liposome solution at 230-300 nm causes some bleaching of the ANTS. The percent ANTS bleaching was determined by comparing the fluorescence measurement after the addition of Triton X-100 for a photolyzed sample to a similar measurement performed on a sample of non-photolyzed liposomes after dividing each by the UV absorbance at 254 nm to factor out any differences in sample preparation,

$$b = I_{photolyzed}/I_{non\text{-}photolyzed} \times A_{non\text{-}photolyzed}/A_{photolyzed}$$

A bleaching factor of between 0.8 and 1.0, depending on the length of photolysis, was obtained, which adjusts the baseline (I_0) to what it would be if the amount of ANTS present before photolysis were equal to that present after photolysis.

The percent leakage at any time is given by the following expression:

$$\% \text{ leakage} = 100 \times (I_t - bI_0)/(1.1I_{100} - bI_0)$$

where I_t is the fluorescence intensity at time (t), I_0 is the fluorescence intensity prior to photolysis, I_{100} is the fluorescence intensity after addition of Triton X-100, and b is the bleaching factor. Because the initial change in concentration inside the liposomes is relatively small, the initial leakage is pseudo-zero order, and the plot is a straight

line. The rate of leakage was calculated from the linear region of the plot using a least squares fit.

5.3 Results

5.3.1. Encapsulation

The fluorescence assay employed in these experiments uses the anionic, water soluble fluorescent marker 8-aminonapthalene-1,3,6-trisulfonic acid (ANTS), and the di-cationic collisional quencher, α,α'-bis-pyridinium-1,4-xylene dibromide (DPX). ANTS has an absorption maximum at 360 nm and a fluorescence maximum at 520 nm. DPX has an absorption maximum at 260 nm and does not fluoresce. When dye and quencher are encapsulated inside the liposome at high concentration (ca. 25 mM ANTS, and 90 mM DPX), the ANTS fluorescence is effectively quenched. When the markers are released into the larger (more than 100 times greater) volume of the cuvette, the fluorescence intensity is no longer quenched, so that the increase in fluorescence intensity is directly proportional to the amount of ANTS released from the liposomes. The percent leakage can be obtained simply by comparing the intensity at any time point with that of completely disrupted liposomes. The absolute ANTS concentration can be obtained if the fluorometer is periodically calibrated with solutions of known ANTS concentration.

The maximum amount of encapsulation of a fluorescent marker or drug molecule into liposomes, without the use of active loading (section 1.8.2.), is the product of the total internal volume of a liposome solution and the concentration of the molecule to be encapsulated. The maximum internal volume of a liposome

suspension was calculated for unilamellar POPC liposomes of various sizes by Pfeiffer *et al* [113]. Though the liposomes that are used in these experiments are of a different composition, Pfeiffer's results give a reasonable approximation of the maximum amount of fluorescent dye that could theoretically be encapsulated by our liposome system. Pfeiffer assumed an area per lipid molecule of 68 square angstroms and a bilayer thickness of 29 angstroms in the calculation. The experimental values of liposome volume determined by entrapment of solute are considerably lower than the values calculated by Pfeiffer. Mayer *et al.* found, by this method, that the actual experimental value for the internal volume of eggPC liposomes, made by the extrusion of freeze-thawed MLVs through two stacked 100 nm polycarbonate membranes, is approximately 0.5 times the theoretical value of 1.5 L/mole (lipid) [114]. Freeze fracture electron microscopy of extruded eggPC/cholesterol liposomes in the absence of cryoprotectants, such as glycerol, shows that the liposomes deviate from the ideal spherical structure [115]. This could result in the lower encapsulated volume that was observed by Mayer. Liposomes in the leakage experiments presented here ranged between 90 and 120 nm in diameter. Because the volume is proportional to r^3 the encapsulated volume in a polydisperse population of liposomes should be dominated by the larger liposomes. Table 5.1 shows the calculated maximum volume and amount of dye that could be encapsulated from a 25 mM ANTS solution into unilamellar liposomes from 90 to 120 nm in diameter.

Table 5.2 indicates the effect of Pegylated lipids on the internal volume of liposomes. As the size of the liposome increases, the effect on the internal volume is reduced as would be expected. The difference between the mushroom and brush

conformations in the Pegylated lipids is mainly due to the amount of hydration associated with the polymers in either of these conformations (Fig. 5.4). The brush conformation requires less water to be associated with it. Therefore the overall area associated with the brush conformation is less then that of the mushroom conformation.

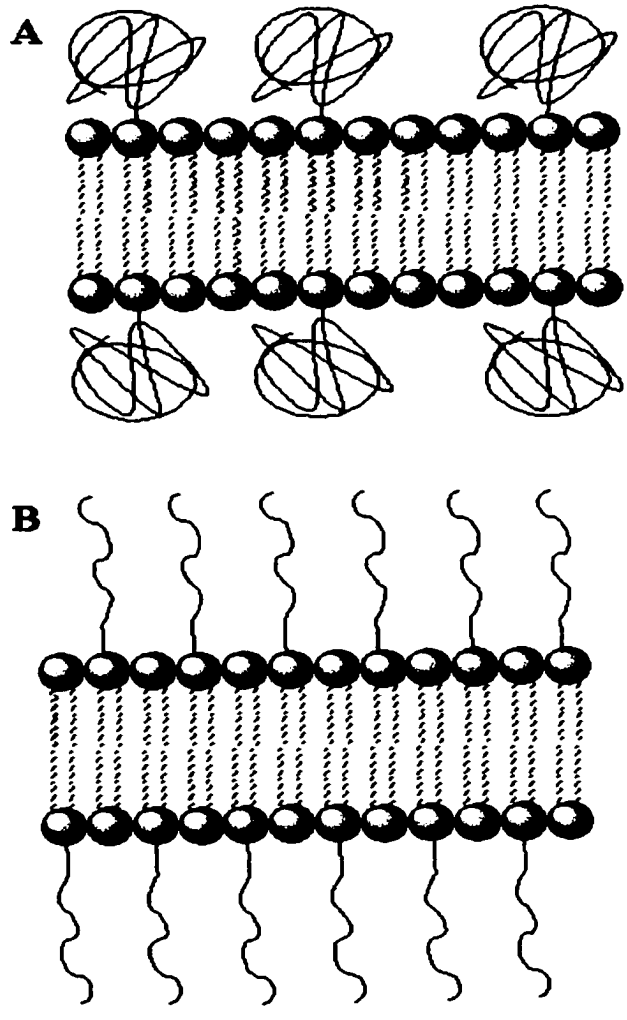

Figure 5.4. Illustration of the mushroom (A) and the brush (B) conformations of the hydrophilic polymer PEG. At low concentrations of the Pegylated lipid (A) the polymer is in a random coil conformation, but at high concentrations (B) (>20 mol %) the polymer is in a brush conformation.

Diameter (nm)	Lipid molecules per liposome	Encapsulated volume (L/mol) of lipid	μM ANTS/ mM lipid
90	69,700	2.70	67.5
100	86,600	3.05	76.1
110	105,300	3.39	84.7
120	125,900	3.73	93.3

Table 5.1. Calculated internal volume, lipid molecules per liposome, and maximum dye encapsulation (assuming 25 mM dye concentration).

Diameter (nm)	Mushroom 10^{-15} mL per liposome	Brush 10^{-15} mL per liposome	Mushroom % of conventional	Brush % of conventional
90	2.3	2.2	83	80
100	3.3	3.1	85	82
110	4.4	4.3	86	84
120	5.9	5.7	87	85

Table 5.2. Calculated internal volume of PEG-liposome with high and low densities as compared to POPC conventional liposomes investigated by Pfeiffer *et al* in Table 5.1.

Table 5.3 indicates the encapsulation efficiency of DOPC liposomes in the liquid crystalline phase. These results are taken from Dr. Bruce Bondurant's dissertation as a relative example of the difficulties that were observed in the

formulations containing DOPC. The encapsulation efficiency maximum value is only 24 % for these formulations, which would certainly disqualify these formulations for commercial use. The effect of having a non-polymerizable lipid such as DOPC with a phase transition temperature of –18 °C, indicating that the lipid would remain in a liquid crystalline state at experimental temperatures, was that the encapsulated dye was able to diffuse out of the liposomal compartment into the external media. This probably occurred rapidly as evidenced by the background fluorescence observed in these formulations. As a result of these studies and the immense amount of experiments Dr. Bondurant was able to perform, a better understanding of the relationship between lipid phases and lipid-lipid interactions led the research group to look towards formulations containing lipids with T_m values above body temperature.

Cholesterol	Background Fluorescence	Encapsulation (μM / mM)	Comparable % Observed in POPC Liposomes (100 nm)
0	34,500	16	21
20	13,500	18	24
30	14,000	17	23
40	11,000	14	18

Table 5.3. Encapsulation of ANTS in liquid crystalline phase liposomes containing differing concentrations of cholesterol. Other membrane components are held constant at the following: PEG-DOPE (15 mol %), bis-SorbPC$_{17,17}$ (25 mol %). DOPC varies to make the sum 100 % [103]. Column four represents the encapsulation efficiency compared to POPC conventional liposomes investigated by Pfeiffer *et al* in Table 5.1.

Table 5.4 indicates the effect on the encapsulation efficiency of varying the concentration of the polymerizable lipid bis-SorbPC$_{17,17}$. There appears to be little change in the encapsulation efficiency of the formulations tested. While there is a decrease in the encapsulation efficiency with an increase in the amount of bis-SorbPC$_{17,17}$, it should also be noted that the formulations did not contain cholesterol. Liposomes formed with bis-SorbPC$_{17,17}$ exclusively did not show the ability to encapsulate ANTS/DPX in the experiments attempted by Dr. Bruce Bondurant (data not published). Light scattering data from liposomes formed from bis-SorbPC$_{17,17}$ exclusively also showed widely varied size distributions, indicating structures other then liposomes are likely formed.

Bis-SorbPC$_{17,17}$	**Background Fluorescence**	**Encapsulation (μM / mM)**	**Comparable % Observed in POPC Liposomes (100 nm)**
0	15,000	24	31
10	15,000	22	29
20	27,000	19	25
25	34,000	16	21

Table 5.4. Encapsulation of ANTS in liposomes containing differing concentrations of bis-SorbPC$_{17,17}$. Other membrane components are held constant at the following: PEG-DOPE (15 mol %), cholesterol (0 mol %). DOPC varies to make the sum 100 % [103].Column four represents the encapsulation efficiency compared to POPC conventional liposomes investigated by Pfeiffer *et al* in Table 5.1.

Table 5.5 indicates the advantage of using lipids with Tm values above body temperature. As discussed above, the previous experiments with low T_m lipids indicated low encapsulation efficiencies, but when using lipids with DAPC (T_m 65 °C) the encapsulation efficiency was increase from 24 % to 70 %. Addition of cholesterol indicated a significant loss in the encapsulation efficiency. This can be explained by the destabilization of solid lipid membranes by cholesterol as discussed in chapter 1.

Cholesterol	Background Fluorescence	Encapsulation (μM / mM)	Comparable % Observed in POPC Liposomes (100 nm)
0	10,500	53	70
20	11,500	40	52
30	19,000	35	46
40	41,000	15	20

Table 5.5. Encapsulation of ANTS in solid phase liposomes containing differing concentrations of cholesterol. Other membrane components are held constant at the following: PEG-DSPE (5 mol %), bis-SorbPC$_{19,19}$ (20 mol %). DAPC varies to make the sum 100 %. Column four represents the encapsulation efficiency compared to POPC conventional liposomes investigated by Pfeiffer *et al* in Table 5.1.

Table 5.6 summarizes the previous tables in a more comparable format. It is clear from this table that an important step has been taken to produce a therapeutically viable formulation. A 3-fold increase in the encapsulation efficiency can be observed between the formulations containing DOPC and those containing DAPC.

T_m	Formulation	Encapsulation (μM / mM)	Comparable % Observed in POPC Liposomes (100 nm)
Low	PEG-DOPE/ DOPE (15/85)	24	31
Low	PEG-DOPE/ bis-SorbPC$_{17,17}$/ DOPE (15/25/60)	16	21
Low	PEG-DOPE/ bis-SorbPC$_{17,17}$/ cholesterol/DOPE (15/25/20/40)	18	24
High	PEG-DSPE/DAPC (5/95)	55	72
High	PEG-DSPE/bis-SorbPC$_{19,19}$/ DAPC (5/20/75)	53	70
High	PEG-DSPE/bis-SorbPC$_{19,19}$/ cholesterol/DAPC (5/20/20/55)	40	52

Table 5.6. Comparison of the encapsulation efficiency of low temperature formulations [103], and the high temperature formulations. The low temperature formulations are in the liquid crystalline phase, whereas the high temperature formulations are in the solid phase at room temperature. Column four represents the encapsulation efficiency compared to POPC conventional liposomes investigated by Pfeiffer *et al* in Table 5.1.

The values for encapsulation in the leakage experiments presented here were much lower than the values obtained from either the internal volumes that were calculated by Pfeiffer or those measured experimentally by Mayer. Tables 5.2 – 5.5 show encapsulation efficiencies of liposomes in which the concentrations of lipids were varied. The highest encapsulation for liposomes containing cholesterol in the low temperature formulations was 24 % of the calculated maximum internal volume for 100 nm POPC LUV for the formulations containing DOPC (Table 5.2). Liposome formulations without cholesterol had a maximum encapsulation value of about 70% (Tables 5.5 & 5.6).

Possible reasons for the lower encapsulation (70 %) include: (1) leakage during or after chromatography, (2) incomplete quenching, (3) volume filled by PEG chains, (4) incorrect area per lipid molecule, or (5) the formation of a sub-population of non-encapsulating or non-spherical structures such as disc-shaped liposomes, toroidal liposomes, rod shaped micelles, or spherical micelles.

Significant differences were observed between DOPC/bis-SorbPC$_{17,17}$ and DAPC/bis-SorbPC$_{19,19}$ formulations (Table 5.6). A possible explanation for the differences in encapsulation efficiency may be explained by the liposomal phase characteristics. The DOPC/bis-SorbPC$_{17,17}$ liposomal formulations should be in a liquid crystalline phase, while the DAPC/bis-SorbPC$_{19,19}$ liposomal formulations should be in a solid phase at room or body temperature. All formulations tested in the current study were maintained at room temperature during gel chromatography and dilution. Because room temperature is below the lowest T_m value in the DAPC/bis-

SorbPC$_{19,19}$ liposomal formulations for the individual lipids, the liposomes can be considered more solid-like in character and less permeable to the encapsulated compounds used in this study.

5.3.1.1. Leakage During Chromatography

Rapid leakage (on the order of 20 min) during size exclusion chromatography results in reduced or no encapsulation with a high background fluorescence as can be seen in the final two entries of table 5.4. If there is some encapsulation, the remaining dye can be observed to leak quickly without photolysis. This behavior was observed with DOPC liposomes that contained 25 mol % bis-SorbPC$_{17,17}$, with no cholesterol. Stable encapsulation could not be achieved with liposomes that contained 30 % or more bis-SorbPC$_{17,17}$ or bis-SorbPC$_{19,19}$ without cholesterol. When 20 to 40 mol % cholesterol is included in the liposomes, dark leakage is reduced by two orders of magnitude [103]. Size exclusion column fractions surrounding the elution of liposomes containing PEG-DSPE/bis-SorbPC$_{17,17}$/cholesterol/DSPC (5/30/35/30) were tested for UV absorbance at 254 nm, background fluorescence, and encapsulation. Higher background fluorescence correlated with higher lipid concentration and encapsulation efficiency [103]. The elution of liposomes and unencapsulated dye did not overlap, indicating that no significant leakage occurs with that lipid mixture during size exclusion chromatography.

5.3.1.2.Incomplete Quenching of ANTS

Incomplete quenching of the ANTS can occur if the DPX is not in a high enough concentration to come into contact with the ANTS upon excitation. This can be due to the use of old media where the DPX has crystallized from the solution or an error in the calculation or formulation of the media. If ANTS is not completely quenched, there could be a significantly higher background fluorescence resulting from encapsulated dye. In the calculation of encapsulation, this fluorescence would be subtracted from the total fluorescence giving an artificially low estimate of encapsulation. If incomplete quenching of encapsulated dye is the only source of background fluorescence, the true encapsulation would be given by comparing the total fluorescence of the ANTS/DPX containing sample after detergent lysis (TX-100 addition) with a sample of liposomes of the same total lipid concentration that contain no encapsulated dye. In other words, the subtraction of the initial ANTS fluorescence intensity would be in error because it is assumed that this is external ANTS and not encapsulated ANTS that is not being efficiently quenched. The fluorescence intensity of empty liposomes with 100 μM total lipid concentration (excitation and emission slit width = 0.4 mm) is 6000 cps, which can simply be explained by the scattering of light by the liposomes and the media. With the exception of samples that contain DOPC and bis-SorbPC$_{17,17}$ without cholesterol, the background intensity of most samples is between 10,000 and 25,000 cps. The maximum error in the calculation of encapsulated dye that could be attributed to incomplete quenching is between 0.5 and 2.5 μM ANTS per mM total lipid (1 to 5 %).

5.3.1.3.Effect of PEG on Liposomal Volume

In contrast to conventional liposomes, PEG-liposomes with PEG on both leaflets have an internal volume that is reduced by the volume occupied by the hydrated polymer. The encapsulated volume of a PEG-liposome can be approximated by a sphere with a radius smaller than the external radius of the liposome by the thickness of the bilayer and of the hydrated PEG layer. The thickness of a hydrated PEG layer for a PEG_{2000}-grafted, supported bilayer has been measured by Leckband *et al.* to be 5.2 nm for a mushroom conformation in the weak overlap regime (4 - 5 % PEG-lipid) and 6.2 nm for a brush regime (> 10 % PEG-lipid) [116]. The calculated volume per liposome for 90 – 120 nm liposomes using the formula for the volume of a sphere ($V = 4/3\ \pi\ r^3$) is given in table 5.2. The reduction in encapsulation is between 13 and 20 %. This trend is demonstrated by the experimental data presented in table 5.3. Although data in tables 5.3 – 5.6 has an uncertainty of about ±10 %, it demonstrates how the encapsulation efficiency varies with changing concentrations of PEG-lipid, cholesterol, and sorbyl lipids.

5.3.1.4.Effect of Cholesterol on Lipid Packing

Cholesterol has been shown in experiments with Langmuir monolayers to cause a considerable decrease in the area per lipid where the lipids are in a liquid crystalline phase [117]. Because the volume is proportional to the $area^{3/2}$, the presence of 40 mol % cholesterol can result in a correspondingly large decrease in the volume per lipid of a DOPC/cholesterol (60/40) liposome, which would be $0.74^{3/2}$ or

0.64 times that of the same size liposome composed of pure DOPC (T_m = -18 °C). That is, it would take a correspondingly larger number of lipid molecules to make up the same size of liposome. If both the effect of cholesterol and the effect of PEG lipid are considered together the volume per lipid (and therefore the maximum encapsulation) of a PEG-DOPE/cholesterol/DOPC (15/40/45) liposome is the product of these factors, which is 45 % of the calculated volume per lipid of a pure DOPC liposome. Table 5.3 shows the encapsulation efficiency of liposomes that vary only in the concentration of cholesterol [103]. The trend toward lower encapsulation efficiency is demonstrated here with the exception of the first entry. The first entry is probably low because of a high rate of dark leakage (4×10^{-2} % s^{-1} at 37 °C), which is supported by the high background fluorescence. If the lower background fluorescence of the second and third entry is used to calculate the encapsulation of the first entry, the efficiency of encapsulation is equal to that of liposomes containing 20 % cholesterol. If the amount of ANTS lost during 20 min of column chromatography is considered, then the adjusted encapsulation efficiency is 24 μM ANTS/mM total lipid, or approximately 32 % of the calculated maximum.

5.3.1.5.Effect of Non-Spherical Structures.

Another trend in encapsulation efficiency is that of decreasing encapsulation with increasing concentration of bis-Sorb lipids. The trend in the absence of cholesterol (Table 5.3) can be explained by the increased rate of leakage (chapter 5.3.1.1.). In the cases where lower concentrations of bis-Sorb lipids (≤ 20 mol %) are present, and leakage is minimized, another possibility may be the effect of non-

spherical structures that do not have an internal aqueous volume. While broadened or bimodal distributions were not observed with 20 mol % bis-Sorb formulations, it is often difficult to detect small structures in the presence of large ones by quasai elastic light scattering (QELS). It might be possible to do this by freeze fracture electron microscopy, or cryo-transmission electron microscopy (cryo-TEM). Also the formulas used to determine size by QELS pre-suppose that structures are spherical. Disk shaped structures have been observed by Edwards *et al* at moderately high PEG-grafted-cholesterol concentrations ($\geq$ 20 mol %) [118]. As QELS experiments would not distinguish these non-spherical shapes, their presence would result in broadened or erroneous size distributions.

5.3.1.6.The Effect of Cholesterol on Solid Phase Liposomes.

Section 5.3.1.4. discussed the effect of cholesterol on the packing of lipids in the liquid crystalline phase. Cholesterol has the opposite effect on lipids in the solid phase [2]. Liposomal formulations, in which the phospholipid T_m values are above 37 °C, indicated much higher encapsulation efficiencies in formulations without cholesterol as shown in table 5.3. Table 5.5 shows the encapsulation efficiencies of liposomes in the liquid crystalline phase versus liposomes in the solid phase. While the low temperature formulation liposomes indicated a range of only 21 to 31 % of calculated for POPC liposomes, the high temperature formulations indicated a range of 70 to 72 %. By factoring in the loss of volume due to the PEG lipid (15 %), the encapsulation efficiency approaches 85 %.

5.3.1.7.Conclusion

The maximum encapsulation for DPPC liposomes as calculated by Pfeiffer *et al* cannot be directly translated to sterically stabilized liposomes because of the data and explanations stated above. Additionally, the inclusion of lipids that phase separate may have an initial effect on the encapsulation efficiency. This conclusion was reached after an extensive discussion with Dr. Vladimir P. Torchilin at Northeastern University, where he relayed unpublished findings during a discussion on the feasibility of using these formulations in vivo. Dr. Torchilin found that liposomes that underwent phase separation were permeable until the phase separation was complete. After the phase separation was completed, the liposome permeability was dependent on the individual lipid characteristics of those domains. Because of the high T_m values in the DAPC/bis-SorbPC$_{19,19}$ formulations, the phase separation should take place very rapidly upon cooling to room temperature after extrusion and minimize the amount of leakage. The addition of cholesterol to formulations would be expected to prolong the time for phase separation and increase the permeability of the liposome, thus reducing the encapsulation efficiency.

5.3.3 Rates of Polymerization

UV photopolymerization of the sorbyl moiety has been extremely well established within the O'Brien group [16, 50, 51, 96, 102]. Figures 5.5 to 5.7 show the UV spectra of three formulations with a total lipid concentration of 150 mM at several photolysis time points for liposomes composed of PEG-DSPE/bis-

SorbPC$_{17,17}$/cholesterol/DSPC (5/30/35/30), PEG-DSPE/bis-SorbPC$_{19,19}$ /DAPC (5/20/75), and PEG-DSPE/bis-SorbPC$_{19,19}$/cholesterol/DAPC (5/20/10/65). Photolysis results in a decrease in the absorbance at ca. 250 nm with a lesser increase in the absorbance at 204 nm, which corresponds to the isolated double bond that is formed in the photo-polymerization. The absence of an isobestic point in most sets of photolysis suggests that there is more than one photo-product. Irradiation of pure bis-SorbPC liposomes in the absence of O_2 yields the 1,4-polymer, but other products are possible as shown in Figure 5.8 [97]. Because the conditions of polymerization in these experiments were different (mixed liposomes and the presence of oxygen), those results do not necessarily hold in this case. It is unlikely that the 3,4-polymerization is occurring in this case, as the absorbance at 210 nm of a double bond in conjugation with a carbonyl group is not observed. Other structures such as poly-*co*-peroxy ethers have been observed, and will be discussed later [119].

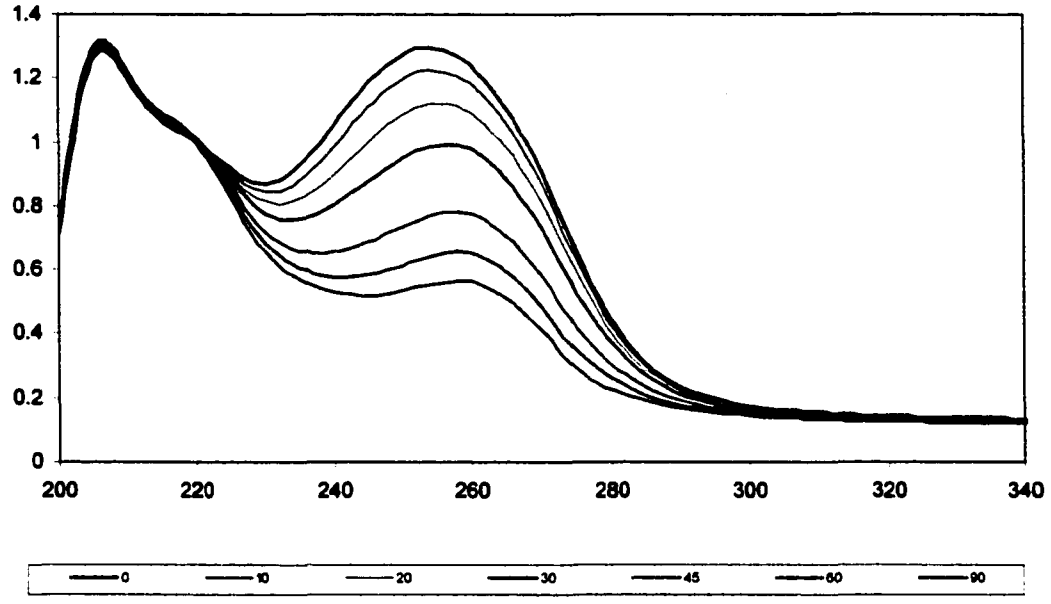

Figure 5.5. UV absorption spectra of DSPC/BisSorbPC$_{17,17}$/PEG-DSPE/Cholesterol (30/30/5/35). Performed with a lipid concentration of 150 mM and at room temperature. Irradiation times (s) are given at the legend (bottom).

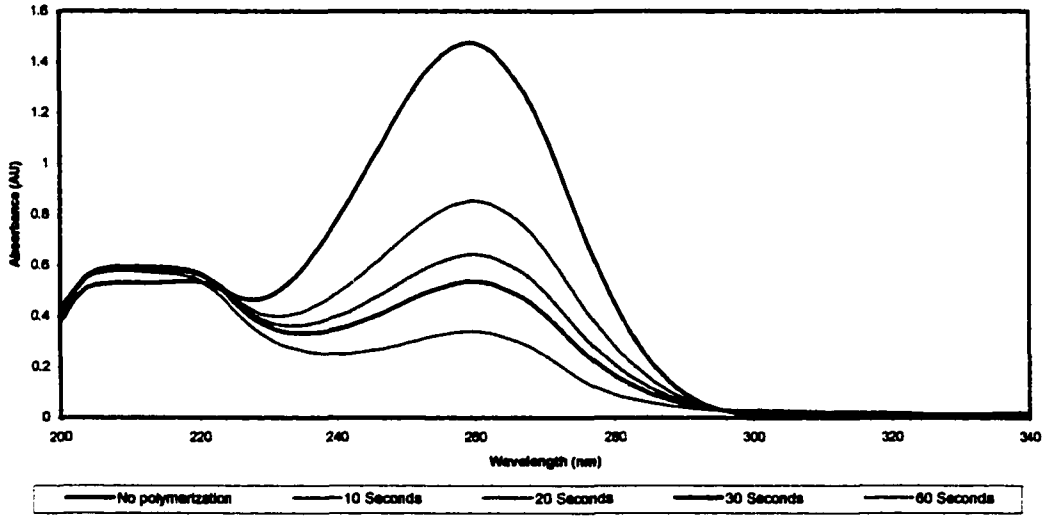

Figure 5.6. Sorbyl UV absorption before and after UV irradiation for different time periods. Irradiation of the PEG-DSPE/bis-SorbPC$_{19,19}$/DAPC (5/20/75) liposomes in MilliQ water at room temperature. The flat peak between 200 – 220 nm is due to absorbance of the fluorescent dye and quencher (ANTS/DPX) encapsulated within the liposomes for leakage assays.

An absorbance remains after 100 % polymerization because of the ANTS and DPX absorbance maxima at 258 and 260 nm respectively. A mixture of 5 parts ANTS to 18 parts DPX (the ratio used in the leakage experiments) has an effective 'molar' (in ANTS) extinction coefficient of 51,000 at 260 nm [103]. This calculation only takes into account the concentration of ANTS, but DPX also has an absorbance at 260 nm. The mixture of ANTS and DPX in PBS, without lipid showed little photobleaching with 11 minutes of UV exposure. For this reason, the absorbance at 260 nm after long exposure times was used as the 100 % loss of monomer point.

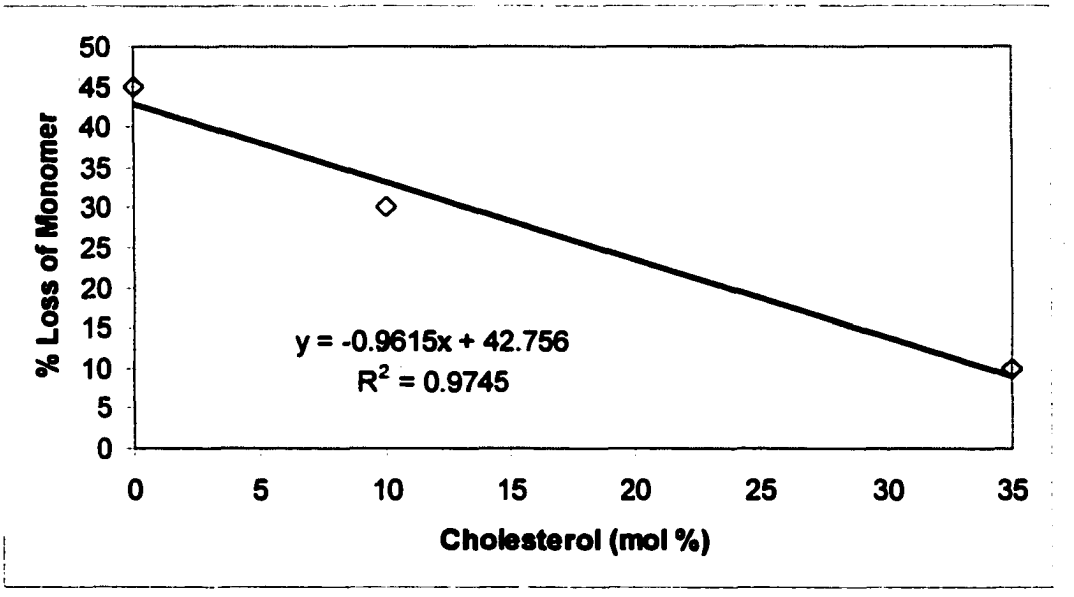

Figure 5.9. Plot of the loss of monomer vs. amount of cholesterol in liposomal formulations after 10 seconds of UV irradiation.

The major difference among the three spectra (Fig. 5.5-5.7) is the rate of polymerization. There appears to be a direct correlation between the amount of cholesterol and the initial rate of polymerization. The amount of polymerization was 10, 30, and 45 percent for the formulations containing 35, 10, and 0 percent cholesterol respectively (Fig. 5.9). This response is likely due to the formation of domains of pure lipid in low cholesterol formulations. Domain formation should allow for a packing of the lipid tails in an assembly where the sorbyl moieties are very closely associated. Because the rate of propagation is dependent upon the concentration of the monomer and in a pure sorb domain where the concentration is maximized, the initial rate of polymerization is expected to be the fastest. When cholesterol is added to the formulation, mixing of the lipids occurs and the monomer is effectively diluted. Fiegenson *et al* were able to show that as cholesterol concentrations increased, domain size decreased until they could no longer be observed with confocal microscopy (Fig. 5.11) [14]. This can clearly be seen in the fifth column where the DLPC/DPPC ratio is maintained at 1:4 and the cholesterol concentration is increased.

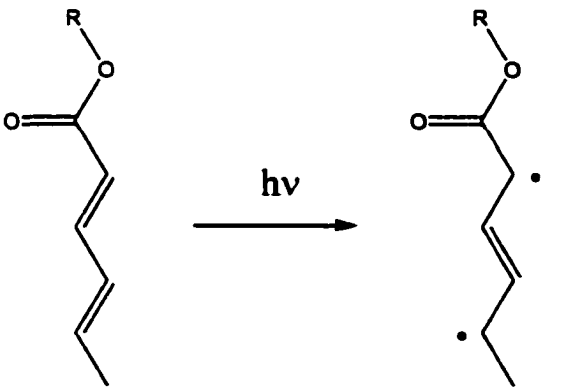

Figure 5.10. UV initiation of the sorbyl moiety.

It should be noted the initiation of the sorbyl moiety is through a direct absorbance of a photon and excitation of an electron to the excited state (Fig. 5.10). Polymerization methodologies that incorporate fewer initiation events would be expected to show an even larger rate disparity in formulations where the concentration of cholesterol is varied. As the size of the domains decrease, and subsequently the number of domains increase, there would need to be more initiation events to obtain a percent conversion equal to systems where the domains are large and the number of domains is decreased. This assumes that the polymer chain lengths are significantly increased in large domains as compared to the smaller domains because of the larger number of monomers present and the low number of initiators [120].

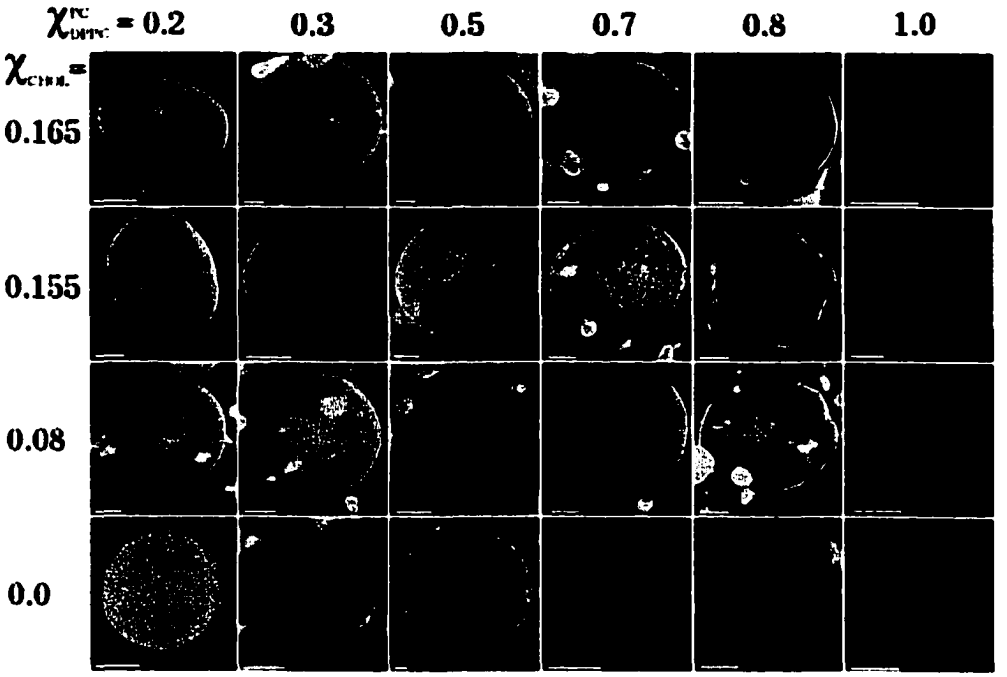

Figure 5.11. Composition dependence of phase behavior in giant unilamellar liposomes of DPPC/DLPC/cholesterol is visualized using confocal fluorescence microscopy. Each image is color-merged from the simultaneously collected fluorescence emission from DiI-C20:0 (orange) and Bodipy-PC (green), with both dyes at mole fraction 0.001 [14].

5.3.4 UV Initiated Destabilization

The use of saturated PEG-DSPE and DSPC in liposome formulations containing cholesterol has a dramatic effect on the photodestabilization of the liposomes. The photolysis of liposomes composed of PEG-DSPE/bis-SorbPC$_{17,17}$/cholesterol/DSPC (15/30/40/15) to 88% loss of monomer at 25°C produces an increase of > 100-fold in the initial rate of leakage (Fig. 5.12). This is approximately ten times the increase in the rate of leakage that was observed with the analogous PEG-DOPE/bis-SorbPC$_{17,17}$/cholesterol/DOPC liposomes at 37°C [51]. The greater increase in the relative rate of leakage can be attributed to both a lower rate of dark leakage and an earlier onset of photoinduced leakage. The initial rate of leakage at 30 sec irradiation in DSPE/bis-SorbPC$_{17,17}$/DSPC liposomes is about three to ten times higher than that which was observed in PEG-DOPE/bis-SorbPC$_{17,17}$/cholesterol/DOPC liposomes, but the rate of dark leakage for DSPE/bis-SorbPC$_{17,17}$/cholesterol/DSPC liposomes is about four to ten times lower than that of PEG-DOPE/bis-SorbPC$_{17,17}$/cholesterol/DOPC. Variations in the PEG and cholesterol mole fractions of DSPE/bis-SorbPC$_{17,17}$/cholesterol/DSPC liposomes had a significant effect on the rate of release upon photolysis. Liposomes with a composition of PEG-DSPE/bis-SorbPC$_{17,17}$/cholesterol/DSPC (5/30/35/30) show as much as a 100 fold increase in the initial rate of leakage, as compared to the dark leakage, with only 5 sec of photolysis.

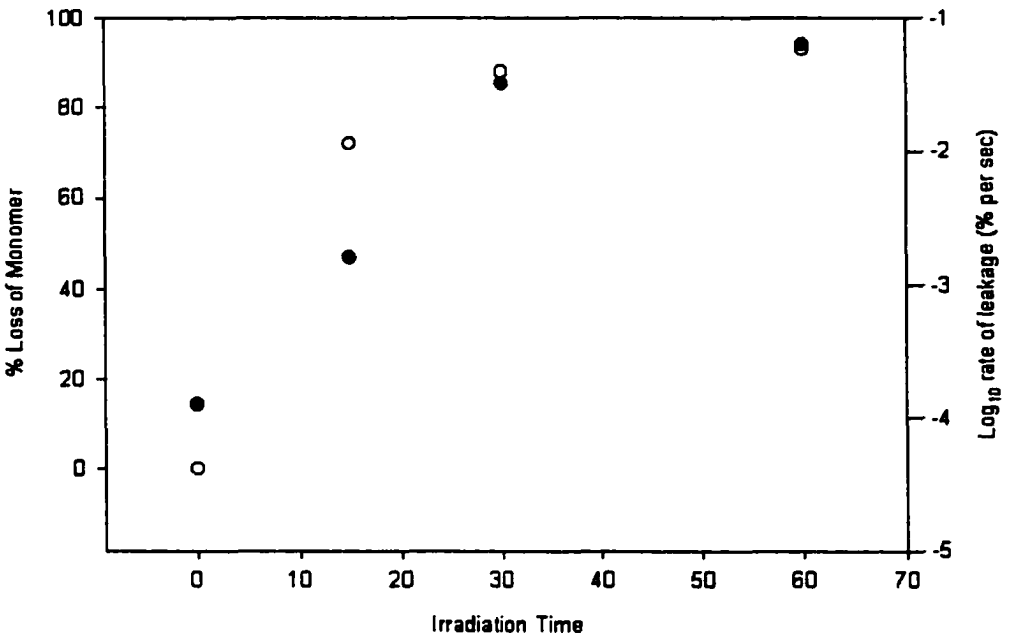

Figure 5.12. PEG-DSPE/bis-SorbPC$_{17,17}$/cholesterol/DSPC (15/30/40/15); Log_{10} of the initial rate of leakage vs. irradiation time (filled circles); Percent loss of monomer vs. irradiation time (open symbols) [103].

Liposome formulations prepared without cholesterol showed an even larger enhancement for the rate of release upon photolysis. Table 5.7 and Figure 5.13 compare the values obtained for the photoinduced leakage of four compositions. The values shown are at 25°C because of the high permeability of liposomes containing lipids with T_m values below 37°C. The minimum increase in the rate of release was 290 fold and the highest was 28,000 fold. Liposomes composed of PEG-DSPE/DAPC/bis-SorbPC$_{19,19}$ had a very low dark leakage at 37°C (3×10^{-5} % s^{-1}) and a photoinduced rate (8.5×10^{-1} % s^{-1}), which was also an increase of 28,000. The photoinduced rate corresponds to 1.9×10^{-8} moles s^{-1}.

Irradiation time (sec)	PEG-IPA/DPPC bis-Sorb$_{17,17}$ (5/75/20)	PEG-IPA/DSPC bis-Sorb$_{17,17}$ (5/75/20)	PEG-DSPE/DSPC bis-Sorb$_{17,17}$ (5/75/20)	PEG-DSPE/DAPC bis-Sorb$_{19,19}$ (5/75/20)
0	0.00004	0.00009	0.0002	0.00002
10	1.1111	0.0258	0.1101	0.1021
X increase	28,000	290	550	5100

Table 5.7. Comparison of the rates of release (% s^{-1}) before and after irradiation at room temperature. Irradiation times were for 10 seconds using the light from a low pressure Hg pen lamp. [Rate of release for the liposomal formulation PEG-DSPE/DAPC/bis-SorbPC$_{19,19}$ (5/75/20) in moles s^{-1} is 1.9×10^{-8}]

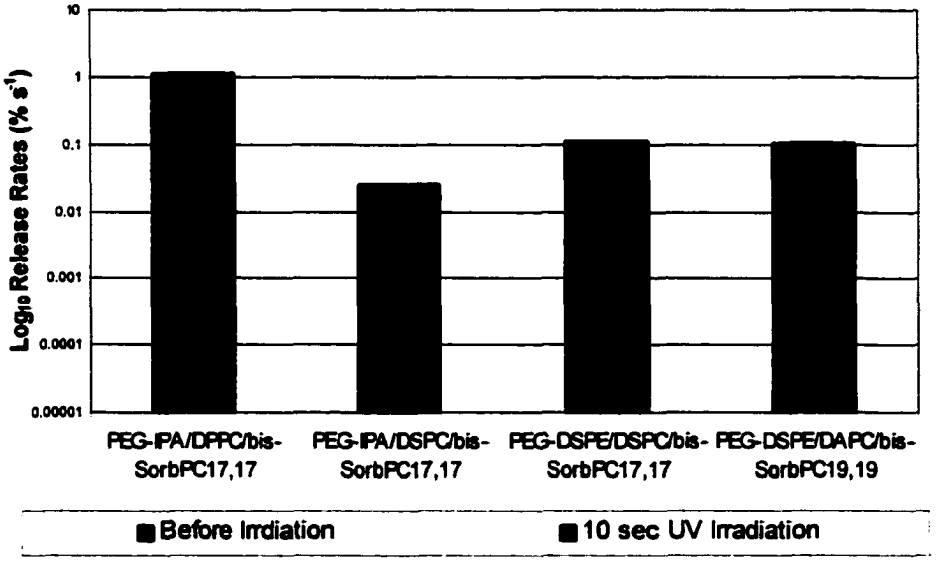

Figure 5.13. Bar Graph representation of Table 5.7.

5.3.5 Conclusion

Liposomes containing a saturated lipid (DAPC), photosensitive lipid (bis-SorbPC$_{19,19}$), and a PEG lipid (PEG-DSPE) have been shown to be thermally stable at temperatures above body temperature (37°C) and have been shown to be responsive to UV irradiation. Phase separation of the lipids based on T_m values may have provided the enhancement to the photoreactivity and increased release of the liposomal contents (greater then 28,000 fold compared to unirradiated liposomes). The large increase in the rate of release was observed with only 10 sec of UV irradiation at 254 nm with a Hg pen lamp. Total release of the liposomal contents was observed within two minutes. This compares very favorably to the commercially available liposomal drug delivery formulations that rely on passive release over days and weeks. Unfortunately UV irradiation is not a biocompatible form of polymerization and in order to perform such experiments in vivo it will be necessary to utilize PEG-liposomes that are sensitive to other forms of polymerization, such as irradiation with visible light or γ-rays.

6 GAMMA IRRADIATION INITIATED DESTABILIZATION OF LIPOSOMES

6.1 Introduction

The need for more effective approaches to the controlled delivery of therapeutic agents continues to be of utmost importance. Passive or active targeting of anticancer agents to tumors is a traditional approach to minimizing side effects. An alternative strategy relies on the activation or release of therapeutic agents only in the vicinity of the diseased tissue. The O'Brien group has previously proposed that the attractive features of photodynamic therapy, i.e. spatial and temporal selectivity, could be significantly broadened if radiant energy were used to release drugs [50, 51, 92-96, 104, 106]. Indeed the selective photolysis of appropriately designed liposomes can trigger the release of their contents. These previous studies now permit the design of sterically stabilized liposomes (PEG-LUV) that are sensitive to ionizing radiation. The selective destabilization of PEG-LUV and release of therapeutic agents upon exposure to clinical doses of radiation holds new promise for controlled drug delivery.

Polymerization in organized assemblies can be initiated by gamma irradiation [107-109]. Unlike photodynamic therapies, ionizing radiation is readily available in most medical centers since it is a principle component of many cancer treatments. The total dose of irradiation can be controlled by regulating the distance from the source and the duration of irradiation. Therapeutic gamma irradiation treatments are generally fractionated over time. In a typical radiation treatment regimen, patients receive a total dose of 200 Rad per day five or six times a week. Typical treatments last 5-7 weeks and the cumulative total dose is 5 – 8.4 Krad [104]. The premise of

fractionating the total dose is that cells with a large proliferative capacity, e.g. tumor cells, generally have a high intrinsic radiative sensitivity [107]. Fractionating the dose reduces damage to the surrounding normal tissue since it probably has a lower radiation sensitivity. Gamma initiation may be especially important in drug delivery systems that require polymerization *in vivo*. UV and visible light do not penetrate deeply beyond the epidermal layer of the body. Red light of 632 nm penetrates the tissue to a maximum of 1 cm. Fiber optic cables must be surgically implanted into the body to deliver light to most targeted areas. The enhanced depth of penetration that gamma rays exhibit is one advantage over UV and visible light initiation. The actual initiating species in gamma polymerizations of hydrated amphiphiles is a hydroxy radical [108, 109]. The mechanism which the production of hydroxyl radicals is shown in Figure 6.1.

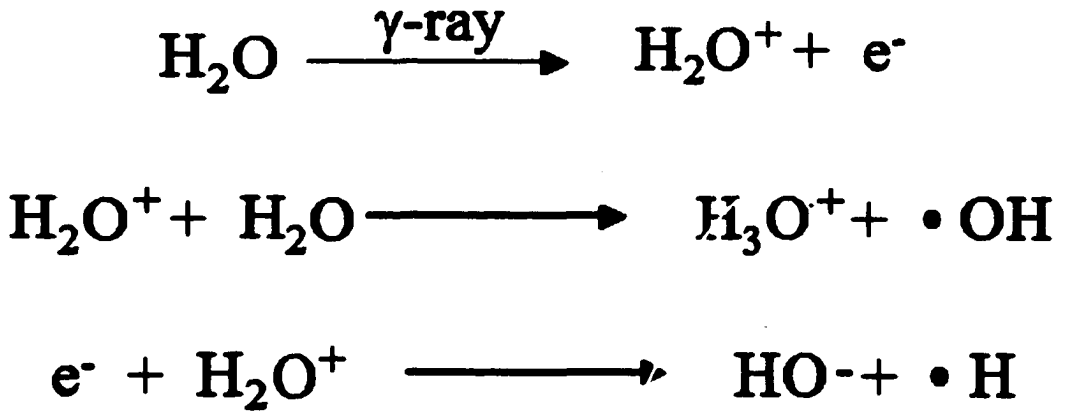

Figure 6.1. Proposed pathway for generation of hydroxyl radicals by gamma irradiation of water.

Organized assemblies such as micelles, multilayers, and vesicle bilayers have each been polymerized through gamma irradiation [108, 121]. These assemblies are

composed of allyl, acrylate, diacetylene, diene, triene, and dienoate functional groups. Paleos *et al* utilized γ-irradiation to polymerize allyl functionalized single and double chained quaternary ammonium amphiphiles as micelles and vesicles respectively. The polymerizable group was attached to the lipid head group in the hydrophilic region. A total dose of 7 MRad was needed for complete polymerization [122]. The polymerization of an allyl functionality located at the acyl chain terminus of a double-chain amphiphile with two acyl chains was investigated [123]. This requires diffusion of the initiating radical into the hydrophobic region of the bilayer and indicated a 50 % loss of monomer after exposed to 1.66 MRad. After exposure to 6 MRad the polymer was no longer soluble in ethanol, indicating a highly crosslinked polymer. This study indicated that polymerizable groups in the hydrophilic and hydrophobic regions of organized assemblies are accessible to radicals generated by gamma irradiation.

A more detailed investigation of gamma irradiation polymerization for mono and bis substituted dienoyl phosphocholine lipids reveals information on termination and molecular weights. The polymerization yield reaches a maximum of 80 % conversion for 1,2-Dihexadeca-2E,4E-dienoyl-*sn*-phosphatidylcholine (bis-DenPC) [124]. The total dose was 0.73 MRad. The polymerization was carried out on large unilamellar vesicles at 4 °C, which is below the T_m. The polymerization rate was proportional to the 1.2^{th} power of the monomer concentration. This indicates that the polymerization was initiated by hydroxy radicals and not direct excitation of the monomeric lipids.

Multiplying the rate of polymerization in percent per Rad (1.1×10^{-4} % Rad^{-1}) times the average daily dosage received in therapeutic treatments (200 Rad), gives a total polymerization of only 0.02 %. This value is extremely low and would not be expected to induce destabilization of the liposomal bilayer. Significant advances and formulations have been able to increase the radiation sensitivity of the liposomes and are discussed in this chapter.

6.2 Materials and Methods

6.2.1 Materials

The collisional quencher, α,α'-bis-pyridinium-1,4-xylene dibromide (DPX) (Fig. 5.1) was prepared as described in section 5.2.1. ANTS was purchased from Molecular Probes Inc. (Eugene, Oregon) and used without further purification. Bis-SorbPC$_{17,17}$ and bis-SorbPC$_{19,19}$ were prepared as described in chapter 2. 1,2-Dipalmitoyl-*sn*-phosphatidylcholine (DPPC), 1,2-Dioleoyl-*sn*-phosphatidylcholine (DOPC), 1,2-distearoyl-*sn*-phosphatidylcholine (DSPC), 1,2-diarachidoyl-*sn*-phosphatidyl-choline (DAPC), PEG$_{2000}$-1,2-dioleoyl-*sn*-phosphatidylethanolamine (PEG-DOPE), and PEG$_{2000}$-1,2-distearoyl-*sn*-phosphatidylethanolamine (PEG-DSPE) were obtained from Avanti Polar Lipids. Cholesterol was purchased from Sigma and used without further purification. Octylphenoxy polyethoxyethanol (Triton X-100) (Sigma) was used in a 5% (wt/wt) solution with Millipore water.

6.2.2 Liposome Formation

Lipids were measured volumetrically into separate weighed 10 mL round bottom flasks from stock solutions of known concentrations. An argon stream was passed over each solution to remove the solvent and the flasks were then placed under high vacuum for a minimum of four hours to complete the drying. The flasks were weighed to obtain the amount of lipid in each flask. Approximately 2 mL of chloroform were then added to all but one of the flasks and the contents were combined and dried as above. A final weight was taken to ensure the complete transfer of lipids. The lipids were then suspended in a sufficient amount of dye containing pH 7 phosphate buffer to make a 10 mM total lipid concentration. The buffer used for the hydration of the lipids contained ANTS (25 mM), DPX (90 mM) and sodium phosphate (10 mM). The osmolarity of the buffer solution was found to be 277 mosmol. The lipid suspension was then subjected to ten freeze thaw cycles and then extruded three times through two stacked 600 nm Nuclepore membranes followed by extrusion three times through two stacked 200 nm Nuclepore membranes and finally extrusion four times through two stacked 100 nm Nuclepore membranes. The resulting ANTS/DPX containing liposomes were eluted through a Sephadex G-75 column with pH 7 buffer solution containing sodium phosphate (10 mM), sodium chloride (139 mM), and having an osmolarity of 277 mosmol. The concentration of the resulting liposome suspensions were determined by UV absorbance at 260 nm (sorbyl $\lambda_{max} = 258_{MeOH}$, $\varepsilon = 47{,}100$) of a 30 µl aliquot in 0.97 mL of HPLC grade methanol. The total lipid concentrations of resulting liposomes were between 1 and 3 mM.

was continued for an additional 45 s. The emission intensity of the sample after addition of Triton X-100 was multiplied by 1.1 to adjust for the dilution by the detergent solution and the difference between this and the initial measurement was compared to the emission intensity of standard solutions of ANTS/DPX (5:18 ratio).

6.2.5 Determination of Liposome Leakage

In order to determine the percent leakage of liposome encapsulated ANTS/DPX, the fluorescence of each sample was measured over 30 s prior to photolysis. Immediately after photolysis, the percent conversion was determined from the sample absorbance with a diode array spectrophotometer, and the fluorescence was measured continuously over several minutes. After the leakage measurement, a 90 s time scan was performed during which a 5% solution of Triton X-100 was added at 45 s. The fluorescence due to 100% leakage was determined from this measurement after correcting for the bleaching of ANTS during photolysis and the dilution factor due to the Triton X-100 solution.

The fluorescent marker, ANTS, has a minor absorption at 258 nm at the sample concentration. For this reason, irradiation of the liposome solution at 230-300 nm causes some bleaching of the ANTS. The percent ANTS bleaching was determined by comparing the fluorescence measurement after the addition of Triton X-100 for a photolyzed sample to a similar measurement performed on a sample of non-photolyzed liposomes after dividing each by the UV absorbance at 254 nm to factor out any differences in sample preparation,

$$b = I_{photolyzed}/I_{non\text{-}photolyzed} \times A_{non\text{-}photolyzed}/A_{photolyzed}$$

A bleaching factor of between 0.8 and 1.0, depending on the length of photolysis, was obtained, which adjusts the baseline (I_0) to what it would be if the amount of ANTS present before photolysis were equal to that present after photolysis.

The percent leakage at any time is given by the following expression:

$$\% \text{ leakage} = 100 \text{ X } (I_t - bI_0)/(1.1I_{100} - bI_0)$$

where I_t is the fluorescence intensity at time (t), I_0 is the fluorescence intensity prior to photolysis, I_{100} is the fluorescence intensity after addition of Triton X-100, and b is the bleaching factor. Because the initial change in concentration inside the liposomes is relatively small, the initial leakage is pseudo-zero order, and the plot is a straight line. The rate of leakage was calculated from the linear region of the plot using a least squares fit.

6.2.6 Ionizing Radiation Polymerization

Ionizing radiation experiments were performed with a ^{60}Co source. Lipid samples were placed 43 cm from the source. The intensity of ionizing radiation was calculated using the equation:

$$\text{Dose} = (DR_c)(PSF)(FDD)(S)[(80+d)/(SSD+d)]^2(0.99)(t-\Delta t)$$

The term DR_c is the calibrated dose rate for the day of the source, PSF is the peak scatter factor, FDD the functional depth dose, s the jaws scatter factor, d the depth of the build up layer, SSD source to sample distance, and t is the time of exposure. In all experiments only the DR_c and time of exposure were varied. The DR_c was calculated using the half-life of ^{60}Co and time since the source was changed.

Monomer conversion was calculated as

$$\% \text{ conversion} = (A_0^{254} - A_R^{254}) / (A_0^{254} - A_4^{254}) \times 100\ \%$$

where A_0 is the absorbance of the non-irradiated sample, A_R is the absorbance of the sample after exposure (Rads) or irradiation, and A_4 is the absorbance of the standard sample after 4 min of UV irradiation exposure with a Hg pen lamp.

6.3 Results

6.3.1 Rates of Polymerization

6.3.1.1 Formulations Excluding Cholesterol

In the ideal situation, γ-irradiated polymerization would correspond directly to the results from section 5.3. Liposomal formulations with 20 mol % of the polymerizable lipid, 5 mol % of the pegylated lipid, and 75 mol % of the saturated lipid would show a rapid rate of polymerization and a rapid rate of release with short exposure times. Unfortunately, and maddeningly so, this is not the case and numerous formulations were tested to determine the optimal lipid ratios. High temperature formulations that excluded cholesterol indicated little or no polymerization upon γ-irradiation.

A considerable amount of this dissertation has been focused on the excellent results obtained with thermally stable formulations because of their low permeability to encapsulated compounds. The same characteristics that contribute to their low permeability may in fact prove to be their downfall when considering ionizing radiation. As described in section 6.1, the mechanism of polymerization initiation with ionizing radiation consists of a hydroxyl radical diffusing into the lipid bilayer. The hydroxyl radical would then initiate the polymerization with the sorbyl moiety as

shown in Figure 6.2. In liposomal formulations with high T_m values, the hydroxyl radicals may be unable to penetrate efficiently to the sorbyl moiety Figure 6.3.

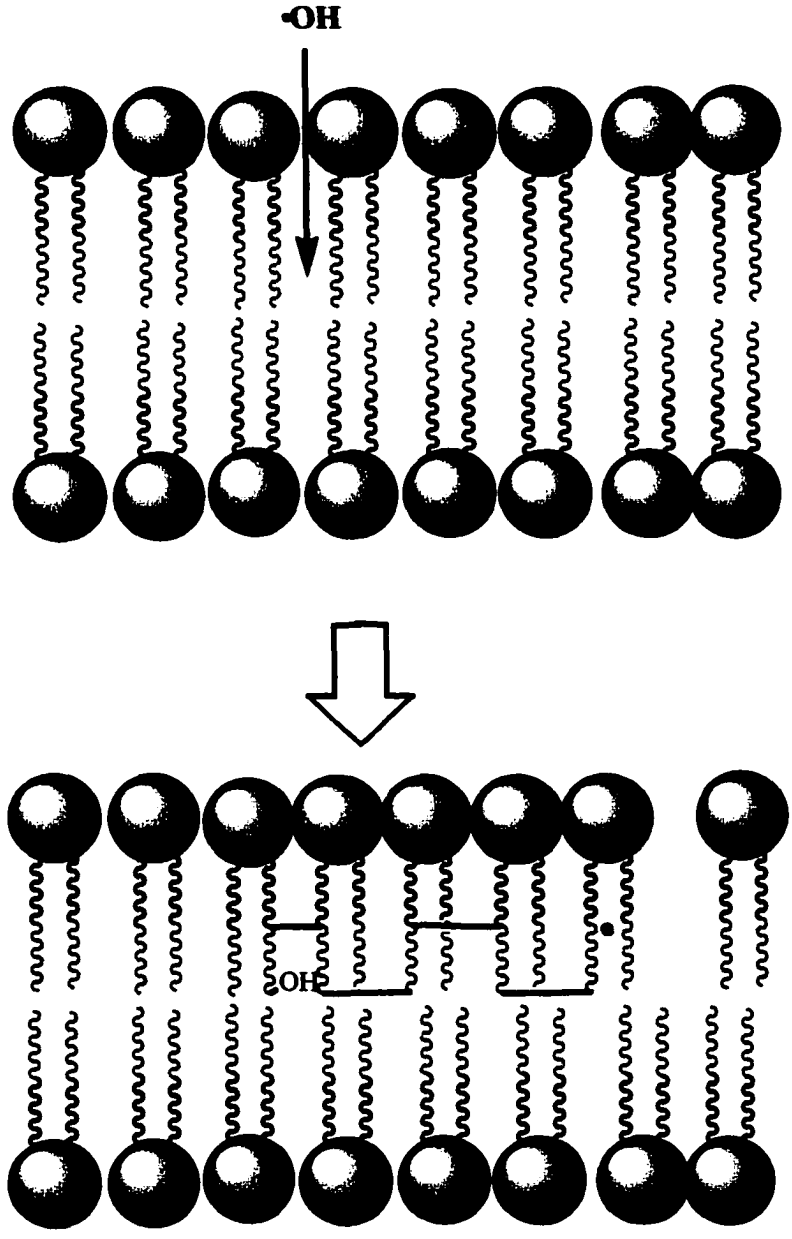

Figure 6.2. Illustration of the initiation in liposomal bilayer polymerizations of ionizing radiation experiments.

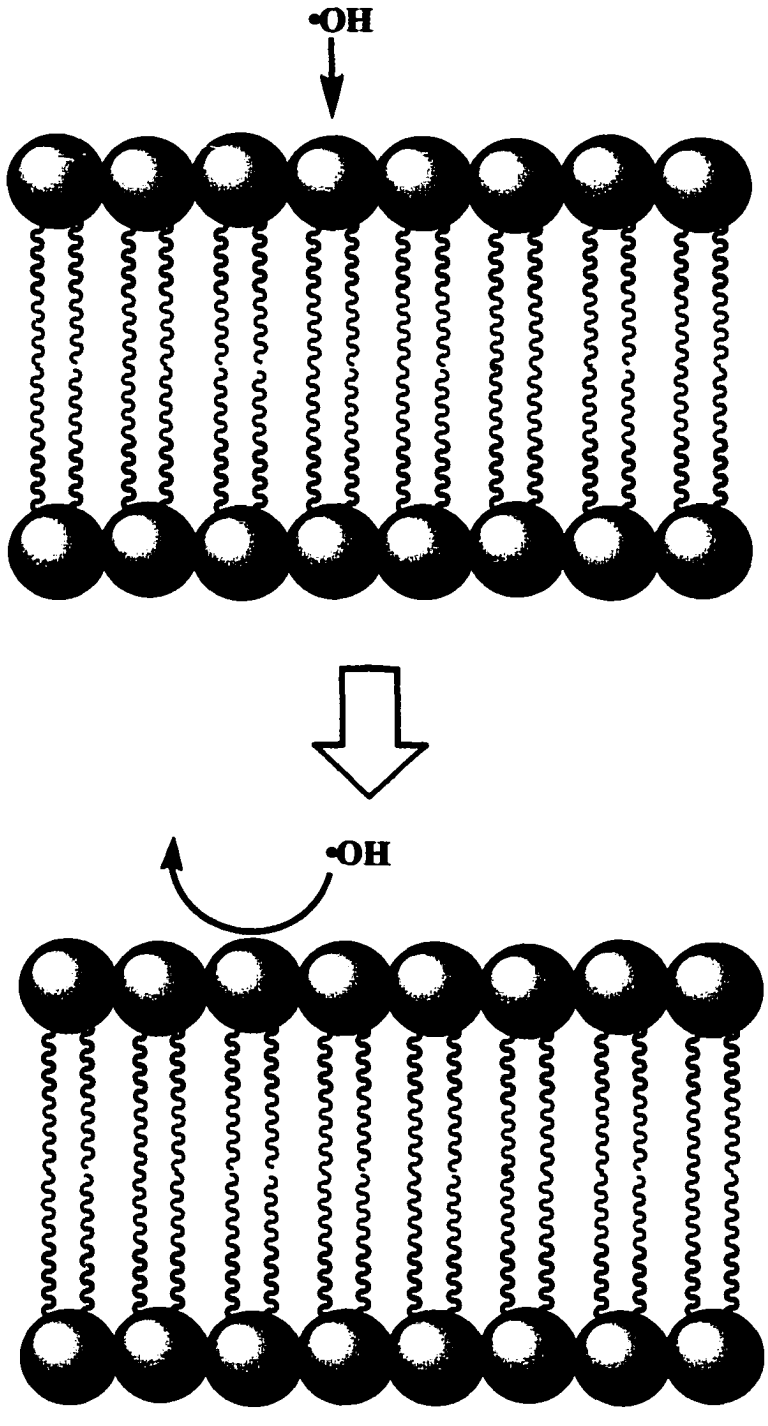

Figure 6.3. Illustration of the high packing efficiency of lipids in the solid phase and the inability of hydroxyl radicals to initiate polymerization in ionizing irradiation experiments.

Tsuchida *et al* provided this possibility when investigating the bis-Den lipids discussed in section 6.1. Polymerizations with γ-irradiation of the lipids in the solid phase indicated a decrease in the rate of polymerization by almost 100 fold [124]. Table 6.1 shows the results for rate of polymerization experiments with high temperature formulations, without cholesterol, which are in the solid phase at room temperature.

T_m	Formulation	Amount of Polymerization (% @ 1000 Rads)
Low	PEG-DSPE/bis-SorbPC$_{17,17}$/DPPC (5/20/75)	4
Low	PEG-DSPE/bis-SorbPC$_{17,17}$/DSPC (5/20/75)	3
Low	PEG-DSPE/bis-SorbPC$_{17,17}$/DAPC (5/20/75)	3
High	PEG-DSPE/bis-SorbPC$_{19,19}$/DSPC (5/20/75)	3
High	PEG-DSPE/bis-SorbPC$_{19,19}$/DAPC (5/20/75)	4

Table 6.1. Rates of polymerization for high temperature formulations under ionizing radiation. All samples were maintained at 150 μM lipid concentrations and in PBS buffer.

Under these conditions, only about 1 % of the sorbyl moieties would be polymerized upon a therapeutic dosage. Therapeutic dosages were insufficient to induce release of the encapsulated dyes, and only at high dosages (> 5,000 Rads), was the release of the encapsulated dye observed. Dr. Anja Mueller, O'Brien group post-doctoral researcher, reported much higher rates of polymerization (≈ 20 % @ 1000 Rads) in formulations that included cholesterol (30 mol %). Unfortunately, each of her formulations exhibited high rates of dark leakage.

6.3.1.2 Formulations Incorporating Cholesterol

Several formulations with varying concentrations (5 to 20 mol %) of cholesterol were investigated for their encapsulation efficiency and their response to ionizing radiation. Consideration of the encapsulation efficiency must be factored in when considering the use of formulations with cholesterol as discussed in section 5.3.1. Table 6.2 shows the comparison of the encapsulation efficiency when the molar amount of cholesterol is varied. The table shows that the encapsulation efficiency is reduced upon the addition of cholesterol as reported in section 5.3.1. A plot of the data (Fig. 6.4) indicates a loss of encapsulation efficiency that is linear with respect to the increase in the molar concentration of cholesterol. The value appears to be a loss of about 1 % in the encapsulation efficiency with a 1 % increase in the amount of cholesterol. This can provide a useful tool in development of formulations and predicting their characteristics.

The rates of polymerization were increased in the formulations containing cholesterol as seen in Table 6.3 (Sample experiment shown in Figure 6.5). The rates

increased from 0.004 to 0.012 % Rad^{-1} when increasing the mol % of cholesterol from 0 to 20. While the rate of polymerization was increased, the rate of leakage was significantly decreased at high concentrations of cholesterol and was effectively stopped at 20 mol % of cholesterol. The rate of polymerization was increased 3 fold in the formulation with 20 mol % cholesterol as compared to the formulation excluding cholesterol. The rates of polymerization for the samples containing 10, 15, and 20 mol % of cholesterol indicated only a slight increase in the rate of polymerization. This suggests that there may be a maximum rate of polymerization with the addition of cholesterol. That is, once the lipid membrane has become fluid enough to allow for diffusion of the hydroxyl radicals to the sorbyl moieties, a further increase in cholesterol will have only a very small effect.

The possible explanation for the increase in the rate of polymerization is illustrated in Figure 6.6. As described in chapter 1, addition of cholesterol to solid phase lipids formulations destabilizes the membranes. The membranes become more permeable to the diffusion of encapsulated compounds as shown in Table 6.2. The destabilization of the membrane appears to allow for the diffusion of hydroxyl radicals into the lipid membrane more freely. The polymerization rates observed in Table 6.3 also suggest this as a possibility. As expected though, there appears to be a give and take balance with the increase in the rate of polymerization and the increase in the rate of dark leakage with an increase in the mole percent of cholesterol.

Cholesterol	Background Fluorescence	Encapsulation (μM / mM)	% of calculated for POPC (100 nm)
0	10,500	53	70
5	12,000	50	66
10	10,000	47	62
15	14,000	41	54
20	11,500	40	52

Table 6.2. Encapsulation of ANTS in solid phase liposomes containing differing concentrations of cholesterol. Other membrane components are held constant at the following: PEG-DSPE (5 mol %), bis-SorbPC$_{19,19}$ (20 mol %). DAPC varies to make the sum 100 %. Column four represents the encapsulation efficiency compared to POPC conventional liposomes investigated by Pfeiffer *et al* in Table 5.1.

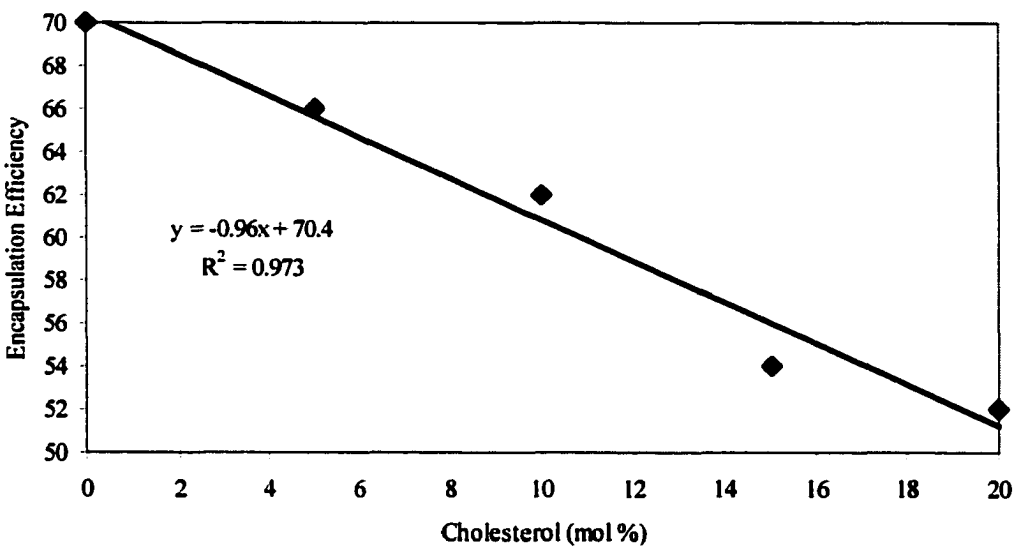

Figure 6.4. Plot of the data presented in table 6.2 with a corresponding trend line. The slope of the line suggests a -1:1 ratio with the respect to the encapsulation efficiency as compared to the molar concentration of cholesterol.

Formulation	Amount of Polymerization (% @ 1000 Rads)
PEG-DSPE/bis-SorbPC$_{19,19}$/DAPC (5/20/75)	4
PEG-DSPE/bis-SorbPC$_{19,19}$/cholesterol/DAPC (5/20/5/70)	5
PEG-DSPE/bis-SorbPC$_{19,19}$/cholesterol/DAPC (5/20/10/65)	10
PEG-DSPE/bis-SorbPC$_{19,19}$/cholesterol/DAPC (5/20/15/60)	11
PEG-DSPE/bis-SorbPC$_{19,19}$/cholesterol/DAPC (5/20/20/55)	12

Table 6.3. Rate of polymerization in % Rad^{-1} in formulations with varying cholesterol concentrations containing PEG-DSPE (5 mol %), bis-SorbPC$_{19,19}$ (20 mol %), and DAPC making up the remaining mol %.

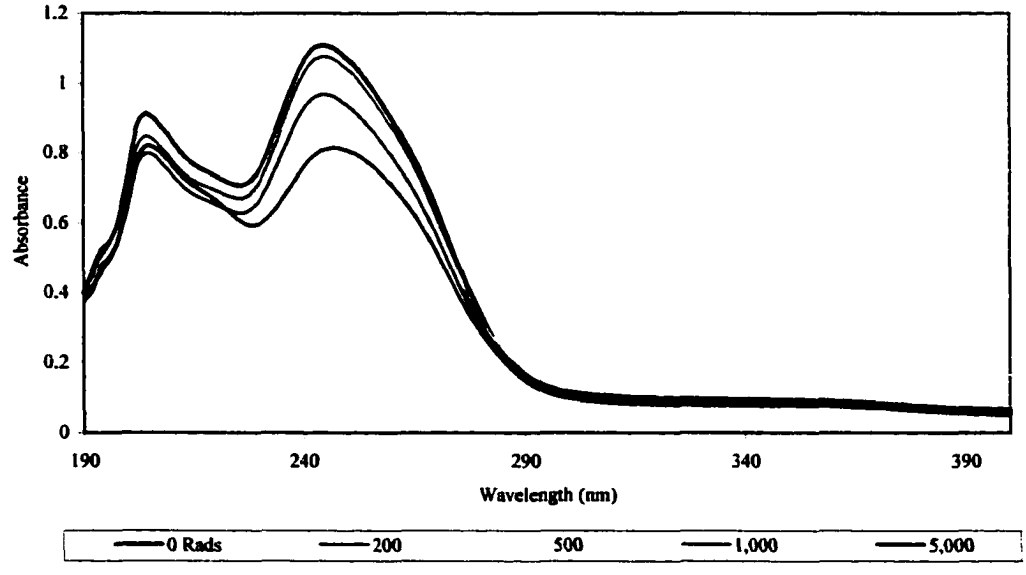

Figure 6.5. UV spectra of the formulation PEG-DSPE/bis-SorbPC$_{19,19}$/cholesterol/ DAPC (5/20/10/65) at varying amounts of exposure to ionizing radiation.

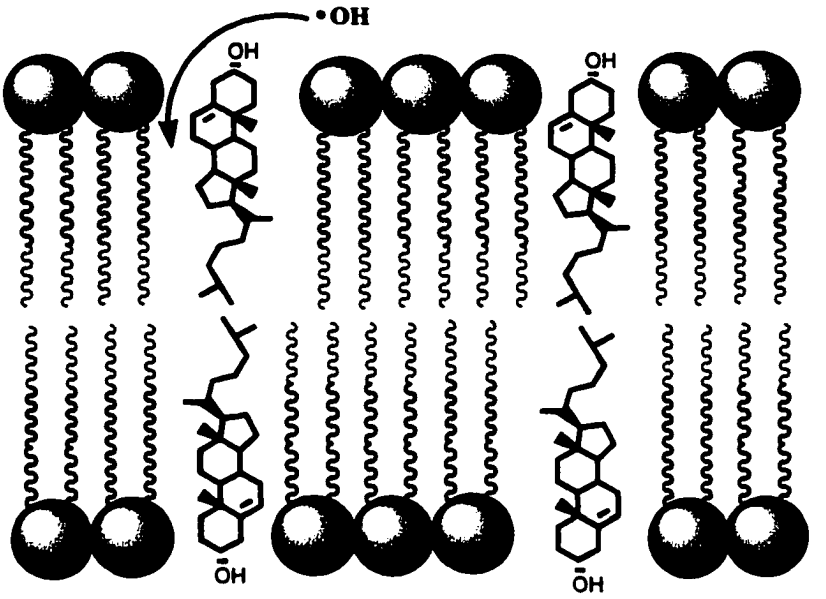

Figure 6.6. The effect of adding cholesterol to the high temperature formulations. Cholesterol disrupts the lipid packing, thus allowing for hydroxyl radical diffusion into the bilayer to initiate polymerization.

6.3.2 Rates of Ionizing Radiation Induced Release

The induced rate of release in UV irradiated samples was greater then 1 % s^{-1} for the formulation: PEG-DSPE/bis-SorbPC$_{19,19}$/DAPC (5/20/75) at 37 °C (section 5.3.4). The amount of release upon exposure to 1,000 Rads of ionizing radiation (5 X the therapeutic dose) is significantly lower in all the experiments to date (Table 6.4). Because of the limited initiation events and subsequent low amount of polymerization, the bilayer membranes are not disrupted at therapeutic dosages and no release of the encapsulated dye was observed in the formulations tested. The values given in table 6.5 and throughout this section are percents of the encapsulated dye released, because of a liposomal release characteristic not observed in UV

polymerization. The liposomes appear to leak only during the ionizing radiation exposure, and release of the encapsulated dye is halted upon removal from the ^{60}Co source. When samples are exposed to 25 times the therapeutic dose (5,000 Rads), the leakage is increased, but it is still well below the amounts observed with only 10 seconds of UV exposure.

Formulation	Percent of Dye Released (1000 Rads)
PEG-DSPE/bis-SorbPC$_{19,19}$/DAPC (5/20/75)	3
PEG-DSPE/bis-SorbPC$_{19,19}$/cholesterol/DAPC (5/20/5/70)	7
PEG-DSPE/bis-SorbPC$_{19,19}$/cholesterol/DAPC (5/20/10/65)	12
PEG-DSPE/bis-SorbPC$_{19,19}$/cholesterol/DAPC (5/20/15/60)	8
PEG-DSPE/bis-SorbPC$_{19,19}$/cholesterol/DAPC (5/20/20/55)	6

Table 6.4. Indicates the amount of dye released upon exposure to 1,000 Rads of ionizing radiation.

Figure 6.7 shows the fluorescence of samples after exposure to ionizing radiation. There is no increase in fluorescence over a 10 minute time period for each of the samples, although each sample shows enhanced fluorescence relative to the unirradiated sample. This suggests two possibilities: (A) Transient Fissures. Once the samples are removed from the ^{60}Co source, and the samples are transported to the fluorometer for measurement, the membrane lipids have had enough time to diffuse and fill any voids where leakage took place, or (B) Permanent Fissures. The fissures

form within the polymerizable domain, and because of the lack of motion of the cross-linked polymer and the absence of saturated lipids in these domains, the fissures are never sealed. The release of the liposomal contents occurs rapidly, and a percentage of the liposomes did not undergo sufficient polymerization to induce release of the liposomal contents. These are illustrated in Figure 6.8.

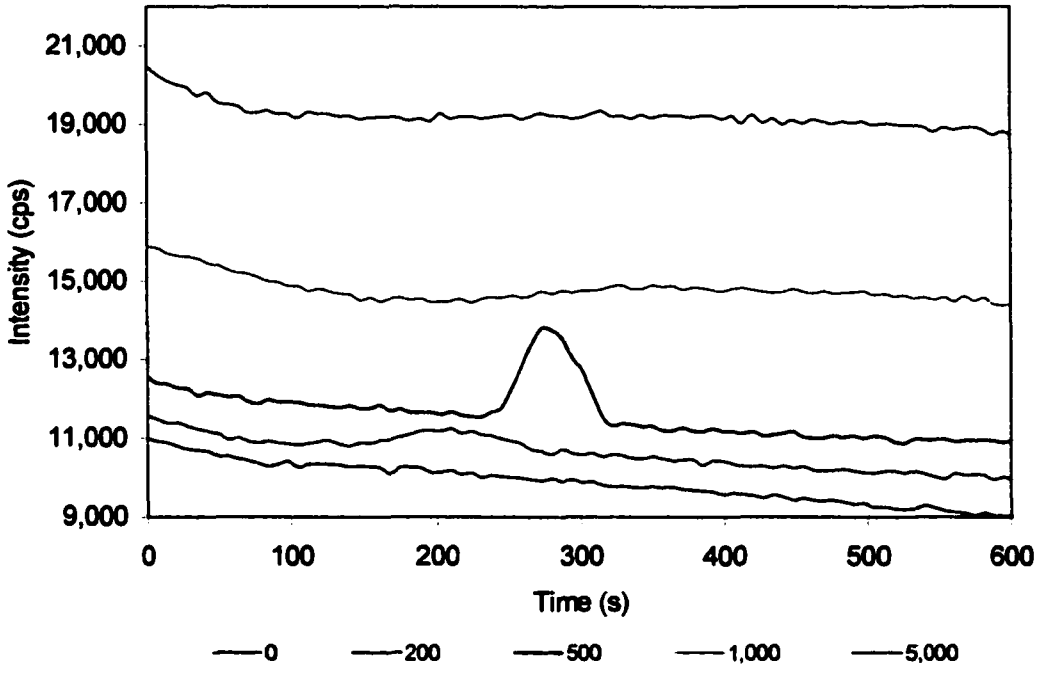

Figure 6.7. Fluorescence intensity graph of PEG-DSPE/bis-SorbPC$_{19,19}$/cholesterol/ DAPC (5/20/10/65) liposomes that have been exposed to various amounts of ionizing radiation (Rads). TX-100 addition gave a maximum intensity of 60,000 cps. The decrease in fluorescence over time is due to a bleaching effect of light source. The peak in the 500 Rad measurement is probably due to an air bubble.

The difficulties in initiating polymerization in the high temperature formulations without cholesterol tend to suggest that the destabilization events are taking place in only a few liposomes (Fig. 6.8 B). This is supported by the amount of

polymerization that is observed in the sample. Conversely, an experimental result that would suggest that the liposome fissures were closing would be a much higher rate of polymerization with a much higher conversion of the monomer. Additionally, the amount of cholesterol in the second possible explanation would play a secondary role. It would not only allow for the diffusion of the hydroxyl radical into the lipid bilayer, but it would also increase the fluidity of the membrane lipids, rate of diffusion, and allow for faster closing of the fissures. In either case, the amount of cholesterol appears to be critical to the diffusion of the hydroxyl radical and the subsequent polymerization of the sorbyl moieties.

As discussed in section 6.3.1, the mol % of cholesterol was varied to give an increased response in the rate of polymerization, as compared to the amount of ionizing radiation exposure. Increases above 20 mol % of cholesterol in the high temperature formulations corresponded to a much higher rate of dark leakage (data not shown). The disruption of the stable liposomal membrane by cholesterol in these formulations made it impossible to measure the induced amount of release for the encapsulated compounds. Because of the low dark leakage, and ionizing radiation induced leakage observed in the PEG-DSPE/bis-SorbPC$_{19,19}$/cholesterol/DAPC (5/20/10/65) formulation, it was considered the most promising formulation for the encapsulation of therapeutic compounds.

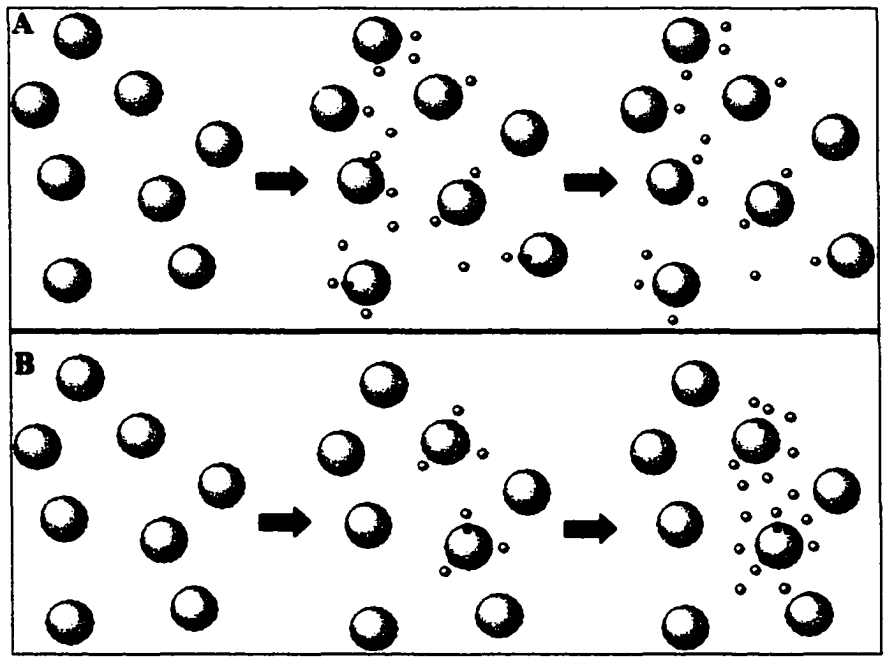

Figure 6.8. Two possibilities for the characteristics observed in the fluorescence measurements upon stimulated release of the liposomal contents with exposure to ionizing radiation. The red spheres represent liposomes, the green spheres represent the encapsulated compounds, and the black areas represent fissures that form during polymerization. In A, the sample is irradiated and a large fraction of the liposomes release a limited amount of their contents, but the fissures are filled by diffusing lipids. In B, the sample is irradiated, but only a few liposomes are induced to release their encapsulated compounds. This occurs because of the low concentration of the hydroxyl radicals in combination with the apparent impermeability of the bilayer.

6.3.3 Conclusion

The amount of released encapsulated compounds, at radiation dosages well above the normal therapeutic dose, is still very minimal. Attempts were made to offset the diffusion difficulties of the hydroxyl radicals with some gain, but at a cost in encapsulation efficiency and stability. It is clear from the results obtained for the

formulations presented here, that there is a trade off in the ability to polymerize the sorbyl moieties with ionizing radiation and the ability to encapsulate compounds.

In chapter 4, a discussion of the use of acryl moieties because of their higher reactivity was presented. However, the data obtained from the polymerization of acryl liposomes indicated that no significant advantage was obtained during the polymerization. The acryl lipids were never incorporated into liposomal formulations with encapsulated compounds to test for the ionizing radiation induced release, but further testing of these formulations may prove beneficial.

Because of the low dark leakage, and ionizing radiation induced leakage observed in the PEG-DSPE/bis-SorbPC$_{19,19}$/cholesterol/DAPC (5/20/10/65) formulation, it was considered the most promising formulation for the encapsulation of therapeutic compounds. In the next chapter, the emphasis is on polymerizable liposomes to indicate any ability to encapsulate chemotherapeutic compounds efficiently and to release the contents upon exposure to ionizing radiation.

7 CHARACTERIZATION OF LIPOSOMES WITH ENCAPSULATED CHEMOTHERAPEUTIC COMPOUNDS

7.1 Introduction

The use of liposomal drug delivery systems has been explored for more then 30 years, but only in the last 10 has the commercial development of liposomal chemotherapy become a reality. Most of the medical applications of liposomes that have reached the preclinical stage are in cancer treatment. Very early studies showed reduced toxicity of liposome-encapsulated drug, but in most of the cases the drug molecules were not bioavailable, resulting in reduced toxicity but also in severely compromised efficacy. Unfortunately, this was even found to be true for primary and secondary liver tumors, where most liposomes are cleared from the bloodstream. Although most of the drug ended up in the liver, it did not diffuse into malignant cells [125, 126].

Several clinical studies did not support the use of conventional liposomes in cancer treatment. Although it is still not clear whether such liposomes can be beneficial in the therapy of some cancers, it has been demonstrated that small, stable liposomes can passively target several different tumors because they can (owing to their biological stability) circulate for prolonged times and (owing to their small size [<50-150 nm]) extravasate in tissues with enhanced vascular permeability, a situation often present in tumors.

Two liposomal formulations have been approved by the Food and Drug Administration (FDA, Washington DC, USA) and are commercially available in the

USA, Europe, and Japan. DOXIL® (ALZA) is a formulation of doxorubicin precipitated in sterically stabilized liposomes, while DaunoXome® (Gilead) is daunorubicin encapsulated in small liposomes with very strong and cohesive bilayers, which can be referred to as mechanical stabilization [125].

Potential Benefits of Liposome Technology	
Limitations of Free Drug	**Advantages of Liposomal Encapsulation**
Instability at blood pH	Improves chemical stability of the drug in the body
Binding to plasma proteins	Protects drug from interacting with plasma proteins
Rapid clearance from the circulation	Greatly increases drug circulation half-life
Lack of site specificity	Increase in efficacy of the drug through site targeting

DaunoXome is a small liposome (DSPC/cholesterol, 2/1, 27 mM, SUV) with daunorubicin (1 mg/mL) loaded by a pH gradient (chapter 1.8.2). These liposomes are relatively stable in the circulation because they are small, and their membrane is electrically neutral and the lipids are very well packed in a solid phase. This reduces the charge-induced and hydrophobic binding of plasma opsonins, but does not protect against adsorption. Also, uncharged liposome formulations are colloidally less stable than charged ones [2].

DOXIL is a liquid suspension of 80 – 100 nm liposomes (PEG-DSPE/HSPC/cholesterol, 20 mM) with doxorubicin HCl at 2 mg/mL. The drug is encapsulated into preformed liposomes by an ammonium sulfate gradient technique and is, additionally, precipitated with encapsulated sulfate anions. These liposomes circulate in patients for several days, which increases their chance to extravasate at those sites with a leaky vascular system. Their stability is due to their surface PEG coating, as well as to their mechanically very stable bilayers. DOXIL was the first liposomal drug approved by the FDA and has been on the market since 1995, while DaunoXome was approved approximately half a year later. Both formulations are used in the treatment of Kaposi's sarcoma. In 1999, Doxil was approved for the treatment of ovarian cancer refractory to paclitaxel- and platinum-based chempotherapy regimens.

DaunoXome was shown to be equally effective as conventional therapies with reduced drug toxicity and improved patient quality-of-life (Gilead web site). The use of DOXIL in Kaposi's sarcoma has shown a high response rate in comparison with standard treatments: 58.7 % response rate as compared to 23.3 % for bleomycin-vincristine therapy and 46.2 % vs. 23.3 % for adriamycin-bleomycin-vincristine [ALZA web site]. Owing to a different biodistribution of DOXIL, the toxicity profile is quite different from that of the free drug or of conventional liposomes. While the dose-limiting toxicity is hand-foot syndrome and stomatitis since liposomes that are not taken by the MPS (mononuclear phagocytic system) or do not extravasate eventually end up in the skin, especially in areas where the vascular system is constantly under pressure and slightly damaged. However, nausea, vomiting, and

alopecia, which are usual after conventional therapy, are notably mild after liposomal (DOXIL) treatment. DOXIL has also been shown to have a 4.5 fold lower medium pathology score for doxorubicin-induced cardiotoxicity than free drug, while neutropenia is similar to the free drug. Despite these convincing results, however, it seems that, in the long run, the potential of this formulation is greater for the treatment of solid tumors. For instance, in salvage therapy of ovarian carcinoma in patients refractory to platinum and paclitaxel, a 13.8 % overall response was recorded with DOXIL.

The difference between the various formulations can be explained by the pharmacokinetic data and biodistribution reports, which have shown significant drug accumulation in tumors in the case of small and stable liposomes; free drug distributes to a large volume (causing systemic toxicity) and is quickly washed away, and because no specific tumor targeting occurs, the activity is relatively low. Conventional liposomes are distributed to a smaller volume. This depends on the drug leakage from liposomes, which is a function of lipid composition and the method of drug encapsulation, and in this case decreases in the following formulations: PC/PG > PC/cholesterol > PC/CL; CL is cardiolipin. Correspondingly, with improved liposome encapsulation, the volume of distribution decreases and the clearance rates are smaller. Because such liposomes typically do not target tumors (short blood circulation times and larger size) and end up in the MPS, the drug activity in most tumor models is compromised and generally, the reduction in drug toxicity does not justify the use of such formulations.

Because of the complexity of systemic drug delivery, the potency of the immune system, and the anatomy of tumors, it is difficult to anticipate that formulations will be prepared that will be much more effective from the drug delivery perspective. Since the early days of liposome applications, scientists have been trying to develop liposomes that would target specific cells via surface attached ligands. Promising in vitro experiments however were not reproduced in vivo because of nonspecific liposome clearance by the MPS. Pegylated liposomes have revived the concept. The immunogenicity of current formulations can be reduced by using fragments of humanized antibodies, so the remaining problems are the accessibility of tumors and cellular uptake of the liposomes. Solid tumors are rather inaccessible and the therapeutic benefit can be expected mostly within the vascular endothelium or in other body fluids, especially in the case of targeting internalizing epitopes. If the therapy proves to be effective, we must also be aware that large-scale manufacturing of targeted liposomes is technically considerably more demanding, and the economics of this will be more critical, than for nontargeted liposomal formulations.

The ultimate goal of the research is to develop a generic formulation that can efficiently encapsulate chemotherapeutic compounds, maintain encapsulation over long periods of time (days) at body temperature, and be induced to release the contents upon stimulation. Ideally, this formulation would be able to incorporate technologies such as targeted antibodies attached to the pegylated lipids without a loss in their stability or reactivity to stimulation. The rest of this dissertation is devoted to the encapsulation of several chemotherapeutic compounds (doxorubicin,

methotrexate, cisplatin, mitoxantrone, and gemcitabine) and the investigation of the liposomal stability and photoreactivity.

7.2 Doxorubicin Encapsulated Liposomes

7.2.1 Materials and Methods

7.2.1.1 Materials

Bis-SorbPC$_{17,17}$ and bis-SorbPC$_{19,19}$ were prepared as described in chapter 2. 1,2-Distearoyl-*sn*-phosphatidylcholine (DSPC), 1,2-diarachidoyl-*sn*-phosphatidylcholine (DAPC), and PEG$_{2000}$-1,2-distearoyl-*sn*-phosphatidylethanolamine (PEG-DSPE) were obtained from Avanti Polar Lipids. Cholesterol was purchased from Sigma and used without further purification. Octylphenoxy polyethoxyethanol (Triton X-100) (Sigma) was used in a 5% (wt/wt) solution with Millipore water. Doxorubicin HCl was purchased from Sigma and used without further purification.

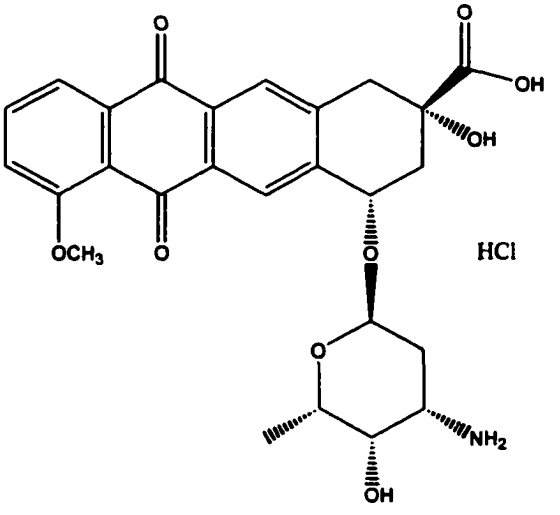

Doxorubicin HCl

7.2.1.2 Liposome Formation

Lipids were measured volumetrically into separate weighed 10 mL round bottom flasks from stock solutions of known concentrations. An argon stream was passed over each solution to remove the solvent and the flasks were then placed under high vacuum for a minimum of four hours to complete the drying. The flasks were weighed to obtain the amount of lipid in each flask. Approximately 2 mL of chloroform were then added to all but one of the flasks and the contents were combined and dried as above. A final weight was taken to ensure the complete transfer of lipids. An ammonium sulfate solution (120 mM $(NH_4)_2SO_4$ in MilliQ water, 270 mOsm, pH 7.0) was added to give a final concentration of 10 mg/mL. The lipid suspension was then subjected to ten freeze thaw cycles and then extruded four times through two stacked 600 nm Nuclepore membranes followed by extrusion three times through two stacked 200 nm Nuclepore membranes and finally extrusion four times through two stacked 100 nm Nuclepore membranes. The resulting ammonium sulfate containing liposomes were eluted through a Sephadex G-75 column with pH 7 solution containing sodium chloride (7.1 g/L, 121 mM), and having an osmolarity of 277 mosmol. A doxorubicin solution was prepared (10 μg of doxorubicin in 100 μl of MilliQ water) and added to the liposomal suspension to give a final concentration of 0.5 mM doxorubicin concentration. The sample was incubated, at 10 °C above the highest T_m of the lipids, for ½ hour then put on ice for 2 minutes, and finally allowed to equilibrate with room temperature. A second Sephadex G-75 column was run to remove the exterior doxorubicin and ammonium sulfate. The concentration of the resulting liposome suspensions were determined by UV absorbance at 260 nm (sorbyl

$\lambda_{max} = 258_{MeOH}$, $\varepsilon = 47{,}100$) of a 30 µl aliquot in 0.97 mL of HPLC grade methanol. The total lipid concentrations of resulting liposomes were between 0.4 and 1.5 mM.

7.2.1.3 Fluorescent Measurements

Fluorescence time based scans were done on 3 mL, 0.15 mM dilutions of the liposome suspensions in a NaCl solution (7.1 g/L), with 560 nm excitation and 600 nm emission on a Spex Fluorolog 2 fluorometer. The slit width for both excitation and emission monochrometers was 4 mm. Complete leakage was determined after lysis of the liposome by addition of 0.3 mL of 5% (v/v) aqueous Triton X-100 to a 3 mL sample. Photopolymerization was carried to between 20 and 99% by exposures of 1 s up to 8 min to light from a low pressure Hg pen lamp at 0.02 to 0.04 W/cm^2. The percent conversion was determined by the change in UV absorbance at 258 nm. A Corning CS-9-54 filter (> 230 nm) was used to prevent photolysis of the polymerization product. Monomer conversion was calculated as

$$\% \text{ conversion} = (A_0^{254} - A_t^{254}) / (A'_0{}^{254} - A'_{20}{}^{254})(A_0^{254}) \times 100\ \%$$

where A_0 is the initial absorbance of the sample, A'_0 is the initial absorbance of the standard sample, A_t is the absorbance of the sample after time (t) or irradiation, and A'_{20} is the absorbance of the standard sample after 20 min of irradiation.

Ionizing radiation experiments were performed with a ^{60}Co source. Lipid samples were placed 43 cm from the source. The intensity of ionizing radiation was calculated using the equation:

$$\text{Dose} = (DR_c)(PSF)(FDD)(S)[(80+d)/(SSD+d)]^2(0.99)(t-\Delta t)$$

The term DR_c is the calibrated dose rate for the day of the source, PSF is the peak scatter factor, FDD the functional depth dose, s the jaws scatter factor, d the depth of the build up layer, SSD sorce to sample distance, and t is the time of exposure. In all experiments only the DR_c and time of exposure were varied. The DR_c was calculated using the half life of ^{60}Co and time since the source was changed.

7.2.1.4 Determination of Liposomal Leakage

In order to determine the percent leakage of liposome encapsulated doxorubicin, the fluorescence of a representative sample was measured over 30 s without photolysis. After irradiation, the percent conversion was determined from the sample absorbance with a diode array spectrophotometer, and the fluorescence was measured continuously over several minutes. After the leakage measurement, a 90 s time scan was performed during which a 5% solution of Triton X-100 was added at 45 s. The fluorescence due to 100% leakage was determined from this measurement after correcting for the dilution factor due to the Triton X-100 solution.

The percent leakage at any time is given by the following expression:

$$\% \text{ leakage} = 100 \text{ X } (I_t)/(1.1I_{100})$$

where I_t is the fluorescence intensity at time (t), I_0 is the fluorescence intensity prior to photolysis, and I_{100} is the fluorescence intensity after addition of Triton X-100. Because the initial change in concentration inside the liposomes is relatively small, the initial leakage is pseudo-zero order, and the plot is a straight line. The rate of leakage was calculated from the linear region of the plot using a least squares fit. Unlike the UV polymerizations, there appears to be no bleaching factor in ionizing

radiation experiments. This was determined by monitoring the UV spectra with increasing ionizing irradiation (data not shown). It should be noted that there is the possibility of direct degradation of the chemotherapeutic compounds with γ-irradiation and no direct testing of this was attempted.

7.2.2 Results and Discussion

Doxorubicin is known to form crystalline structures inside of liposomes during active loading procedures. This can be observed when viewing cryoelectron micrographs of liposomes encapsulating doxorubicin as shown in Figure 7.1 [2]. Unfortunately, this has proven to have very severe side effects for the lipid formulations tested. The formation of crystals, and the subsequent change in the shape of the liposome, probably caused a disruption in the lipid packing. Dark leakage in all the formulations was very high and could not be corrected through the addition or exclusion of cholesterol (Table 7.1).

The rates of dark leakage for doxorubicin were about two orders of magnitude higher then the dark leakage in the ANTS/DPX formulations. It is somewhat peculiar that the formulations with 10 mol % cholesterol indicated an increase of 2 and 3 fold for the PEG-DSPE/bis-SorbPC$_{17,17}$/cholesterol/DSPC and PEG-DSPE/bis-SorbPC$_{19,19}$/cholesterol/DAPC formulations respectively (Table 7.1). This suggests that cholesterol destabilizes a portion of the membrane and allows for diffusion of the doxorubicin. Because of the oval shape of the liposomes, the cholesterol may concentrate in those areas of high curvature to relieve the strain. The areas of high cholesterol concentration would be permeable to most compounds and allow for the

diffusion of the doxorubicin from the entrapped liposomal compartment. Upon increasing the concentration of cholesterol to 30 mol %, the membrane stability was slightly increased, and could be explained by an increase in the overall fluidity of the bilayer. The more fluid structure of the bilayer membrane could more readily incorporate areas of high curvature.

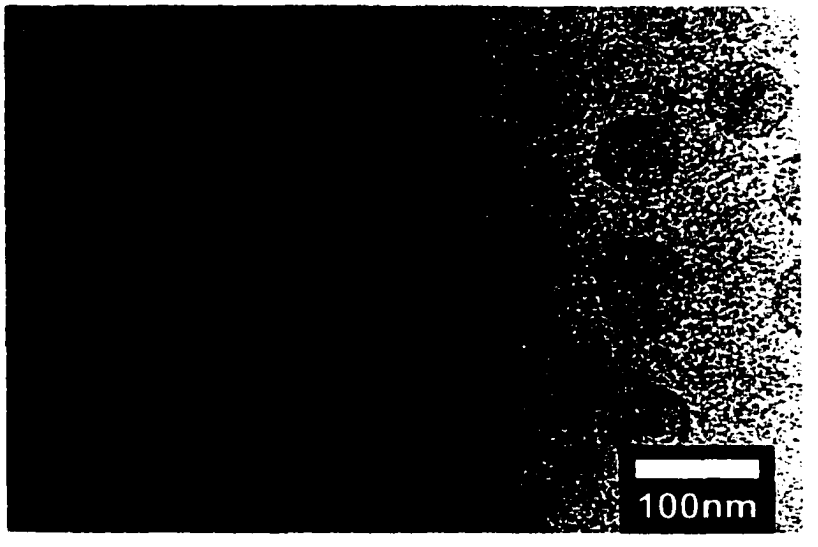

Figure 7.1. Cryoelectron micrograph of doxorubicin encapsulated in sterically stabilized liposomes. In the interior of the liposomes fibers of $(DoxH^{+})_2SO_4$ crystals can be observed that also change the shapes of the liposomes from spherical into oval. Higher magnification (not shown) shows that fibers in the bundles exhibit a helical arrangement [2].

Formulation	Rate of Dark Leakage ($\% s^{-1}$)
PEG-DSPE/bis-SorbPC$_{17,17}$/DSPC (5/20/75)	0.003
PEG-DSPE/bis-SorbPC$_{17,17}$/cholesterol/DSPC (5/20/10/65)	0.006
PEG-DSPE/bis-SorbPC$_{17,17}$/cholesterol/DSPC (5/30/30/35)	0.002
PEG-DSPE/bis-SorbPC$_{19,19}$/DAPC (5/20/75)	0.004
PEG-DSPE/bis-SorbPC$_{19,19}$/cholesterol/DAPC (5/20/10/65)	0.012

Table 7.1. Rates of release for doxorubicin in liposomal formulations. The liposomal samples were not irradiated and all experiments were performed at room temperature for the low temperature formulations and at 37 °C for the high temperature formulations. The sample with the lowest rate of release (0.002 % s^{-1}) would completely release the contents after only 14 hours.

T_m	Formulation	Amount of Polymerization (% @ 1000 Rads)
Low	PEG-DSPE/bis-SorbPC$_{17,17}$/DSPC (5/20/75)	5
Low	PEG-DSPE/bis-SorbPC$_{17,17}$/cholesterol/DSPC (5/20/10/65)	12
Low	PEG-DSPE/bis-SorbPC$_{17,17}$/cholesterol/DSPC (5/30/30/35)	15
High	PEG-DSPE/bis-SorbPC$_{19,19}$/DAPC (5/20/75)	4
High	PEG-DSPE/bis-SorbPC$_{19,19}$/cholesterol/DAPC (5/20/10/65)	10

Table 7.2. Rates of polymerization for liposomal formulations with encapsulated doxorubicin at room temperature for the low temperature formulations and at 37 °C for the high temperature formulations.

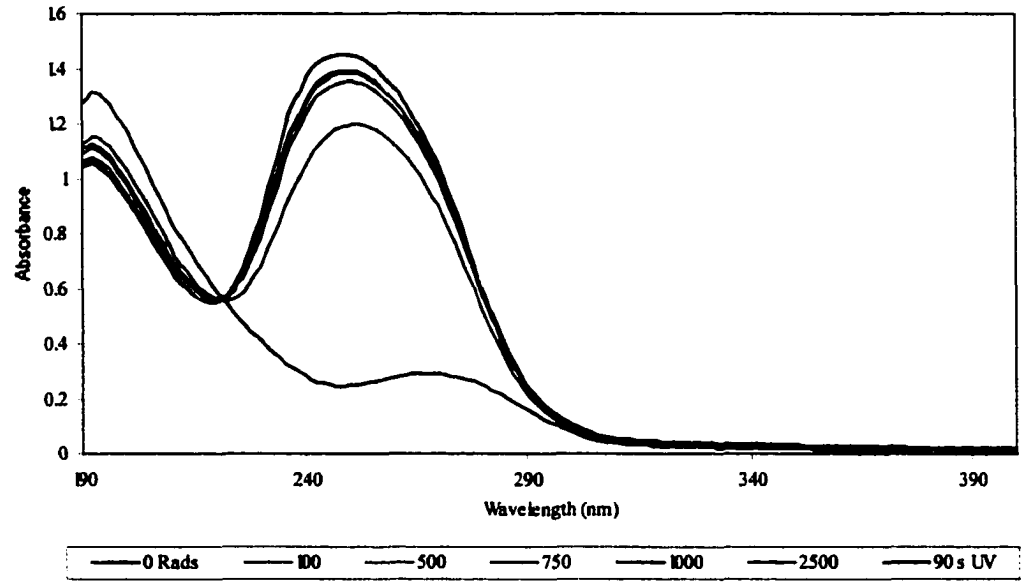

Figure 7.2. Ionizing radiation polymerization of PEG-DSPE/bis-SorbPC$_{19,19}$/ cholesterol/DAPC (5/20/10/65). Polymerization was performed at 37 °C with a lipid concentration of 150 μM.

Ionizing radiation indicated similar results to the liposome experiments discussed in chapter 6. Representative UV spectra are shown in Figure 7.2. Table 7.2 shows the rate of polymerization observed for liposomes encapsulating doxorubicin. It is obvious from the numerous experiments to this point, that the addition of cholesterol to liposomal formulations increases the rate of polymerization (Tables 6.1, 6.3, and 7.2). Unfortunately, the amount of the encapsulated compound is dependent upon the amount of cholesterol as well. As the amount of cholesterol is increased, the encapsulation efficiency is reduced. This was observed in the liposomes with encapsulated ANTS/DPX and also in the doxorubicin encapsulated liposomes.

Ionizing radiation induced leakage of liposomes encapsulating doxorubicin was also similar to the results reported in chapter 6 for ANTS/DPX leakage (Table

7.3). It should be noted that the amount of leakage has a large amount of error, because of the high dark leakage rates and the amount of time to transport the samples between facilities. Typically, greater than 50 % of the encapsulated doxorubicin had diffused out of the liposome before the measurements are taken.

The fluorescent measurements for the samples encapsulating doxorubicin indicated a constant maximum value for the fluorescence of the sample similar to the ANTS/DPX samples in chapter 6. That is, the samples indicated a constant fluorescence intensity, allowing for the rate of dark leakage, at the time the samples were tested. As discussed in chapter 6, this could be due to either the formation of transient fissures forming in a large portion of the liposomes or permanent fissures forming in only a few liposomes.

Formulation	**Amount of Released Doxorubicin (% @ 1000 Rads)**
PEG-DSPE/bis-SorbPC$_{17,17}$/DSPC (5/20/75)	5
PEG-DSPE/bis-SorbPC$_{17,17}$/cholesterol/DSPC (5/20/10/65)	6
PEG-DSPE/bis-SorbPC$_{17,17}$/cholesterol/DSPC (5/30/30/35)	6
PEG-DSPE/bis-SorbPC$_{19,19}$/DAPC (5/20/75)	4
PEG-DSPE/bis-SorbPC$_{19,19}$/cholesterol/DAPC (5/20/10/65)	2

Table 7.3. The amount of released doxorubicin after 1000 Rads of ionizing radiation. The values are corrected for dark leakage by taking the fluorescence of a sample that has not been irradiated.

The data strongly suggests that the limiting factor in the polymerization and the release of the encapsulated compounds is the polymerization initiation by the hydroxyl radicals. Additionally, the high dark leakage observed in the doxorubicin liposomes suggests an incompatibility between doxorubicin and the formulations being tested. This is probably due to the crystal structures formed by the doxorubicin within the encapsulated compartment, and the subsequent deformation of the liposome. An attempt to find a more appropriate chemotherapeutic agent that does not form crystals will be the focus of the next several sections.

7.3 Methotrexate Encapsulated Liposomes

7.3.1 Materials and Methods

7.3.1.1 Materials

Bis-SorbPC$_{19,19}$ was prepared as described in chapter 2. 1,2-Diarachidoyl-*sn*-phosphatidyl-choline (DAPC), and PEG$_{2000}$-1,2-distearoyl-*sn*-phosphatidyl-ethanolamine (PEG-DSPE) were obtained from Avanti Polar Lipids. Cholesterol was purchased from Sigma and used without further purification. Octylphenoxy polyethoxyethanol (Triton X-100) (Sigma) was used in a 5% (wt/wt) solution with Millipore water. Methotrexate • $3H_2O$ was purchased from Sigma and used without further purification.

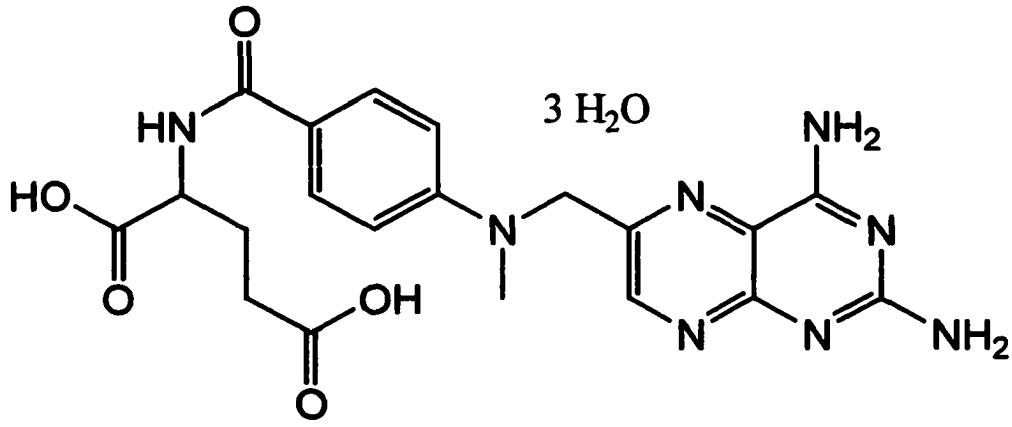

Methotrexate $3H_2O$

7.3.1.2 Liposome Formation

Lipids were measured volumetrically into separate weighed 10 mL round bottom flasks from stock solutions of known concentrations. An argon stream was passed over each solution to remove the solvent and the flasks were then placed under high vacuum for a minimum of four hours to complete the drying. The flasks were weighed to obtain the amount of lipid in each flask. Approximately 2 mL of chloroform were then added to all but one of the flasks and the contents were combined and dried as above. A final weight was taken to ensure the complete transfer of lipids. The lipids were then suspended in a sufficient amount of methotrexate (2 mg/mL) containing pH 7 phosphate buffer to make a 10 mM total lipid concentration. The osmolarity of the buffer solution was found to be 270 mosmol. The lipid suspension was then subjected to ten freeze thaw cycles and then extruded three times through two stacked 600 nm Nuclepore membranes followed by extrusion three times through two stacked 200 nm Nuclepore membranes and finally

extrusion four times through two stacked 100 nm Nuclepore membranes. The resulting methotrexate containing liposomes were eluted through a Sephadex G-75 column with pH 7 buffer solution containing sodium phosphate (10 mM), sodium chloride (139 mM), and having an osmolarity of 270 mosmol. The concentration of the resulting liposome suspensions were determined by UV absorbance at 260 nm (sorbyl $\lambda_{max} = 258_{MeOH}$, $\varepsilon = 47{,}100$) of a 30 µl aliquot in 0.97 mL of HPLC grade methanol. The total lipid concentrations of resulting liposomes were between 1 and 3 mM.

7.3.1.3 Fluorescent Measurements

Fluorescence time based scans were done on 3 mL, 0.15 mM dilutions of the liposome suspensions in a NaCl solution (7.1 g/L), with 392 nm excitation and 472 nm emission on a Spex Fluorolog 2 fluorometer. The slit width for both excitation and emission monochrometers was 4 mm.

7.3.2 Results and Discussion

There are no convenient procedures to determine the liposomal leakage of methotrexate, and the methodology to determine the concentration of methotrexate involves UV analysis of samples [76, 127]. Procedures are available to determine liposomal leakage with (^{3}H) methotrexate, but they involve equipment that is not readily available [128]. An attempt was made to determine the fluorescence of methotrexate, and a very interesting phenomenon was discovered; methotrexate degrades rapidly with UV exposure. In addition it degrades, at a slower rate, when

stored at 25 °C and above. This can be observed in a fluorescence intensity increase at 472 nm with an excitation at 392 nm (Fig. 7.3).

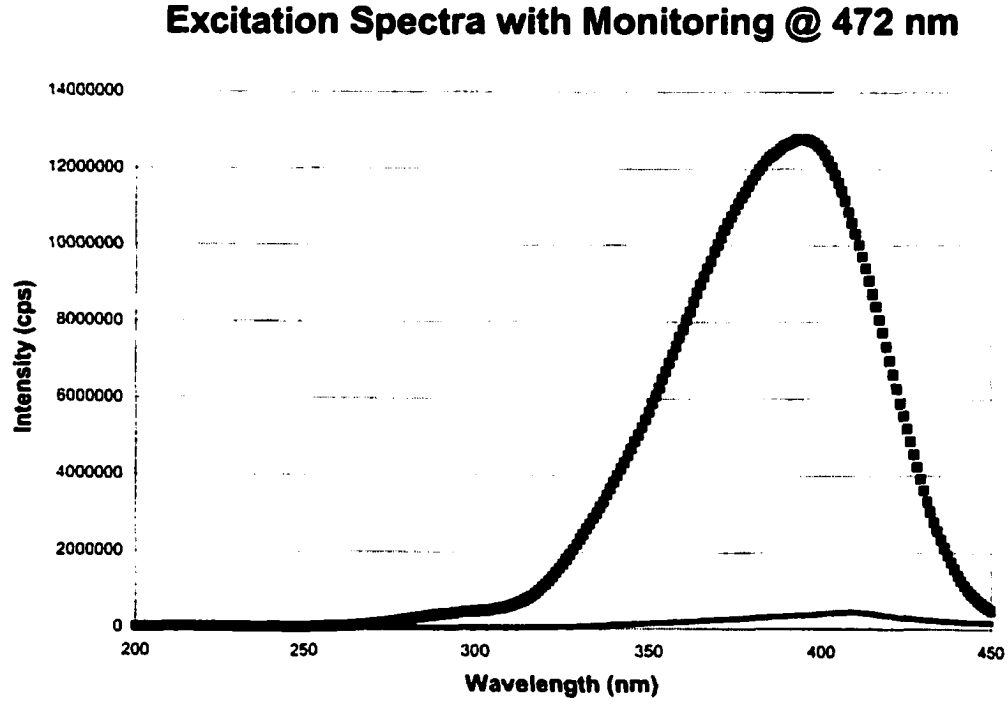

Figure 7.3. Fluorescence emission intensity of methotrexate (1 mg/mL in PBS buffer). Excitation proceeded from 200 to 450 nm with monitoring at 472 nm. The lower line represents the initial fluorescence, and the upper line represents the fluorescence intensity after 1 hour at 37 °C. The increase in fluorescence intensity is probably due to the degradation of the methotrexate.

Methotrexate solubility is a major factor in attempting to load liposomes with the chemotherapeutic compound. The solubility is about 2 mg/mL in buffer and less in MilliQ water. Additionally, the reported encapsulation efficiency for methotrexate is only 5 % [127]. The inability to get an accurate concentration from fluorescence, the low solubility, and the low encapsulation efficiency hindered any attempt to quantify the rates of release for liposomal samples. UV analysis of dialysis samples

that were exposed to ionizing radiation, UV irradiation, and no irradiation was attempted, but the UV spectra indicated no methotrexate in the dialysate released from the liposomes. This can be explained by assuming that there is no release of the methotrexate under any of the conditions, or more likely, the concentration of the methotrexate in the dialysis samples was below detection limits because of the low encapsulation efficiency and solubility.

Polymerization of liposomes encapsulating methotrexate also produced an unexpected result. There was little to no apparent polymerization of the sorbyl moieties up to 10,000 Rads (Fig. 7.4). The experiment was repeated twice to determine whether these results were correct, and in each experiment the results were similar. Polymerization with UV irradiation was normal and agreed with previous results for liposomes encapsulating ANTS/DPX as discussed in chapter 5. A possible explanation for the lack of polymerization in ionizing radiation experiments could be the amount of amines present in methotrexate. Amines are known to be radical scavengers [120], and may be scavenging the hydroxyl radicals prior to their diffusion into the lipid bilayer to initiate polymerization. Additionally, because of the low water solubility of methotrexate, the compound may be associated with the lipid bilayer and form a protective layer that prevents diffusion of the radicals by scavenging them as they reach the bilayer membrane.

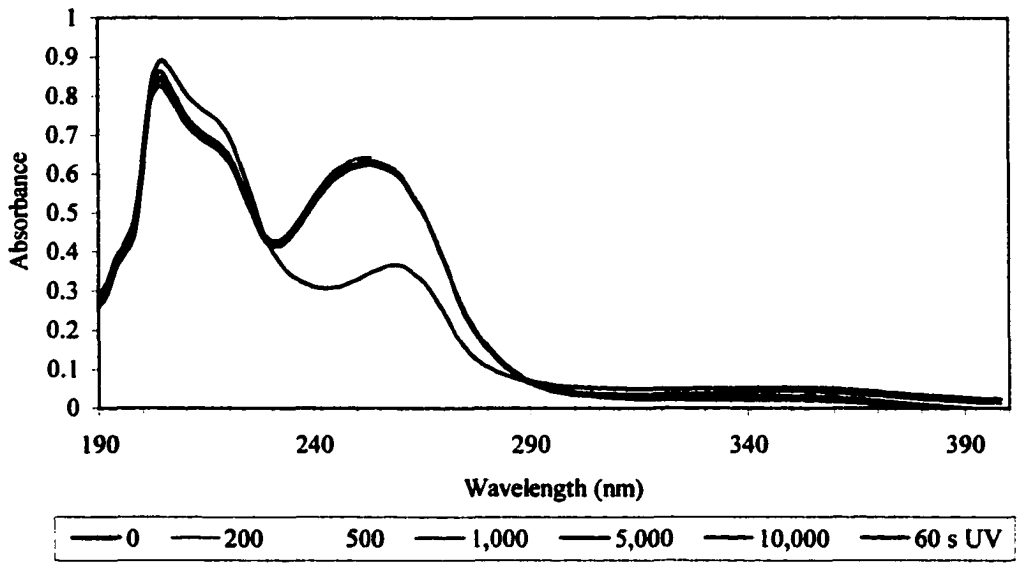

Figure 7.4. UV spectra of methotrexate encapsulated liposomes at various exposures to ionizing irradiation. The liposomal formulation was PEG-DSPE/bis-SorbPC$_{19,19}$/ DAPC (5/20/75)

Tumor cells that were exposed to liposomes with encapsulated methotrexate indicated no toxicity to the level of chemotherapeutic compound present. These test were performed with liposomes that were irradiated with UV and ionizing radiation. Methotrexate was determined to be a poor possibility for encapsulation in the formulations used.

7.4 Cisplatin Encapsulated Liposomes

7.4.1 Materials and Methods

7.4.1.1 Materials

Bis-SorbPC$_{19,19}$ was prepared as described in chapter 2. 1,2-Diarachidoyl-*sn*-phosphatidyl-choline (DAPC), and PEG$_{2000}$-1,2-distearoyl-*sn*-phosphatidyl-

ethanolamine (PEG-DSPE) were obtained from Avanti Polar Lipids. Cholesterol was purchased from Sigma and used without further purification. Octylphenoxy polyethoxyethanol (Triton X-100) (Sigma) was used in a 5% (wt/wt) solution with Millipore water. Cisplatin was purchased from Sigma and used without further purification.

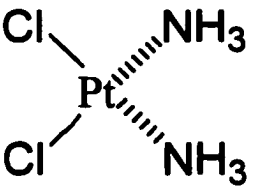

Cisplatin

7.4.1.2 Liposome Formation

Lipids were measured volumetrically into separate weighed 10 mL round bottom flasks from stock solutions of known concentrations. An argon stream was passed over each solution to remove the solvent and the flasks were then placed under high vacuum for a minimum of four hours to complete the drying. The flasks were weighed to obtain the amount of lipid in each flask. Approximately 2 mL of chloroform were then added to all but one of the flasks and the contents were combined and dried as above. A final weight was taken to ensure the complete transfer of lipids. The lipids were then suspended in a sufficient amount of cisplatin (2 mg/mL) containing pH 7, 3,3-dimethylglutaric acid (DMG) buffer to make a 10 mM total lipid concentration. DMG buffer was used instead of the typical PBS buffer because of the testing procedures discussed in chapter 7.4.1.3. The osmolarity of the

buffer solution was found to be 270 mosmol. The lipid suspension was then subjected to ten freeze thaw cycles and then extruded three times through two stacked 600 nm Nuclepore membranes followed by extrusion three times through two stacked 200 nm Nuclepore membranes and finally extrusion four times through two stacked 100 nm Nuclepore membranes. The resulting cisplatin containing liposomes were eluted through a Sephadex G-75 column with pH 7 buffer solution containing 3,3-dimethylglutaric acid (10 mM), sodium chloride (139 mM), and having an osmolarity of 270 mosmol. The concentration of resulting liposome suspensions were determined by UV absorbance at 260 nm (sorbyl $\lambda_{max} = 258_{MeOH}$, $\varepsilon = 47{,}100$) of a 30 μl aliquot in 0.97 mL of HPLC grade methanol. The total lipid concentrations of resulting liposomes were between 1 and 3 mM.

7.4.1.3 Sample Preparation for ICP-MS

The samples were irradiated with ionizing radiation at a lipid concentration of 800 μM to maximize the concentration of platinum for testing procedures. The samples then underwent dialysis for 48 hours with a 2 mL sample placed in a dialysis bag (50,000 MW pore size) and diluted in a 2 L sample of DMG buffer. After irradiation and dialysis, the liposomal samples were digested in 50 weight % HNO_3 solutions overnight at 40 °C. The inductively coupled plasma/mass spectrometry (ICP-MS) testing was performed by Gavin Buttigieg at the University of Arizona. The platinum concentration was compared to the phosphorus concentration, present from the lipid headgroups, as a normalization factor. Because phosphorus was used as the normalization factor in the ICP-MS experiments, the buffer could not contain

additional phosphorus. DMG was chosen after testing several liposomal formulations for polymerization rates under ionizing radiation and UV exposure conditions. The results were identical to PBS solutions.

7.4.2 Results and Discussion

Cisplatin is a potent anticancer drug and well established in the chemotherapy of a variety of solid tumors in patients. However, administration of cisplatin is associated with myelosuppression, gastrointestinal toxicity, peripheral neuropathy, ototoxicity and nephrotoxicity, which is the dose-limiting factor [129]. As discussed in chapter 1, the ability to encapsulate cisplatin within liposomes could provide protection from the serious side effects and allow for a higher concentration to be used for the direct application to solid tumors.

Cisplatin has no UV absorbance and no fluorescence. The techniques that have been employed to determine the concentration of cisplatin take advantage of platinum [130, 131]. Both of these methodologies involved atomic absorption (electrothermal atomic absorption spectrometry and ICP-MS). An attempt to use ICP-MS, in coordination with Gavin Buttigieg of the Bonner Denton group at the University of Arizona, was undertaken to evaluate the ability to use these procedures in liposomal formulations.

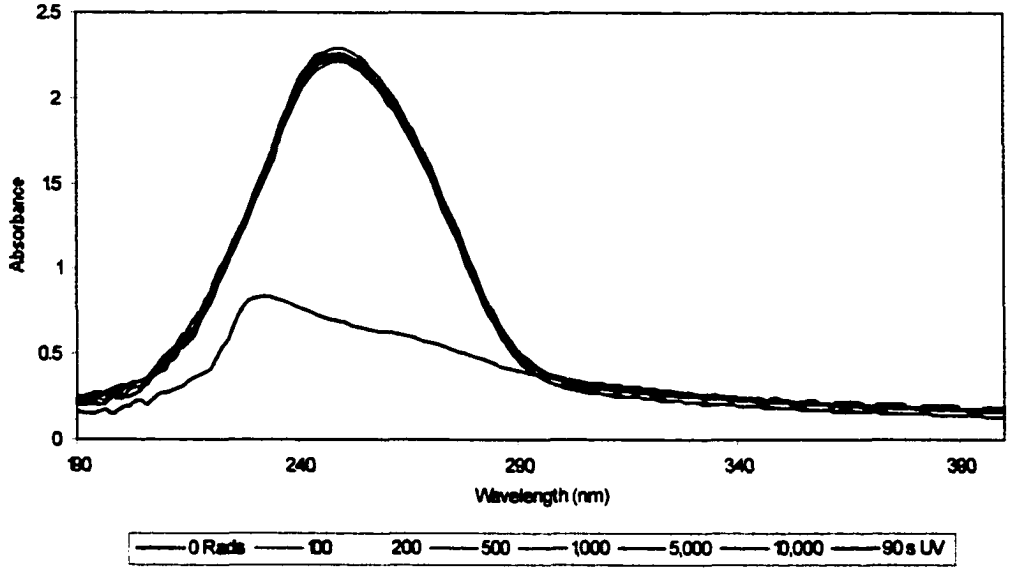

Figure 7.5. Cisplatin formulation polymerization upon the exposure to ionizing radiation (Rads). PEG-DSPE/bis-SorbPC$_{19,19}$/DAPC (5/20/75) in DMG buffer at a lipid concentration of 800 μM.

As in the case of the methotrexate formulations that were exposed to ionizing radiation, the liposome formulations encapsulating cisplatin indicated little or no polymerization up to 10,000 Rads (Fig. 7.5). This was additionally frustrating due to the much higher concentration of the lipids in the samples irradiated then typically used. A higher concentration of the sorbyl moiety should indicate a higher rate of conversion upon exposure to ionizing radiation.

ICP-MS analysis of the samples indicated some release of the cisplatin after exposure to ionizing radiation, but the data is erratic (Fig. 7.6). Cisplatin solubility is about 2 mg/mL at 60 °C (6 mM). The initial concentration of platinum in the liposomal formulations without dialysis indicates an encapsulation efficiency of only 3 %. Furthermore, a large amount (> 50 %) of the cisplatin appears to have leaked

during the dialysis. A precipitate formed in the samples that had been irradiated for 1,000 or more Rads. No tests were performed to determine the nature of the precipitate, but it may have interfered with the ICP-MS results. An attempt was made to extract the entire sample from the vials for injection into the equipment, but the solid that was observed was difficult to transfer and may have remained in the vial. This may explain the apparent loss of platinum in those samples. The sample where polymerization was done with UV irradiation did indicate a loss of platinum without the appearance of a precipitate.

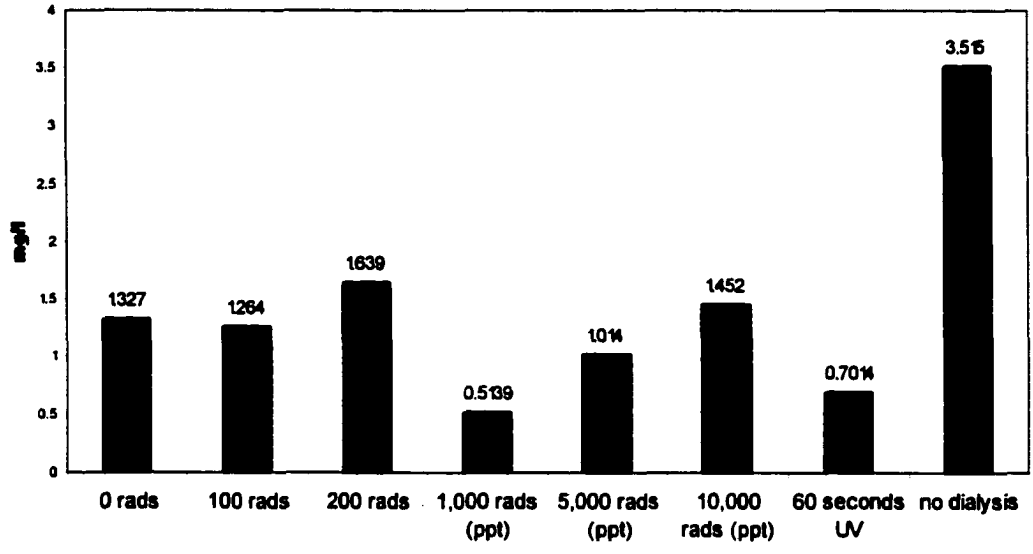

Figure 7.6. ICP-MS results indicating the concentration of Pt in the liposomal samples after exposure to ionizing radiation and dialysis. The (ppt) indicates a precipitate formed in the samples after ionizing radiation exposure.

As in the case of the methotrexate, it is believed that the lack of polymerization after ionizing radiation exposure is due to the presence of the amines on cisplatin. Because of the lack of polymerization and consistent results obtained

from cisplatin, it was determined that cisplatin was a poor candidate for the liposomal encapsulation formulations that are currently being considered. An additional problem is the lack of readily available equipment for testing and the extended periods necessary for sample preparation.

7.4 Mitoxantrone Encapsulated Liposomes

7.4.1 Materials and Methods

7.4.1.1 Materials

Bis-SorbPC$_{19,19}$ was prepared as described in chapter 2. 1,2-Diarachidoyl-*sn*-phosphatidyl-choline (DAPC), and PEG$_{2000}$-1,2-distearoyl-*sn*-phosphatidyl-ethanolamine (PEG-DSPE) were obtained from Avanti Polar Lipids. Cholesterol was purchased from Sigma and used without further purification. Octylphenoxy polyethoxyethanol (Triton X-100) (Sigma) was used in a 5% (wt/wt) solution with Millipore water. Mitoxantrone • 2 HCl was purchased from Sigma and used without further purification.

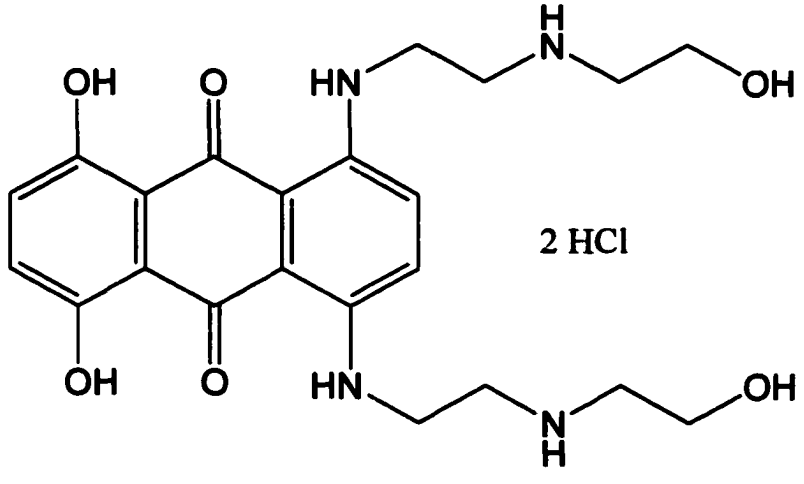

7.4.1.2 Liposome Formation

Lipids were measured volumetrically into separate weighed 10 mL round bottom flasks from stock solutions of known concentrations. An argon stream was passed over each solution to remove the solvent and the flasks were then placed under high vacuum for a minimum of four hours to complete the drying. The flasks were weighed to obtain the amount of lipid in each flask. Approximately 2 mL of chloroform were then added to all but one of the flasks and the contents were combined and dried as above. A final weight was taken to ensure the complete transfer of lipids. The lipids were then suspended in a sufficient amount of mitoxantrone (10 mg/mL) containing solution. The solution was prepared with mitoxantrone in MilliQ and the pH of the solution was taken to 7 with the addition of dilute NaOH. NaCl was added to give a final mOsm of 270. A NaCl solution was used because of the high solubility of mitoxantrone and the high osmolarity when a PBS buffer solution was attempted. The lipid suspension was then subjected to ten freeze thaw cycles and then extruded three times through two stacked 600 nm Nuclepore membranes followed by extrusion three times through two stacked 200 nm Nuclepore membranes and finally extrusion four times through two stacked 100 nm Nuclepore membranes. The resulting mitoxantrone containing liposomes underwent dialysis to remove the external mitoxantrone. Typically the lipid solution was 3 mL and placed in a 50,000 MW dialysis bag. The dialysis solution was 2 L of a NaCl solution (14.2 g/2L) in MilliQ that had been taken to a pH of 7. The concentration of resulting liposome suspensions were determined by UV absorbance at 260 nm (sorbyl

$\lambda_{max} = 258_{MeOH}$, $\varepsilon = 47,100$) of a 30 µl aliquot in 0.97 mL of HPLC grade methanol. The total lipid concentrations of resulting liposomes were between 8 and 10 mM.

7.4.2 Results and Discussion

Mitoxantrone was chosen because of its solubility in aqueous solutions (10 mg/mL) and its fluorescence characteristics (excitation at 609 nm and a strong emission at 690 nm). The emission intensity of the mitoxantrone was comparable to ANTS, which had worked extremely well as discussed in chapters 5 and 6. There was some initial concern about the amines present in the structure, but two of the amines are conjugated to the aromatic ring and the other amines are secondary amines. A hypothesis was put forth: the more hindered the amines, the less availability to scavenge radicals. Additionally, mitoxantrone was found to be extremely efficient in causing cell death by collaborators at the University of Arizona Cancer Center. The toxicity was about 1000 fold higher for mitoxantrone than for doxorubicin, which had shown the highest toxicity before this candidate. One more advantage to using mitoxantrone, initially, was the blue color of the mitoxantrone solutions even at 100 nM concentrations. At typical concentrations (µM), the drug could be easily followed during column chromatography or dialysis.

Two formulations were tested: PEG-DSPE/bis-SorbPC$_{19,19}$/DAPC (5/20/75) and PEG-DSPE/bis-SorbPC$_{19,19}$/cholesterol/DAPC (5/20/10/65), which had appeared to be the most promising to date. Ionizing radiation and UV light exposure indicated excellent polymerization results in the sample with the formulation PEG-DSPE/bis-SorbPC$_{19,19}$/cholesterol/ DAPC (5/20/10/65) (Fig. 7.7). The formulation without

cholesterol indicated that only 3 % of the sorbyl moiety had reacted after 1,000 Rads, while the formulation with cholesterol indicated that 12 % of the sorbyl moiety had reacted. Both of these results are consistent with the results obtained in chapter 6 and chapter 7.2 with doxorubicin.

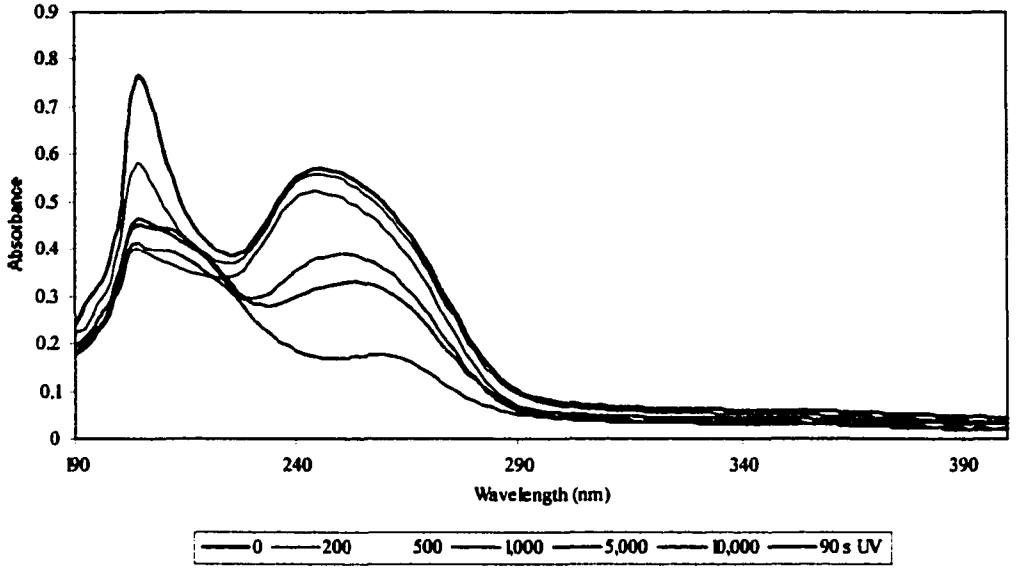

Figure 7.7. Ionizing radiation polymerization of mitoxantrone encapsulated liposomes. PEG-DSPE/bis-SorbPC$_{19,19}$/cholesterol/DAPC (5/20/10/65) at a lipid concentration of 150 μM in a NaCl solution.

Maintaining the encapsulation of mitoxantrone in the liposomes proved to be extremely difficult when added to cell cultures. Although mitoxantrone is more water soluble then the previous compounds, it appeared to rapidly diffuse out of the liposomes upon addition to cell cultures. All cell samples that had the mitoxantrone liposomes added to them indicated complete cell death even without stimulation to release the encapsulated compound. The samples had undergone dialysis for at least two days with several exchanges of the external media after 8-12 hour intervals. The

external solution was colorless and UV analysis indicated no presence of the mitoxantrone, whereas the solution within the dialysis bag was dark blue.

This suggests that something occurs during transport of the samples to the testing facility (Cancer Center) or upon addition to the cell culture media. It is well known that cells release compounds into the external media, and these compounds may interfere with the encapsulation of the chemotherapeutic agents within the formulations tested. Compounds such as proteins or enzymes released from the cells may interact with the liposomes and cause release of the encapsulated agents by disrupting the liposomal bilayer. Additional tests would need to be undertaken to determine the extent of the disruption from the media and those are currently underway at the Cancer Center.

7.4 Conclusion

This research was designed to develop a general formulation that could readily encapsulate numerous chemotherapeutic compounds and release the compounds under normal radiation treatment therapies. Unfortunately, the chemotherapeutic compounds chosen for testing appear to have been too lipophilic and may have interfered with the stability of the liposomal bilayer. What has been shown, is that a formulation was developed that is thermally stable at body temperature and that it is responsive to ionizing radiation and UV light exposure.

The formulation with the most promise to this point is PEG-DSPE/bis-SorbPC$_{19,19}$/cholesterol/DAPC (5/20/10/65). This formulation probably allows for phase separation and domain formation to enhance the polymerization of the sorbyl

moieties as well as release the encapsulated compounds upon either UV light or ionizing radiation stimulation. That is not to say that this formulation should not be modified. Enhancement of the phase separation even in the presence of cholesterol may be accomplished through the substitution of sphingolipids for the saturated phospholipid (DAPC). Additionally, a more reactive polymerizable moiety that is less dependent upon the presence of molecular oxygen could enhance the rate of polymerization and the response to ionizing radiation to give a better rate of release at a lower dosage of Rads.

APPENDIX A CONTENTS

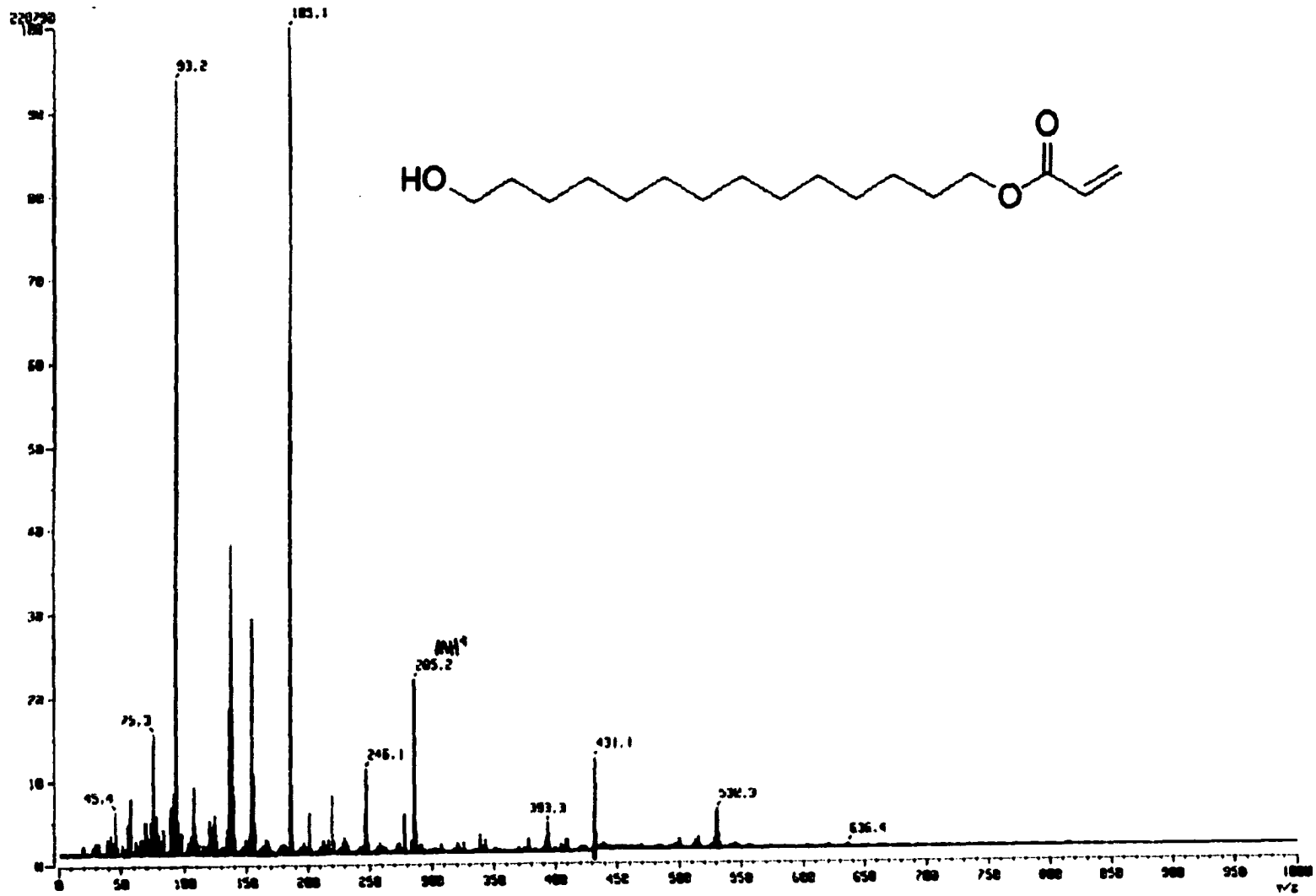
HO
O
O
93.2
185.1
205.2
431.1

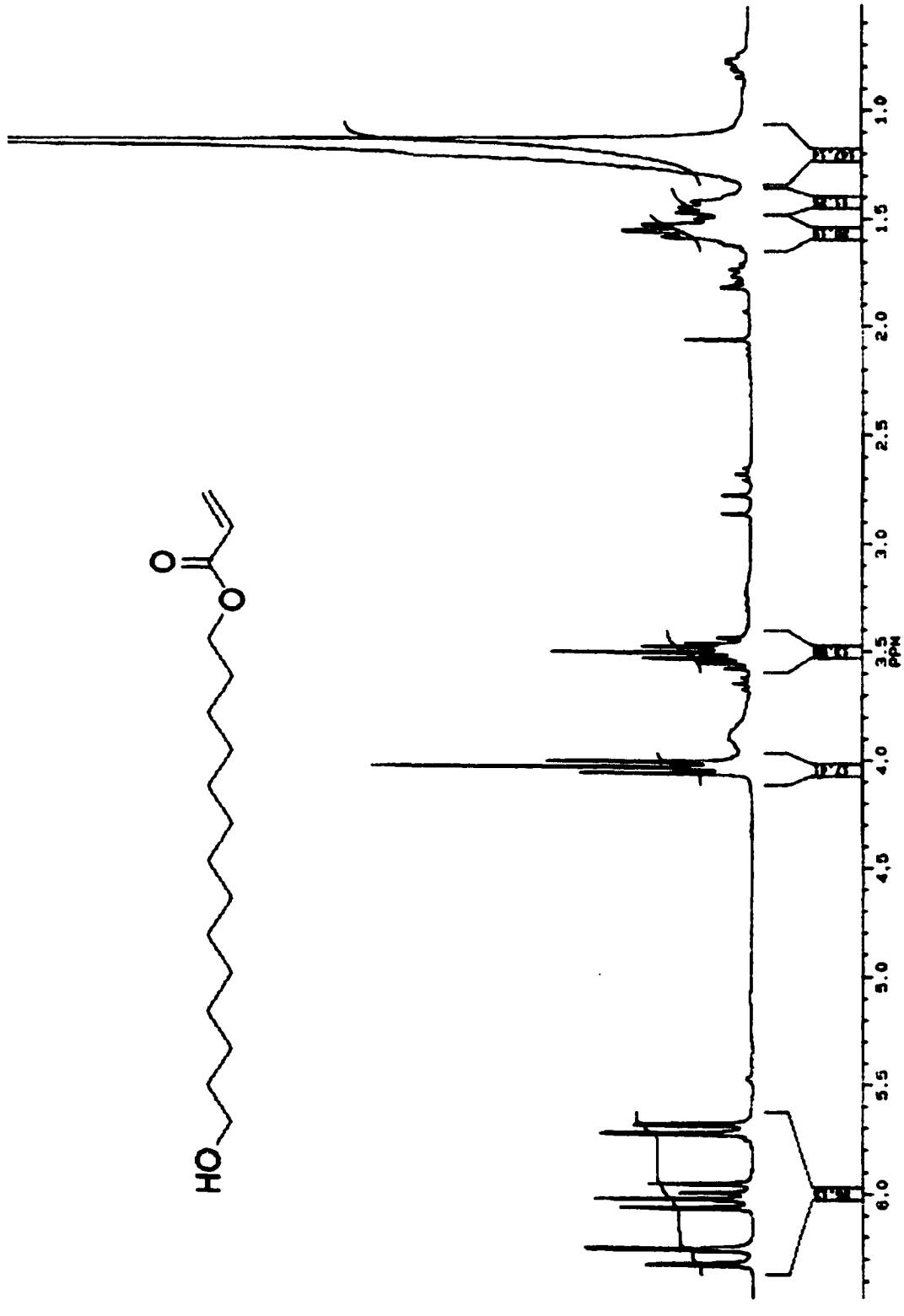
HO
O
O
6.0
5.5
5.0
4.5
4.0
3.5
PPM
3.0
2.5
2.0
1.5
1.0

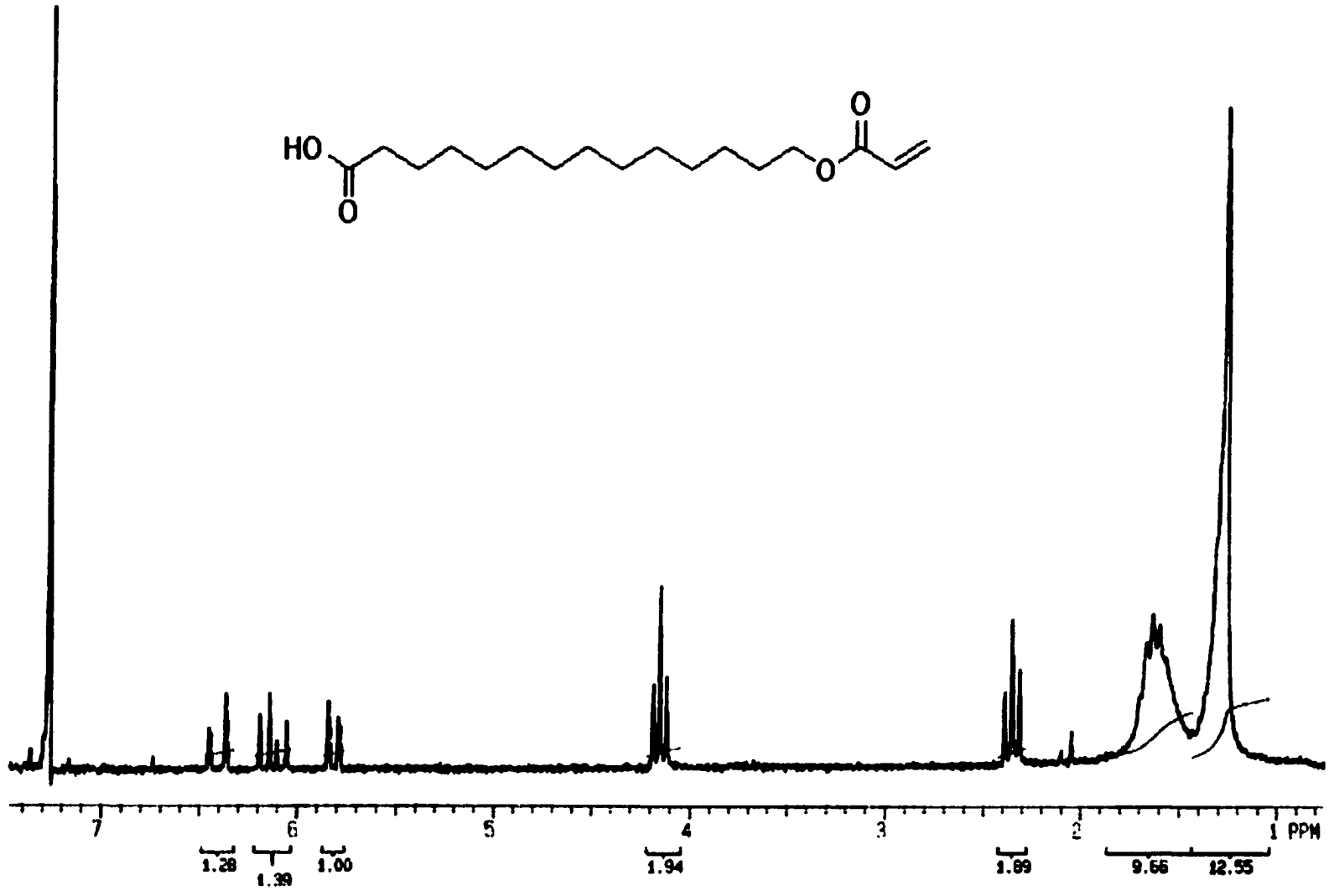
HO
O
O
O
7
6
5
4
3
2
1 PPM
1.28
1.39
1.00
1.94
1.89
9.66
12.55

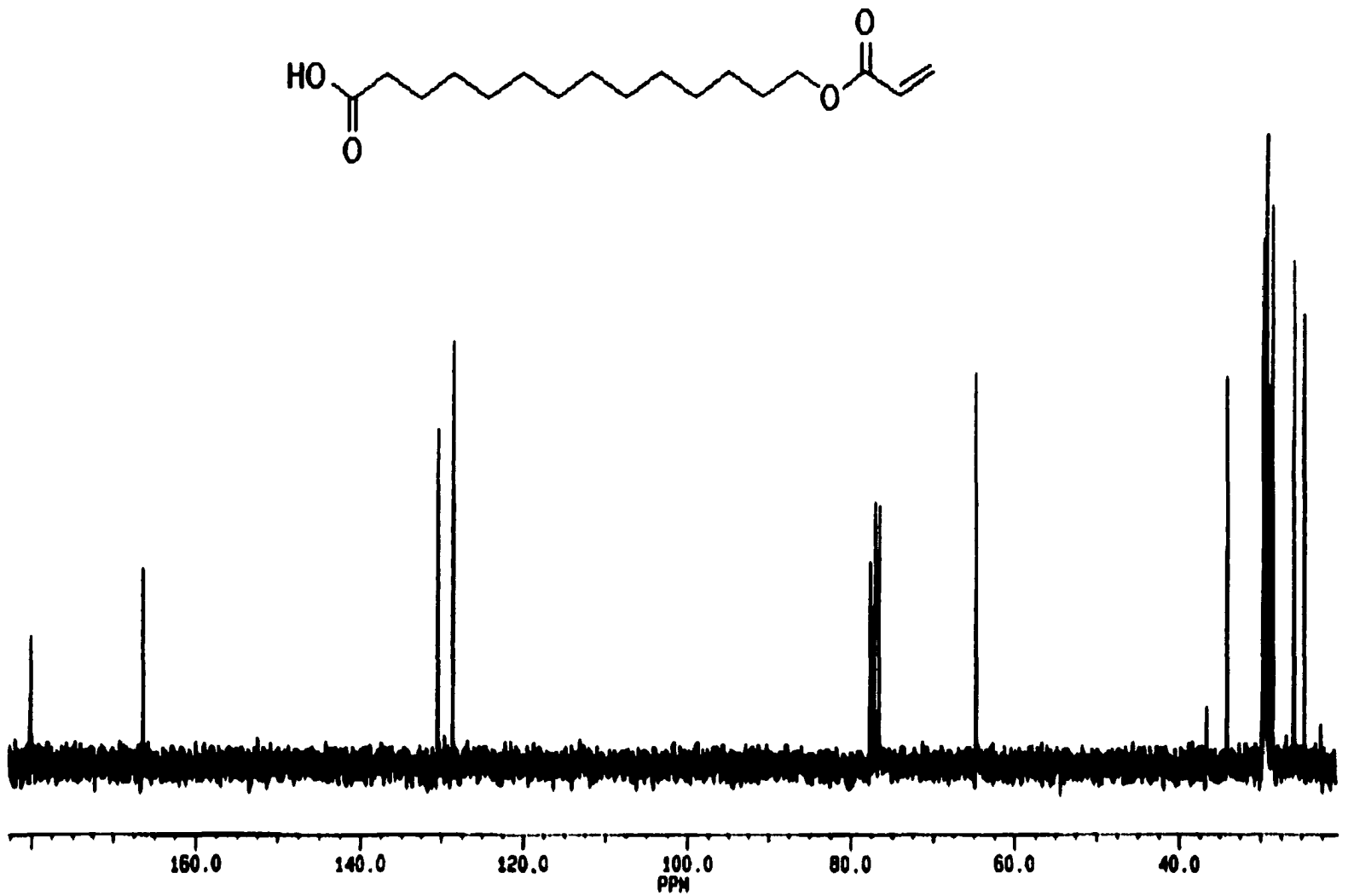
HO
O
O
O
160.0
140.0
120.0
100.0
PPM
80.0
60.0
40.0

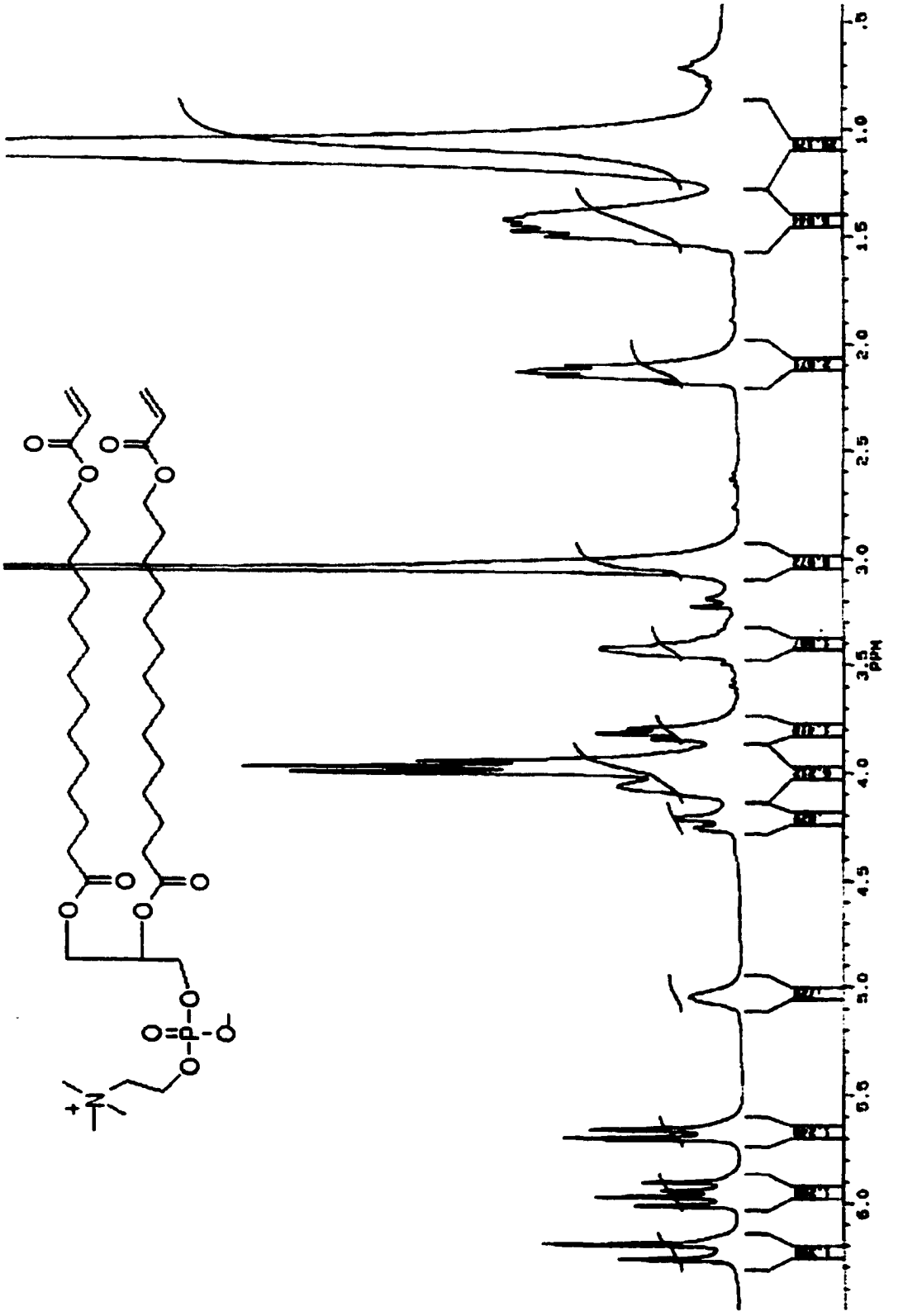
.5
1.0
1.5
2.0
2.5
3.0
3.5
PPM
4.0
4.5
5.0
5.5
6.0

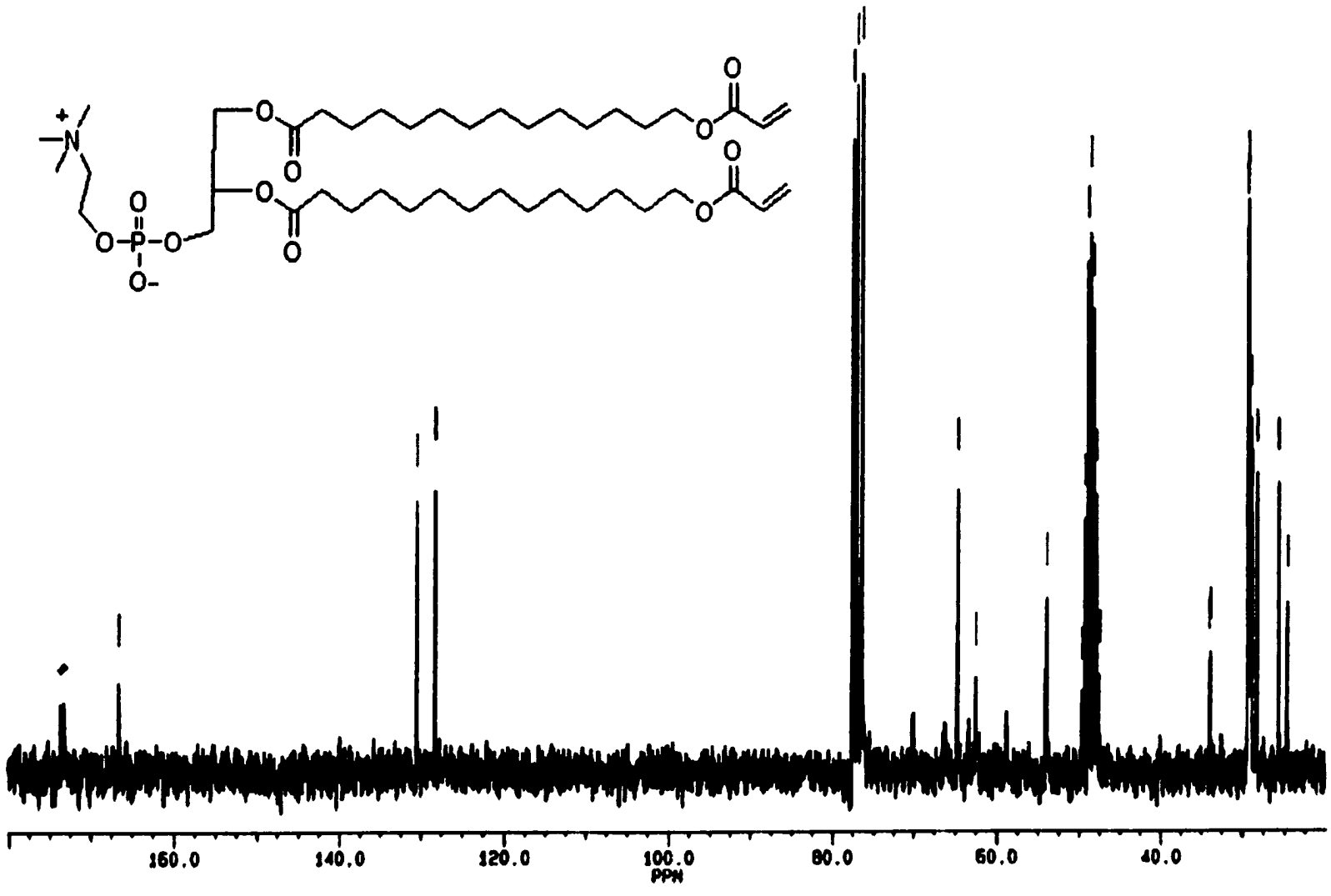
160.0
140.0
120.0
100.0
PPM
80.0
60.0
40.0

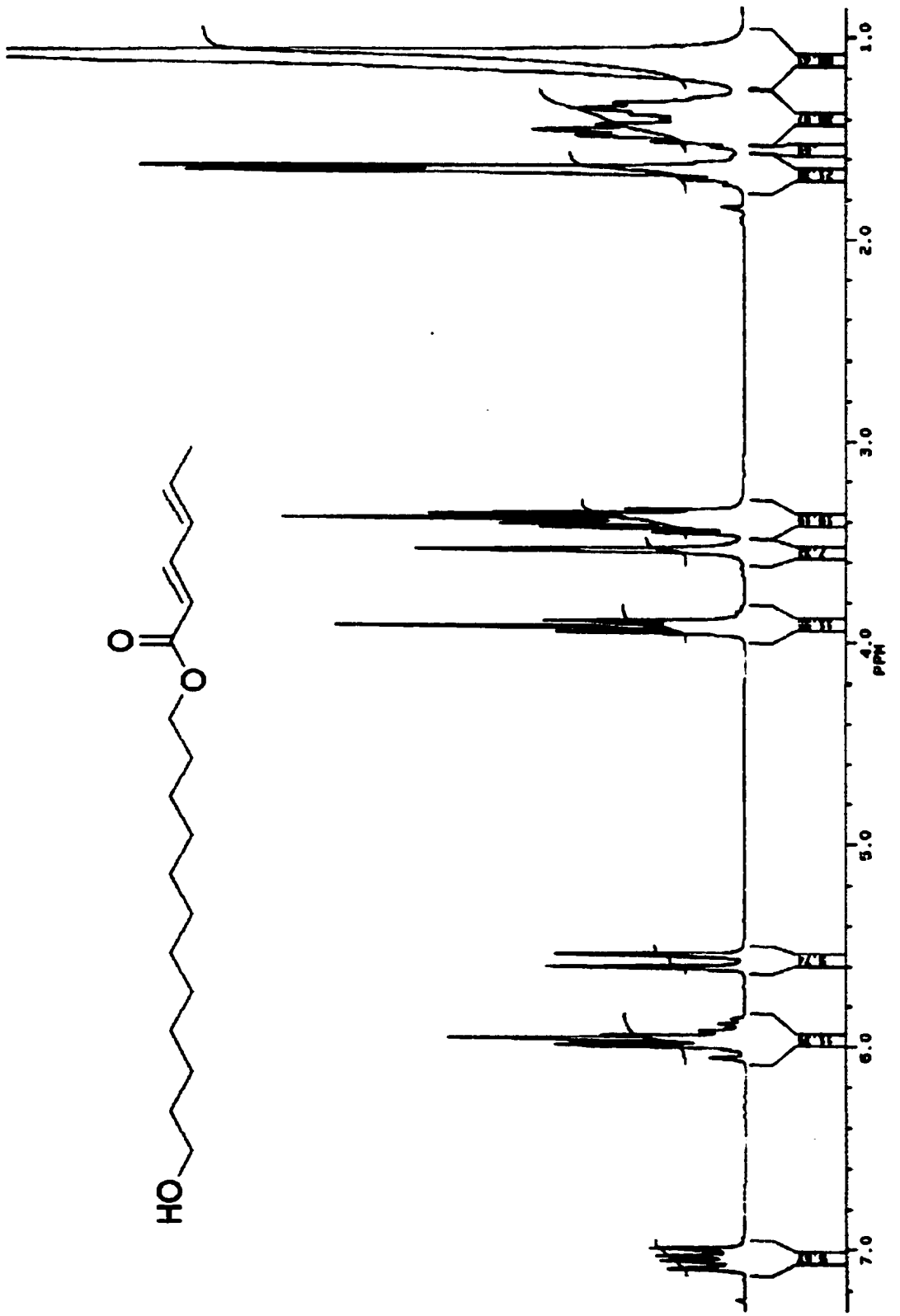
HO
O
O
1.0
2.0
3.0
4.0
PPM
5.0
6.0
7.0

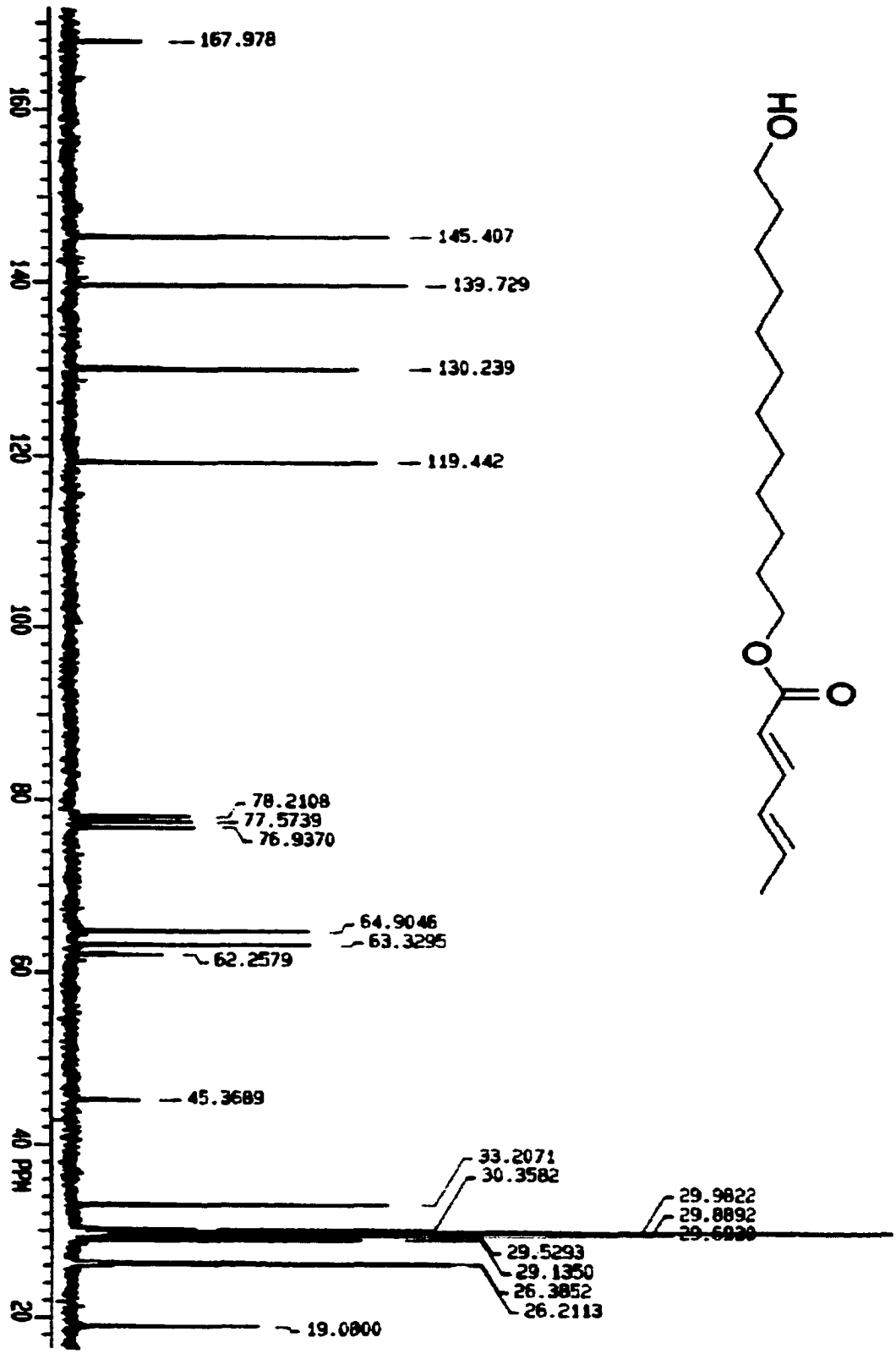
167.978
145.407
139.729
130.239
119.442
78.2108
77.5739
76.9370
64.9046
63.3295
62.2579
45.3689
33.2071
30.3582
29.9822
29.8892
29.6020
29.5293
29.1350
26.3852
26.2113
19.0800
160
140
120
100
80
60
40
20
PPM
OH
O
O

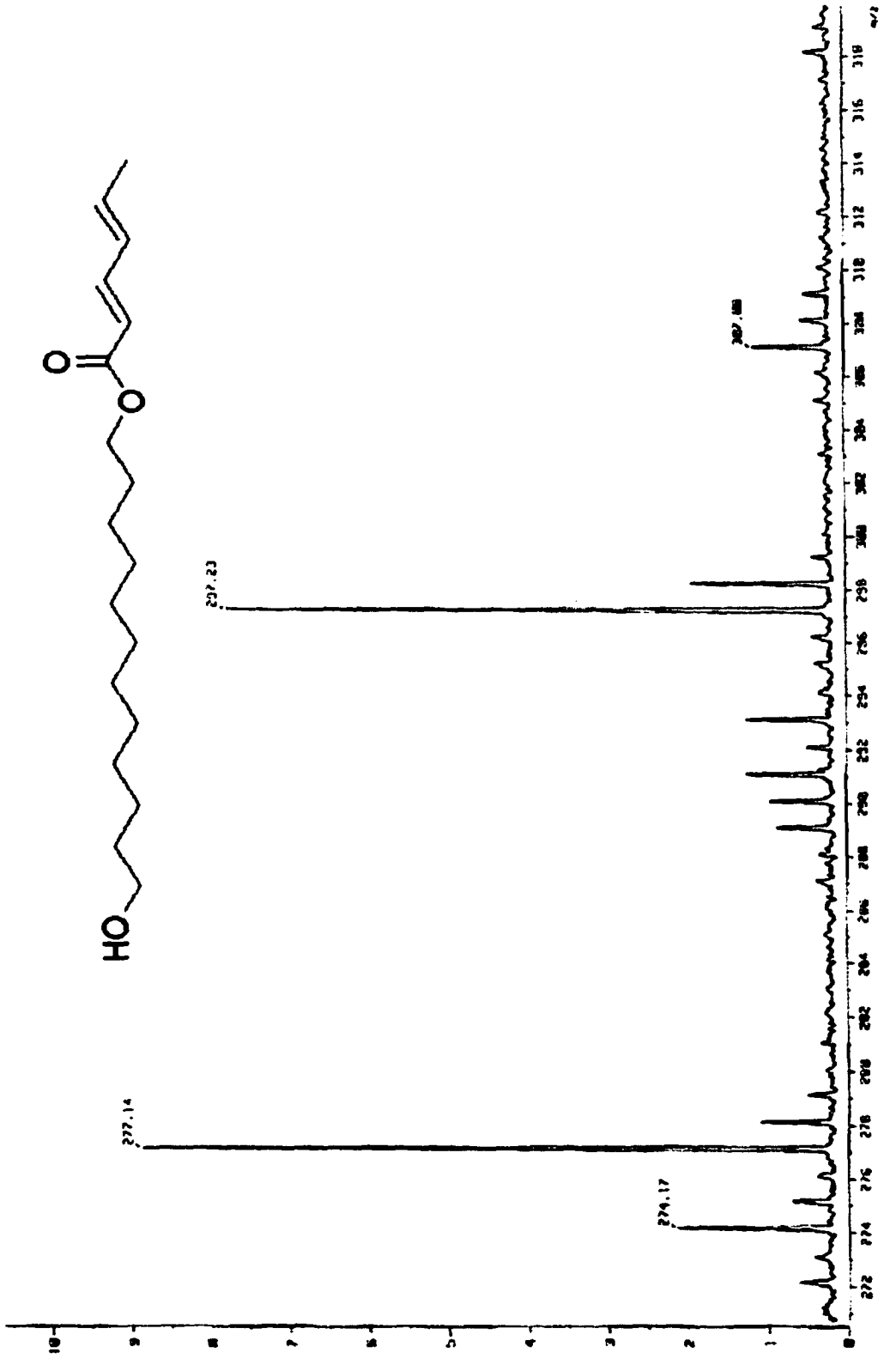
HO
O
O
277.14
274.17
297.23
307.08

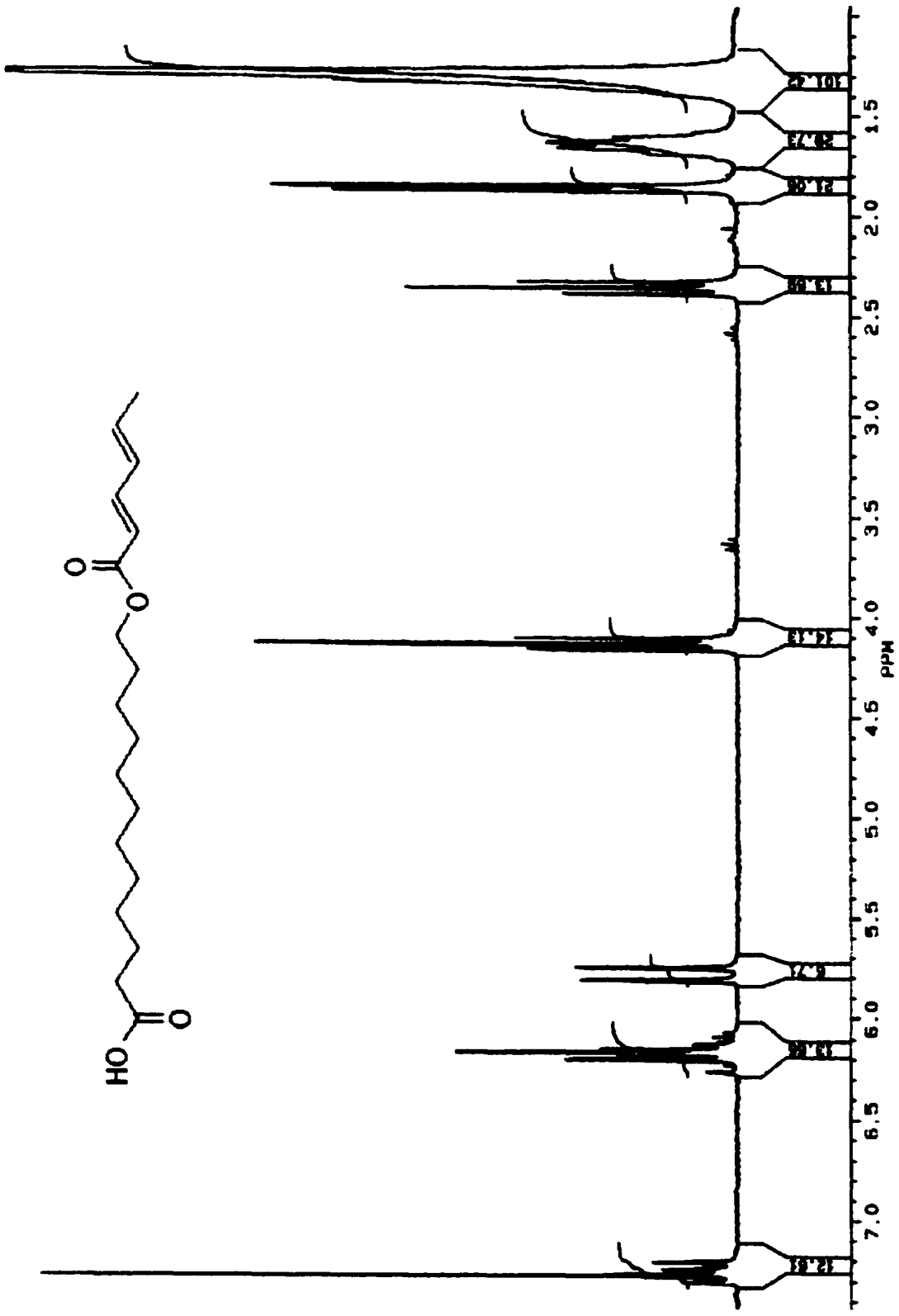
HO
O
O
O
PPM
1.5
2.0
2.5
3.0
3.5
4.0
4.5
5.0
5.5
6.0
6.5
7.0

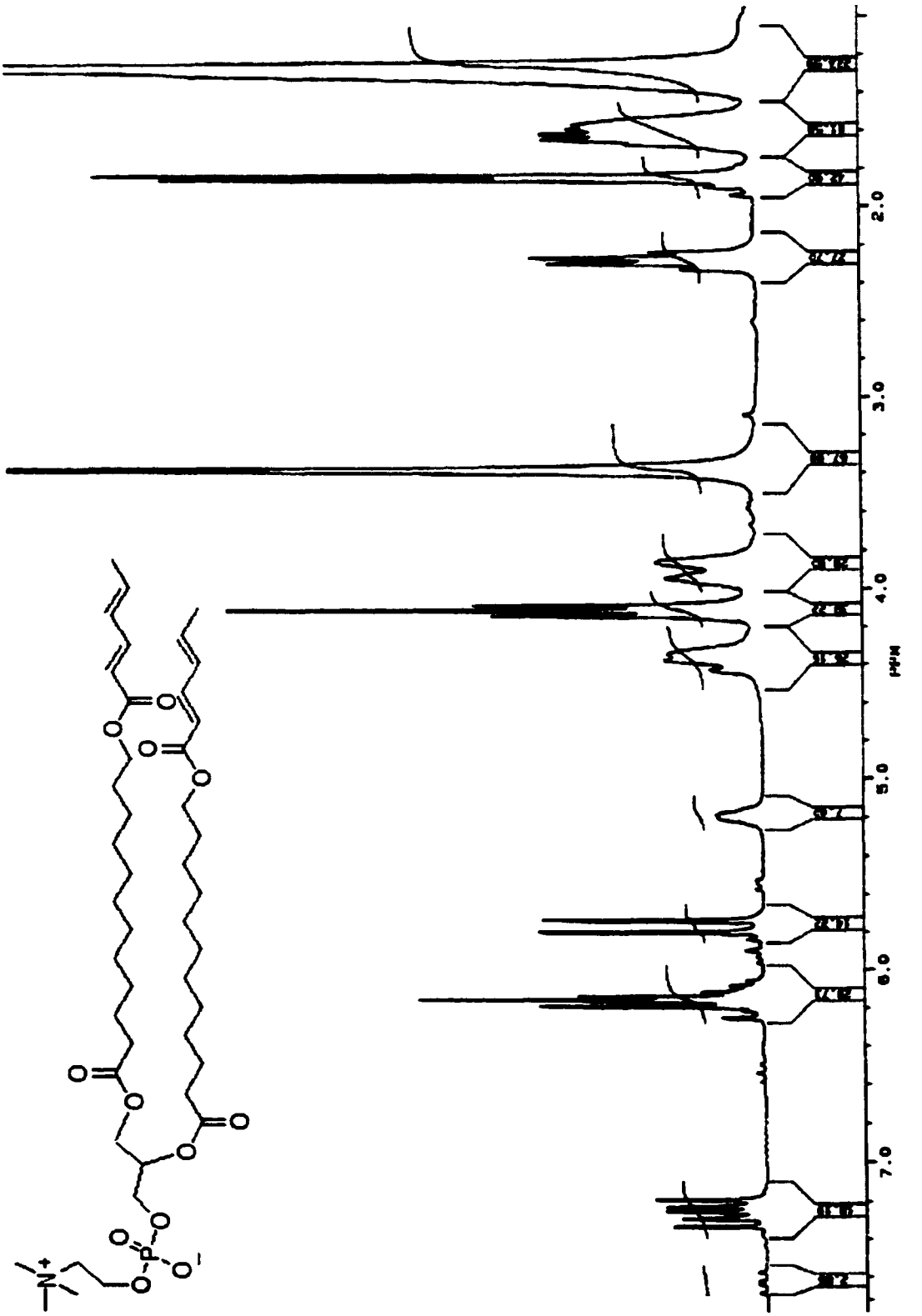
2.0
3.0
4.0
5.0
6.0
7.0
PPM

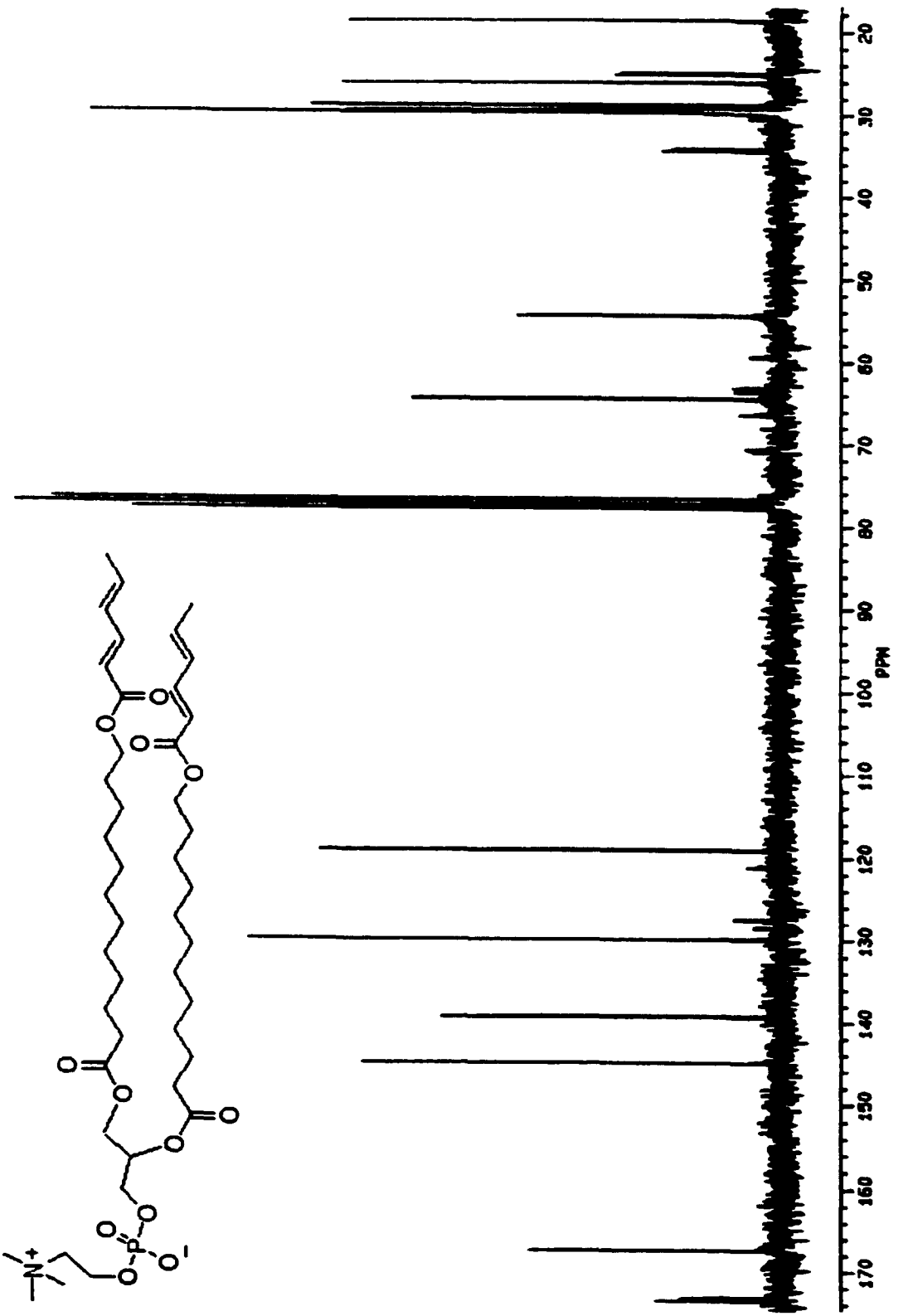
20
30
40
50
60
70
80
90
100
110
120
130
140
150
160
170
PPM

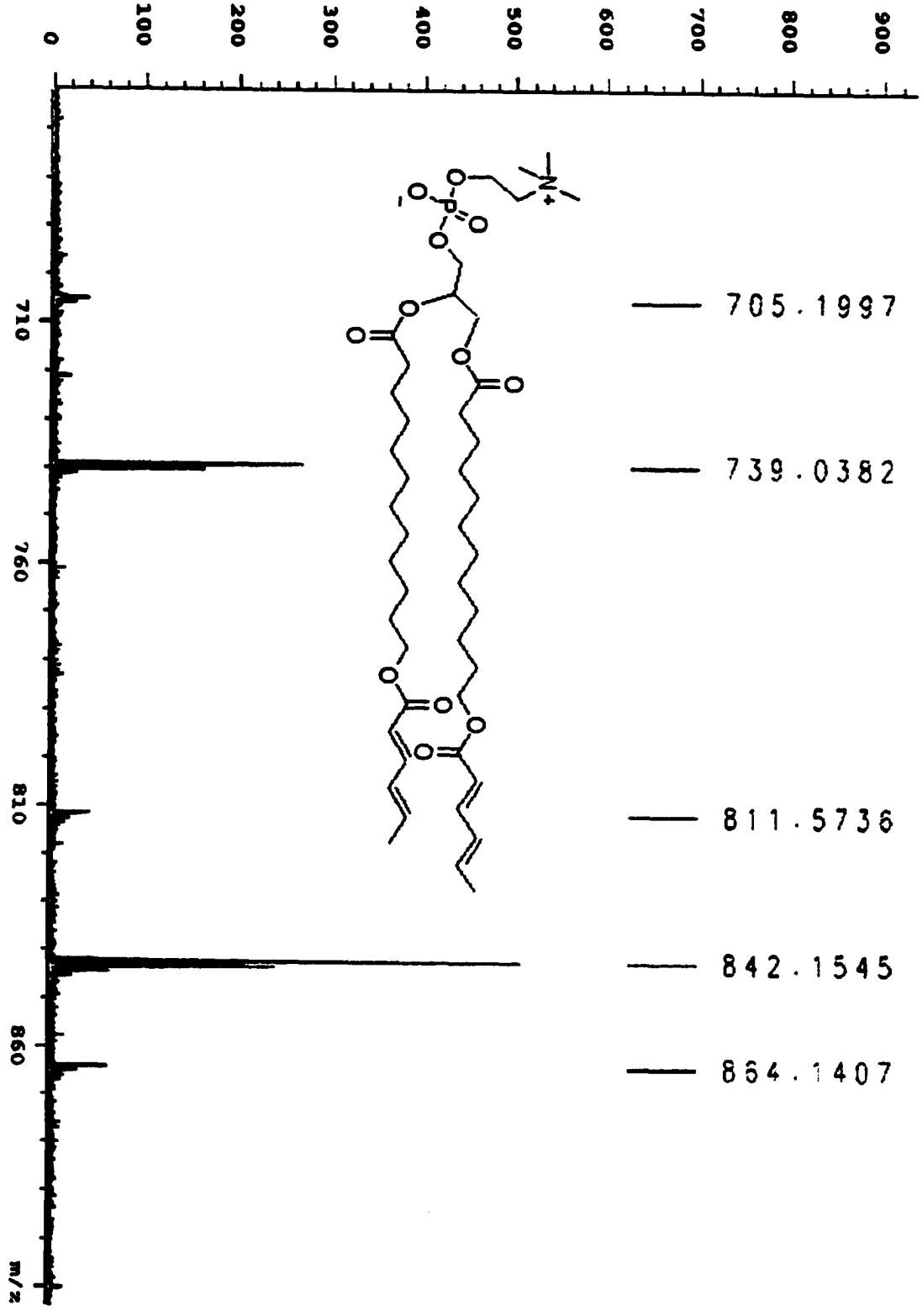
0
100
200
300
400
500
600
700
800
900
710
760
810
860
m/z
705.1997
739.0382
811.5736
842.1545
864.1407

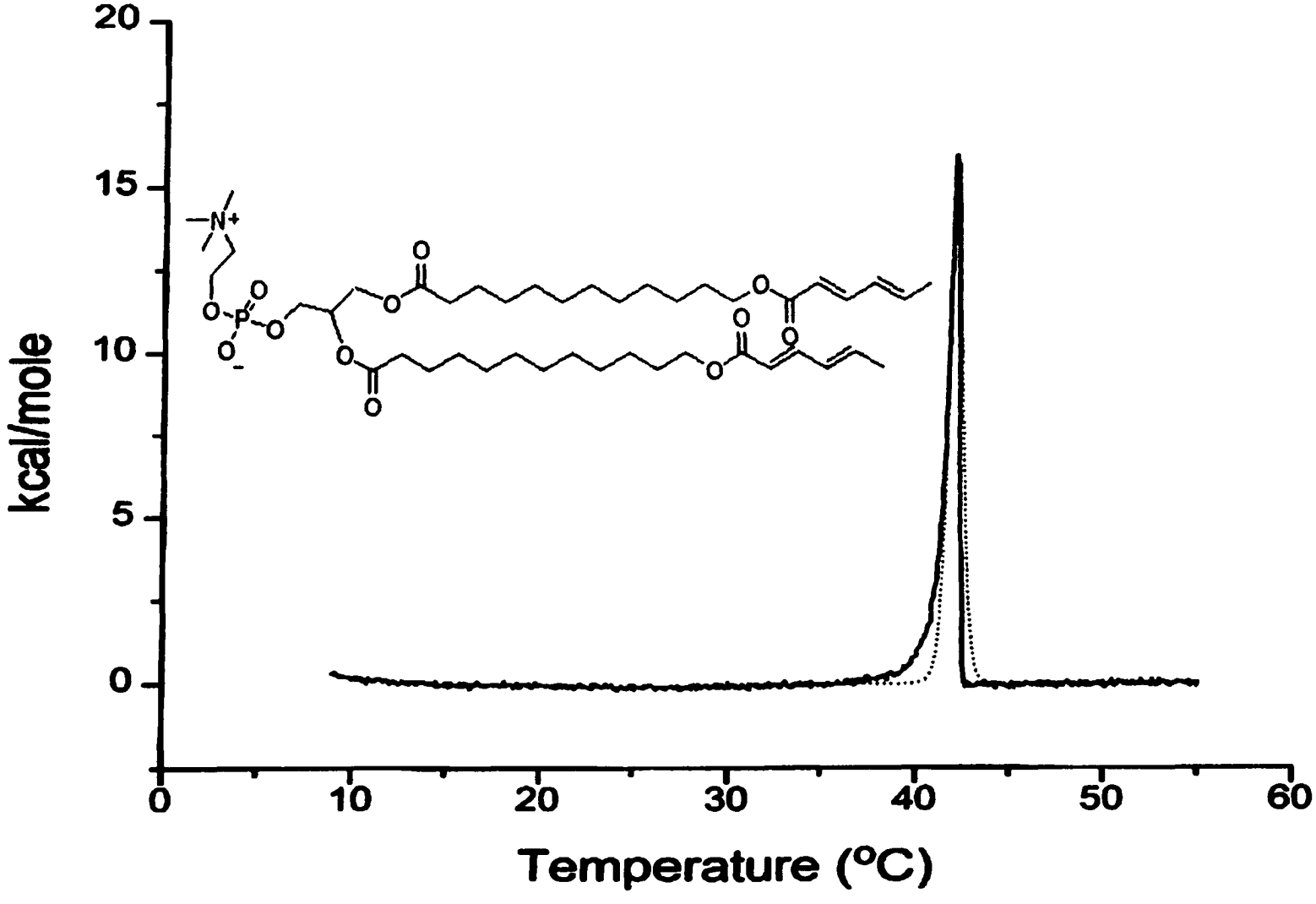
20
15
10
5
0
kcal/mole
0
10
20
30
40
50
60
Temperature (°C)

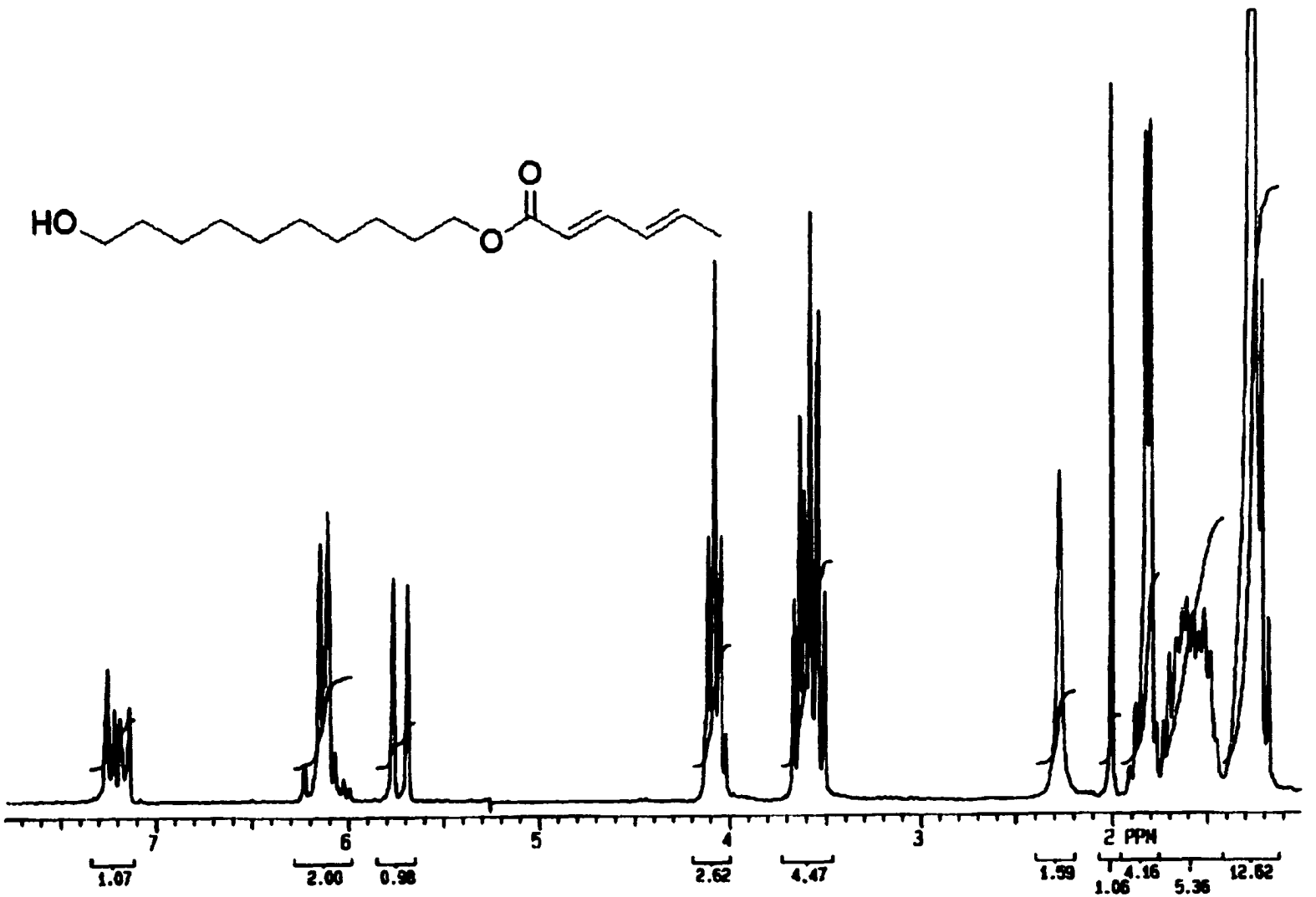
HO
O
O
7
6
5
4
3
2 PPM
1.07
2.00
0.98
2.62
4.47
1.99
1.06
4.16
5.36
12.62

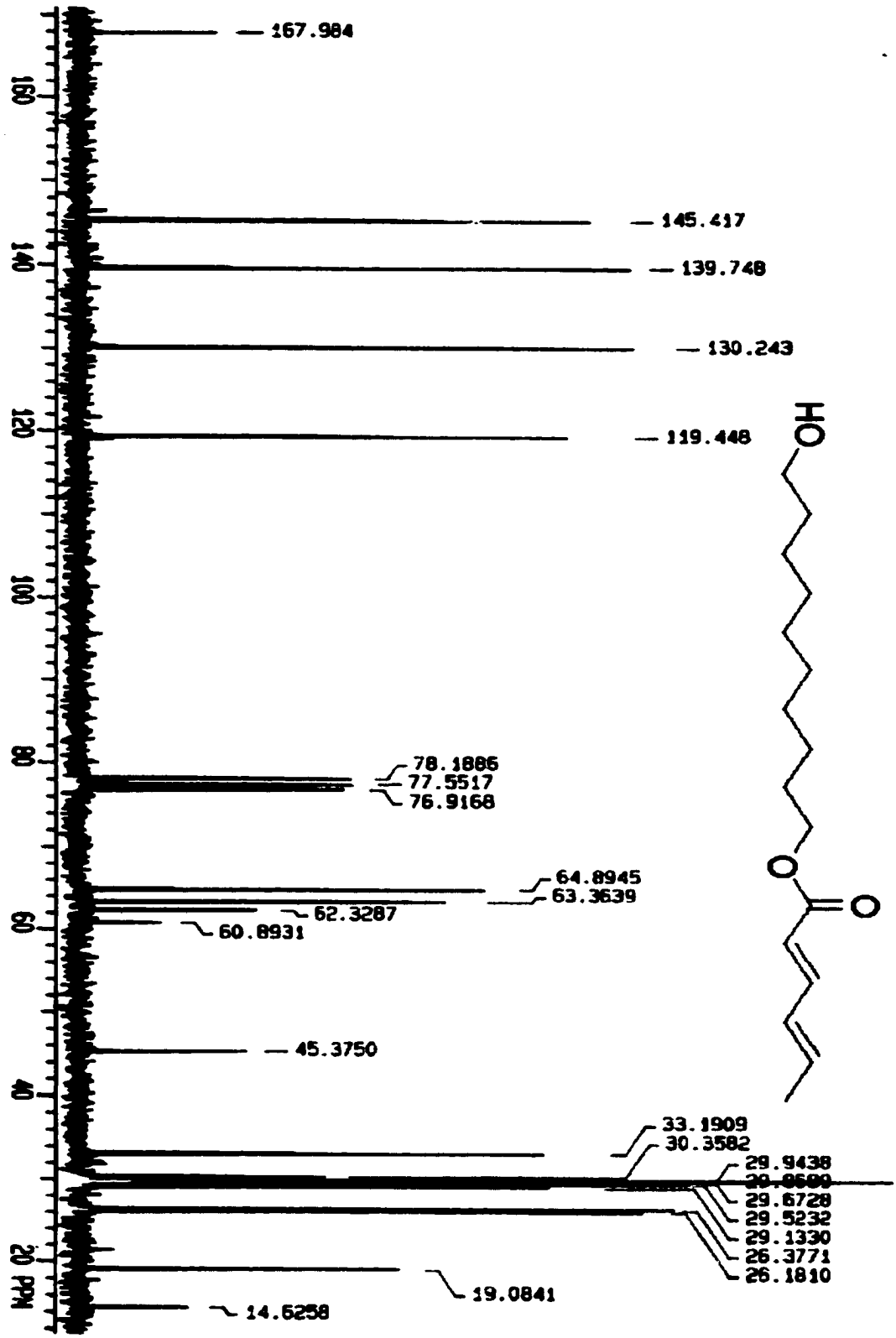
167.984
145.417
139.748
130.243
119.448
78.1886
77.5517
76.9168
64.8945
63.3639
62.3287
60.8931
45.3750
33.1909
30.3582
29.9438
29.6728
29.5232
29.1330
26.3771
26.1810
19.0841
14.6258
ppm
OH
O
O

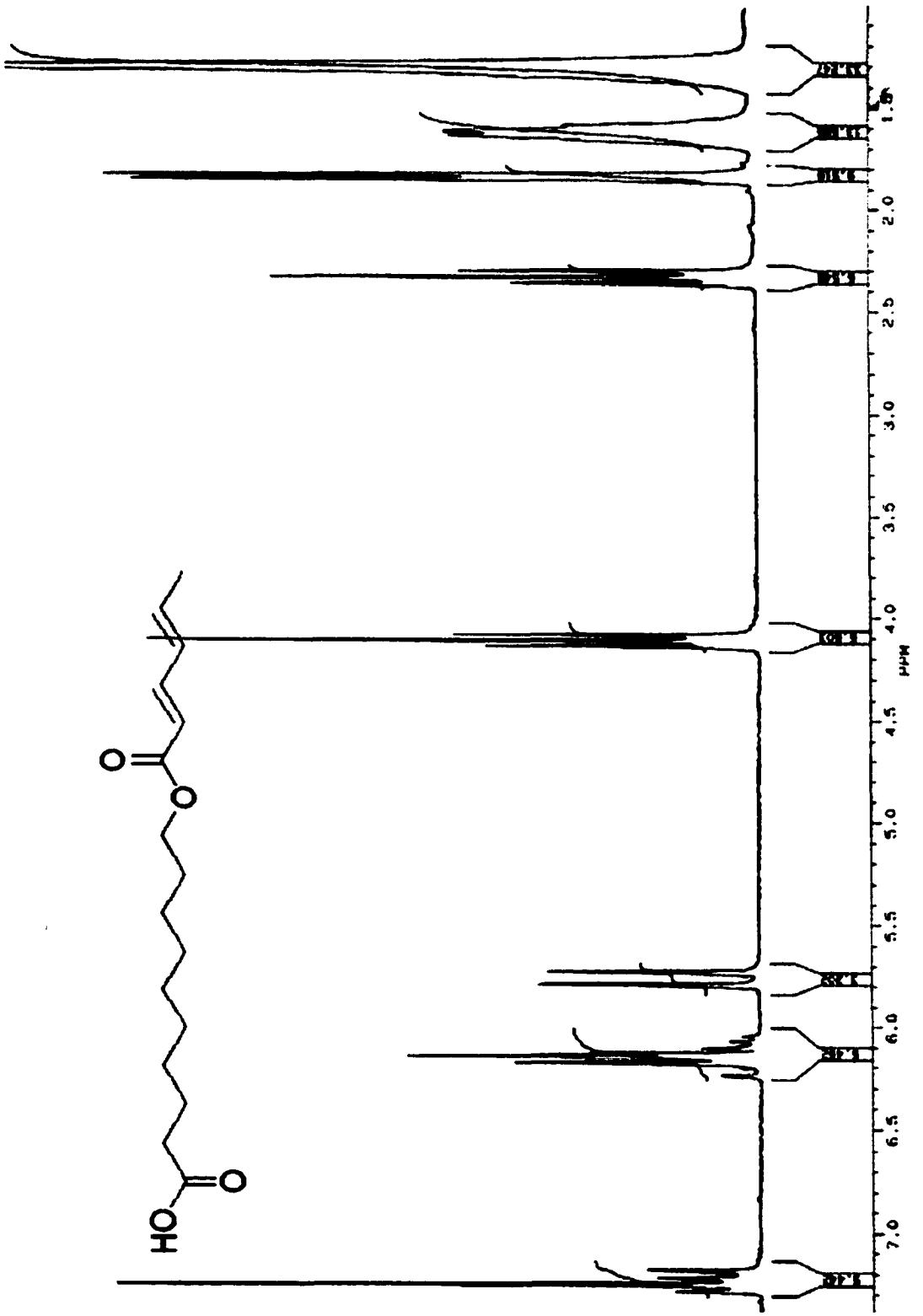
O
O
HO
O
1.5
2.0
2.5
3.0
3.5
4.0
4.5
5.0
5.5
6.0
6.5
7.0
PPM

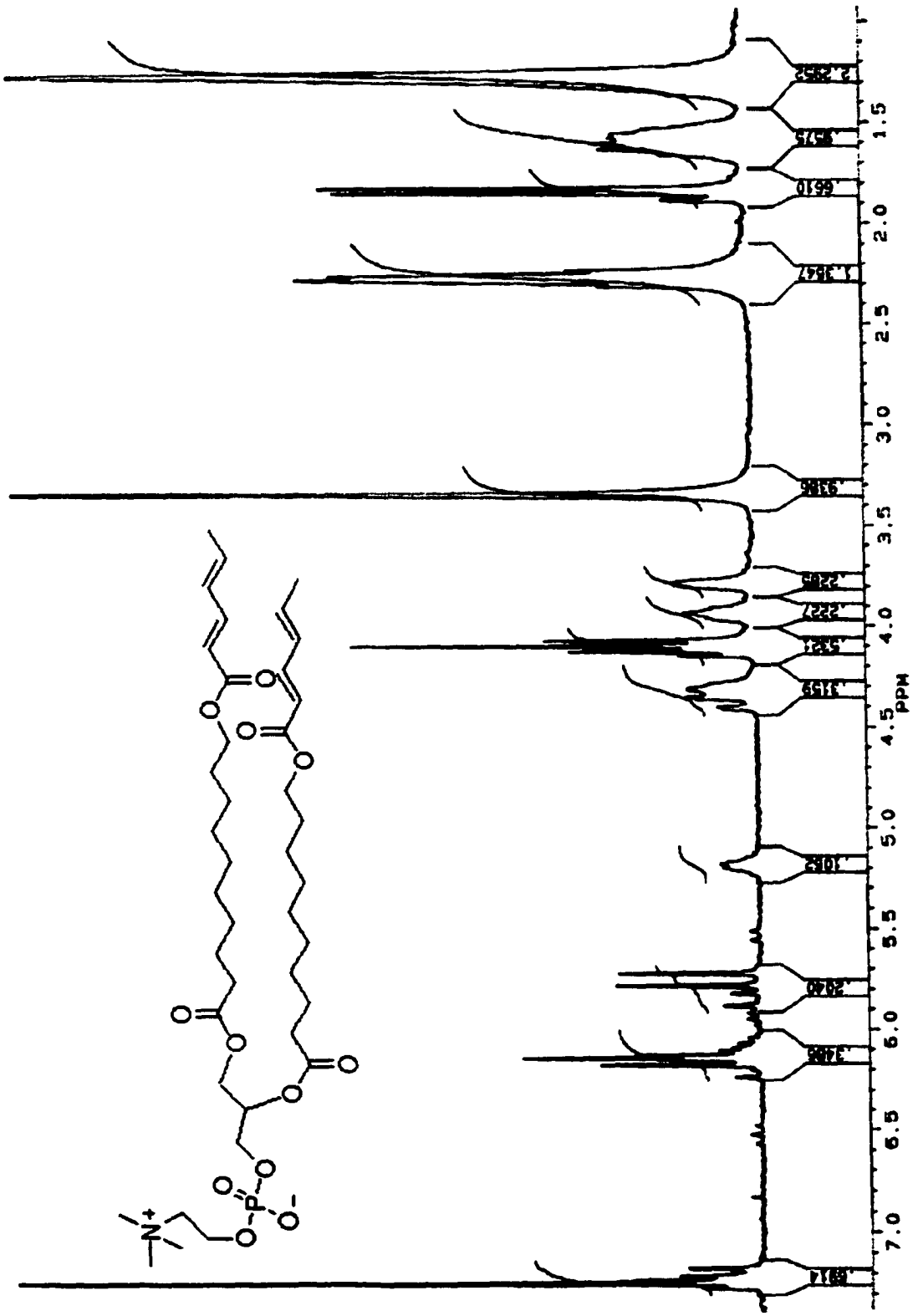
PPM
1.5
2.0
2.5
3.0
3.5
4.0
4.5
5.0
5.5
6.0
6.5
7.0

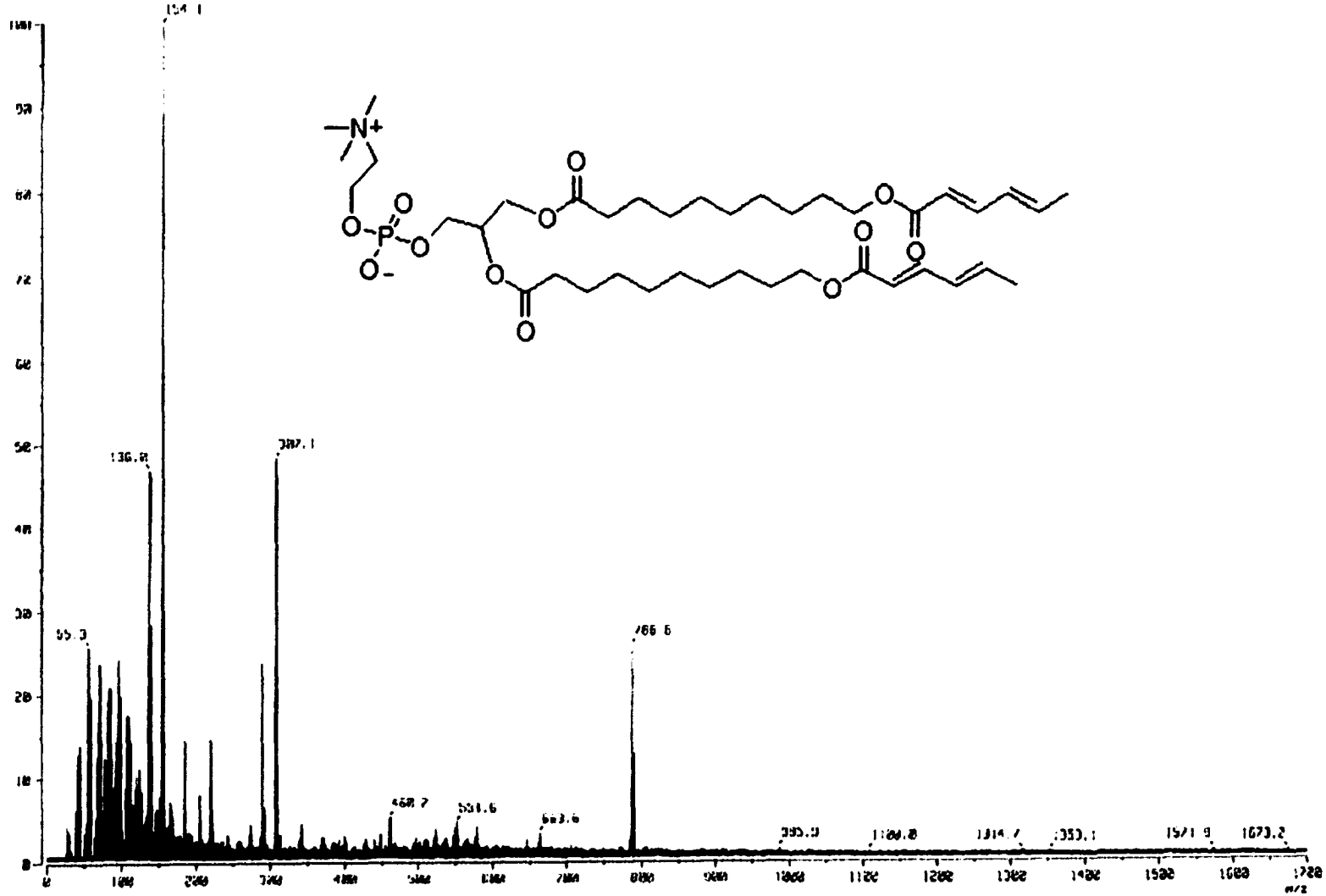

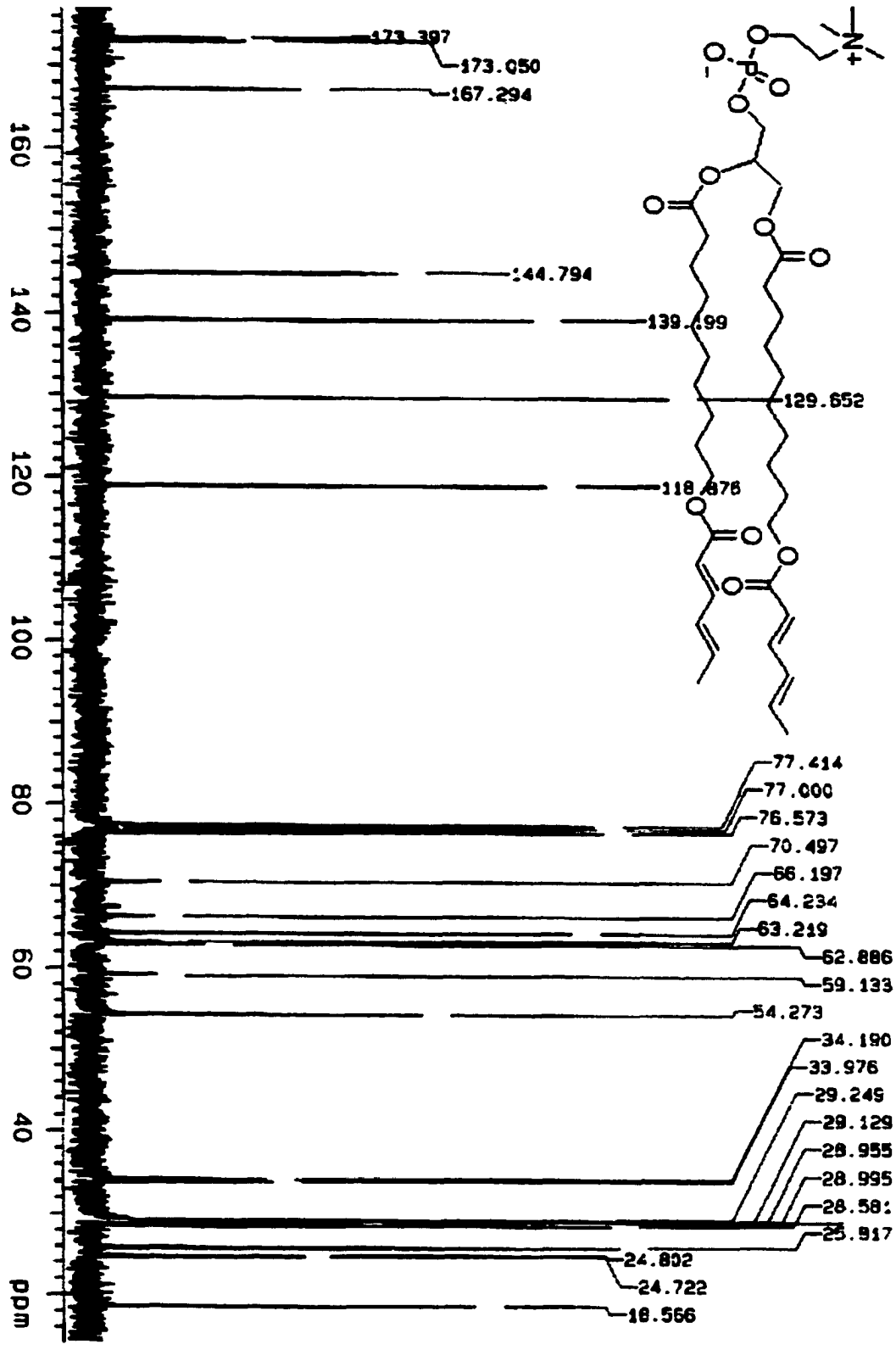
173.397
173.050
167.294
144.794
139.199
129.652
118.876
77.414
77.000
76.573
70.497
66.197
64.234
63.219
62.886
59.133
54.273
34.190
33.976
29.249
29.129
28.955
28.995
28.581
25.917
24.802
24.722
18.566
160
140
120
100
80
60
40
ppm

References

1. Hui, S.W., T.P. Stewart, and L.T. Boni, *The nature of lipidic particles and their roles in polymorphic transitions.* Chem. Phys. Lipids, 1983. **33**: p. 113.

2. Zhang, Y.P., B. Ceh, and D.D. Lasic, *Liposomes in Drug Delivery*, in *Polymeric Biomaterials*, S. Dumitriu, Editor. 2002, Marcel Dekker: New York.

3. Bangham, A.D., M.M. Standish, and J.C. Watkins, *Diffusion of univalent ions across the lamellae of swollen phospholipids.* J. Mol. Biol., 1965. **13**: p. 238.

4. Lehninger, A.L., D.L. Nelson, and M.M. Cox, *Principles of Biochemistry, Pt. 1. 2nd Ed.* 1993. 666 pp.

5. Petursson, S., *Clarification and expansion of formulas in AOCS recommended practice Cd 1c-85 for the calculation of iodine value from FA composition.* Journal of the American Oil Chemists' Society, 2002. **79**(7): p. 737.

6. Lewis, R.N.A.H., N. Mak, and R.N.A. McElhaney, *A differential scanning calorimetric study of the thermatropic phase behavior of model membranes composed of phosphatidylcholines containing linear saturated fatty acyl chains.* Biochemistry, 1987: p. 6118.

7. Lewis, R.N.A.H., B.D. Sykes, and R.N.A. McElhaney, *Thermotropic phase behavior of model membranes composed of phosphatidylcholines containing cis-monounsaturated acyl chain homologues of oleic acid: differential scanning calorimetric and ^{31}P NMR spectroscopic studies.* Biochemistry, 1988. **27**: p. 880.

8. Marsh, D., *General features of phospholipid phase transitions.* Chemistry and Physics of Lipids, 1991. **57**: p. 109.

9. Zhang, Y.P., R.N.A.H. Lewis, R.N.A. McElhaney, and R.O. Ryan, *Calorimetric and spectroscopic studies of the interaction of Manduca sexta apolipophorin III with zwitterionic, anionic, and nonionic lipids.* Biochemistry, 1993. **32**: p. 3942.

10. Boggs, J.M., *Lipid intermoleculer hydrogen bonding: influence on structural organization and membrane function.* Biochimica et Biophysica Acta, 1987. **906**: p. 353.

11. Boggs, J.M., G. Rangaraj, and K.M. Koshy, *Effect of hydrogen-bonding and non-hydrogen-bonding long chain compounds on the phase transition temperatures of phospholipids.* Chem. Phys. Lipids, 1986. **40**: p. 23.

12. Seddon, J.M., G. Cevc, and D. Marsh, *Calorimetric studies of the gel-fluid (L_β-L_α) and lamellar-inverted hexagonal (L_α-L_β) phase transitions in dialkyl- and diacylphosphatidylethanolamines.* Biochemistry, 1983. **22**: p. 1280.

13. Marsh, D., *Handbook of Lipid Bilayers.* 1990, Boca Raton, Fl: CRC Press.

14. Fiegenson, G.W. and J.T. Buboltz, *Ternary Phase Diagram of Dipalmitoyl-PC/Dilauroyl-PC/Cholesterol: Nanoscopic Domain Formation Driven by Cholesterol.* Biophysical Journal, 2001. **80**: p. 2775.

15. New, R.R.C., *Influence of Liposome Characteristics on Their Properties and Fate*, in *LIPOSOMES as TOOLS in BASIC RESEARCH and INDUSTRY*, R.R.C. New, Editor. 1995, CRC Press: Boca Raton.

16. O'Brien, D.F., B. Armitage, A. Benedicto, D.E. Bennett, H.G. Lamparski, Y.-S. Lee, W. Srisiri, and T.M. Sisson, *Polymerization of Preformed Self-Organized Assemblies.* Accounts of Chemical Research, 1998. **31**(12): p. 861.

17. Fahey, P.F. and W.W. Webb, *Lateral diffusion in phospholipid bilayer membranes and multilamellar liquid crystals.* Biochemistry, 1978. **17**: p. 3046.

18. Liu, S., T.M. Sisson, and D.F. O'Brien, *Synthesis and Polymerization of Heterobifunctional Amphiphiles to Cross-Link Supramolecular Assemblies.* Macromolecules, 2001. **34**(3): p. 465.

19. Srisiri, W., Y.S. Lee, and D.F. O'Brien, *Chemical synthesis of a polymerizable bis-substituted phosphoethanolamine.* Tetrahedron Lett., 1995. **36**: p. 8945.

20. Blume, G. and G. Cevc, *Liposomes for the sustained drug release in vivo.* Biochimica et Biophysica Acta, 1990. **1029**(1): p. 91.

21. Allen, T.M., *Long-circulating (sterically stabilized) liposomes for targeted drug delivery.* Trends in Pharmacological Sciences, 1994. **15**(7): p. 215.

22. Monfardini, C. and F.M. Veronese, *Stabilization of Substances in Circulation.* Bioconjugate Chem., 1998. **9**: p. 418.

23. Allen, T.M., G.A. Austin, A. Chonn, L. Lin, and K.D. Lee, *Uptake of liposomes by cultured mouse bone marrow macrophages: influence of liposome composition and size.* Biochimica et Biophysica Acta, 1991. **1061**: p. 56.

24. Allen, T.M. and A. Chonn, *Large unilamellar liposomes with low uptake into the reticuloendothelial system.* FEBS Letters, 1987. **284**: p. 263.

25. Charrois, G.J.R. and T.M. Allen, *Stealth liposome size influences biodistribution: Implications for toxicity and therapeutic activity.* Proceedings

- 28th International Symposium on Controlled Release of Bioactive Materials and 4th Consumer & Diversified Products Conference, San Diego, CA, United States, June 23-27, 2001, 2001. **1**: p. 576.

26. Ishida, T., M.J. Kirchmeier, E.H. Moase, S. Zalipsky, and T.M. Allen, *Targeted delivery and triggered release of liposomal doxorubicin enhances cytotoxicity against human B lymphoma cells.* Biochimica et Biophysica Acta, 2001. **1515**(2): p. 144.

27. Mayer, L.D., R. Krishna, and M.B. Bally, *Liposomes for Cancer Therapy Applications*, in *Polymeric Biomaterials*, S. Dumitriu, Editor. 2002, Marcel Dekker: New York. p. 823.

28. Gabizon, A. and F. Martin, *Polyethylene glycol-coated (pegylated) liposomal doxorubicin. Rationale for use in solid tumors.* Drugs, 1997. **54**: p. 15.

29. Lasic, D.D. and Y. Barenholz, *Handbook of Nonmedical Applications of Liposomes: Theory and Basic Sciences.* 1996, Boca Raton: CRC Press.

30. Gregoriadis, G., *Liposomes as Drug Carrier Recent Trends and Progress.* 1988, New York: john Wiley and Sons.

31. Nassander, U.K., G. Storm, P.A.M. Peters, and D.J.A. Crommelin, *Liposomes*, in *Biodegradable Polymers as Drug Delivery Systems*, M. Chasin and R. Langer, Editors. 1990, Marcel Dekker: New York.

32. Senior, J.H., *Fate and behavior of liposomes in vivo: a review of controlling factors.* Crit. Rev. Ther. Drug Carriers Syst., 1987. **3**: p. 123.

33. Yasuda, T., *Direct injection of liposome-encapsulated doxorubicin inhibits tumor growth.* International Journal of Cancer, 2000. **88**: p. 645.

34. Gregoriadis, G. and J.H. Senior, *The phospholipid component of small unilamellar liposomes control the rate of clearance of entrapped solutes from the circulation.* FEBS Letters, 1980. **119**: p. 43.

35. Senior, J.H. and G. Gregoriadis, *Is half-life of circulating small unilamellar liposomes determined by changes in their permeability?* FEBS Letters, 1982. **145**: p. 109.

36. Senior, J.H., J.C.W. Crawley, and G. Gregoriadis, *Tissue distribution of liposomes exhibiting long half-lives in the circulation after intravenous injection.* Biochimica et Biophysica Acta, 1985. **839**: p. 1.

37. Gregoriadis, G., *Fate of Liposomes in Vivo and Its Control: A Historical Perspective*, in *Stealth Liposomes*, D.D. Lasic and F.J. Martin, Editors. 1995, CRC Press: Boca Raton.

38. Hwang, K.J., *Liposome pharmacokinetics*, in *Liposomes from Biophysics to Therapeutics*, M.J. Ostro, Editor. 1987, Marcel Dekker: New York.

39. and T.M. Allen, *Stealth^{TM} liposomes: avoiding reticuloendothelial uptake in liposomes*, in *Liposomes in the Therapy of Infectious Diseases and Cancer*, G. Lopez-Berestein and I.J. Fidler, Editors. 1989, Alan R. Liss: New York. p. 405.

40. Papahadjopoulos, D., T.M. Allen, A. Gabizon, E. Mayhew, S.K. Huang, K.D. Lee, M.C. Woodle, D.D. Lasic, C. Redemann, and F.J. Martin, *Sterically stabilized liposomes - improvements in pharmacokinetics and antitumor therapeutic efficacy.* Proc. Natl. Acad. Sci. U.S.A., 1991. **88**: p. 11460.

41. Klibanov, A.L., K. Maruyama, A.M. Beckerleg, V.P. Torchilin, and L. Huang, *Activity of amphipathic poly(ethylene glycol) 5000 to prolong the circulation time of liposomes depends on the liposome size and is unfavorable for immunoliposome binding to target.* Biochimica et Biophysica Acta, 1992. **1062**: p. 142.

42. Klibanov, A.L., K. Maruyama, V.P. Torchilin, and L. Huang, *Amphipathic polyethyleneglycols effectively prolong the circulation time of liposomes.* FEBS Letters, 1990. **268**: p. 235.

43. Torchilin, V.P., A.L. Klibanov, L. Huang, S. O'Donnell, N.D. Nossiff, and B.A. Khaw, *Targeted accumulation of polyethylene glycol-coated immunoliposomes in infarcted rabbit myocardium.* FASEB J., 1992. **6**: p. 2716.

44. Gabizon, A. and D. Papahadjopoulos, *The role of surface charge and hydrophilic groups on liposome clearance in vivo.* Biochimica et Biophysica Acta, 1992. **1103**: p. 94.

45. Lasic, D.D., F.G. Martin, A. Gabizon, S.K. Huang, and D. Papahadjopoulos, *Sterically stabilized liposomes - a hypothesis on the molecular origin of the extended circulation times.* Biochimica et Biophysica Acta, 1991. **1070**: p. 187.

46. Needham, D., T.J. McIntosh, and D.D. Lasic, *Repulsive interactions and mechanical stability of polymergrafted lipid membranes.* Biochimica et Biophysica Acta, 1992. **1108**: p. 40.

47. Torchilin, V.P., V.G. Omelyanenko, M.I. Papisov, A.A. Bogdanov, Jr., V.S. Trubetskoy, J.N. Herron, and C.A. Gentry, *Poly(ethylene glycol) on the liposome surface: on the mechanism of polymer-coated liposome longevity.* Biochimica et Biophysica Acta, 1994. **1195**: p. 11.

48. Juliano, R.L., M.J. Hsu, S.L. Regen, and M. Sing, *Photopolymerized phospholipid vesicles. Stability and retention of hydrophilic and hydrophobic marker substances.* Biochimica et Biophysica Acta, 1984. **770**: p. 109.

49. Wagner, N., H. Dose, H. Koch, and H. ringsdorf, *Incorporation of ATP synthetase into long-term stable liposomes of polymerizable synthetic sulfolipid.* FEBS Letters, 1981. **132**: p. 313.

50. Bennett, D.E., H. Lamparski, and D.F. O'Brien, *Photosensitive liposomes.* J. Liposome Res., 1994: p. 331.

51. Bondurant, B., A. Mueller, and D.F. O'Brien, *Photoinitiated destabilization of sterically stabilized liposomes.* Biochimica et Biophysica Acta, 2001. **1511**(1): p. 113.

52. Mayer, L.D., M.J. Hope, P.R. Cullis, and A.S. Janoff, *Solute distributions and trapping efficiencies observed in freeze-thawed multilamellar vesicles.* Biochimica et Biophysica Acta, 1985. **817**: p. 193.

53. Cullis, P.R., L.D. Mayer, M.B. Bally, T.D. Madden, and M.J. Hope, *Generating and loading of liposomal systems for drug-delivery applications.* Advanced Drug Delivery Reviews, 1989. **3**: p. 267.

54. Amselem, S., A. Gabizon, and Y. Barenholz, *Optimization and upscaling of doxorubicin-containing liposomes for clinical use.* Journal of Pharmaceutical Sciences, 1990. **79**(12): p. 1045.

55. Haran, G., R. Cohen, L.K. Bar, and Y. Barenholz, *Transmembrane ammonium sulfate gradients in liposomes produce efficient and stable entrapment of amphipathic weak bases.* Biochimica et Biophysica Acta, 1993. **1151**: p. 201.

56. Lasic, D.D., B. Ceh, M.C.A. Stuart, L. Guo, P.M. Frederik, and Y. Barenholz, *Transmembrane gradient driven phase transitions within vesicles: lessons for drug delivery.* Biochimica et Biophysica Acta, 1995. **1239**: p. 145.

57. Bally, M.B., H. Lim, P.R. Cullis, and L.D. Mayer, *Controlling the Drug Delivery Attributes of Lipid-Based Drug Formulations.* Journal of Liposome Research, 1998. **8**: p. 299.

58. Costin, G.E., M. Trif, M. Michita, R. Dwek, and S.M. Petrescu, *pH-sensitive liposomes are efficient carriers for endoplasmic reticulum-targeted drugs in mouse melanoma cells.* Biochemical and Biophysical Research Communications, 2002. **293**(3): p. 918.

59. Hong, M.-S., S.-J. Lim, Y.-K. Oh, and C.-K. Kim, *pH-sensitive, serum-stable and long-circulating liposomes as a new drug delivery system.* Journal of Pharmacy and Pharmacology, 2002. **54**(1): p. 51.

60. Lee, K.-Y., E. Chun, and B.L. Seong, *Investigation of Antigen Delivery Route in Vivo and Immune-Boosting Effects Mediated by pH-Sensitive Liposomes Encapsulated with Kb-Restricted CTL Epitope.* Biochemical and Biophysical Research Communications, 2002. **292**(3): p. 682.

61. Roux, E., M. Francis, F.M. Winnik, and J.-C. Leroux, *Polymer based pH-sensitive carriers as a means to improve the cytoplasmic delivery of drugs.* International Journal of Pharmaceutics, 2002. **242**(1-2): p. 25.

62. Roux, E., R. Stomp, S. Giasson, M. Pezolet, P. Moreau, and J.-C. Leroux, *Steric stabilization of liposomes by pH-responsive N-isopropylacrylamide copolymer.* Journal of Pharmaceutical Sciences, 2002. **91**(8): p. 1795.

63. Shi, G., W. Guo, S.M. Stephenson, and R.J. Lee, *Efficient intracellular drug and gene delivery using folate receptor-targeted pH-sensitive liposomes composed of cationic/anionic lipid combinations.* Journal of Controlled Release, 2002. **80**(1-3): p. 309.

64. Wang, H., L. Hu, Z. Chen, S. Wang, and Z. Wang, *Research on optimized recipe and preparation conditions of pH-sensitive liposomes of gene transfection with orthogonal design methods.* Zhongguo Yaoxue Zazhi (Beijing, China), 2002. **37**(1): p. 29.

65. Holland, J.W., C. Hui, P.R. Cullis, and T.D. Madden, *Poly(ethylene glycol)-Lipid Conjugates Regulate the Calcium-Induced Fusion of Liposomes Composed of Phosphatidylethanolamine and Phosphatidylserine.* Biochemistry, 1996. **35**: p. 2618.

66. Kirpotin, D., K. Hong, N. Mullah, D. Papahadjopoulos, and S. Zalipsky, *Liposomes with Detachable Polymer Coating: Destabilization and Fusion of Dioleoylphosphatidylethanolame Vesicles Triggered by cleavage of Surface-grafted Poly(ethylene glycol).* FEBS Letters, 1996. **388**: p. 115.

67. Kono, K., K.-i. Zenitani, and T. Takagishi, *Novel pH-Sensitive Liposomes: Liposomes bearing a Poly(ethylene glycol) Derivative with Carboxyl Groups.* Biochimica et Biophysica Acta, 1994. **1193**: p. 1.

68. Kono, K., T. Igawa, and T. Takagishi, *Cytoplasmic Delivery of Calcein Mediated by Liposomes Modified with a pH-Sensitive Poly(ethylene glycol) derivative.* Biochimica et Biophysica Acta, 1997. **1325**: p. 143.

69. Rui, Y., S. Wang, P.S. Low, and D.H. Thompson, *Diplasmenylcholine-Folate Liposomes: An Efficient Vehicle for Intracellular Drug Delivery.* J. Am. Chem. Soc., 1998. **120**: p. 11214.

70. Boomer, J. and D.H. Thompson, *Synthesis of Acid Labile Diplasmenyl Lipids for Drug and Gene Delivery Applications.* Chemistry and Physics of Lipids, 1999. **99**: p. 145.

71. Collier, J.H., B.-H. Hu, J.W. Ruberti, J. Zhang, P. Shum, D.H. Thompson, and P.B. Messersmith, *Thermally and photochemically triggered self-assembly of peptide hydrogels.* Journal of the American Chemical Society, 2001. **123**(38): p. 9463.

72. Kakinuma, K. and R. Tanaka, *Targeting chemo-thermotherapy for malignant gliomas by thermosensitive liposome.* Shinkei Kenkyu no Shinpo, 1999. **43**(3): p. 431.

73. Needham, D., *Materials engineering of lipid bilayers for drug carrier performance.* MRS Bulletin, 1999. **24**(10): p. 32.

74. Kono, K., *The37rmosensitive polymer-modified liposomes.* Advanced Drug Delivery Reviews, 2001. **53**(3): p. 307.

75. Kono, K., R. Nakai, K. Morimoto, and T. Takagishi, *Thermosensitive Polymer-Modified Liposomes that Release Contents Around Physiological Temperature.* Biochimica et Biophysica Acta, 1999. **1416**: p. 239.

76. Kono, K., R. Nakai, K. Morimoto, and T. Takagishi, *Temperature-dependent interaction of thermo-sensitive polymer-modified liposomes with CV1 cells.* FEBS Letters, 1999. **456**: p. 306.

77. Kono, K., K. Yoshino, and T. Takagishi, *Effect of poly(ethylene glycol) grafts on temperature-sensitivity of thermosensitive polymer-modified liposomes.* Journal of Controlled Release, 2002. **80**(1-3): p. 321.

78. Maruyama, K., S. Unezaki, N. Takahashi, and M. Iwatsuru, *Enhanced Delivery of Doxorubicin to Tumor by Long-Circulating Thermosensitive Liposomes and Local Hyperthermia.* Biochimica et Biophysica Acta, 1993. **1149**: p. 209.

79. Gaber, M.H., K. Hong, S.K. Huang, and D. Papahadjopoulos, *Thermosensitive Sterically Stabilized Liposomes: Formulation and in Vitro Studies on Mechanism of Doxorubicin Release by Bovine Serum and Human Plasma.* Pharmaceutical Research, 1995. **12**: p. 1407.

80. Oku, N., R. Naruse, K. Doi, and S. Okada, *Potential Usage of Thermosensitive Liposomes for Macromolecule Delivery.* Biochimica et Biophysica Acta, 1994. **1191**: p. 390.

81. Hayashi, H., K. Kono, and T. Takagishi, *Temperature Controlled Release Property of Phospholipid Vesicles bearing a Thermo-Sensitive Polymer.* Biochimica et Biophysica Acta, 1996. **1280**: p. 127.

82. Bisby, R.H., C. Mead, and C.G. Morgan, *Wavelength-Programmed Solute Release from Photosensitive Liposomes.* Biochemical and Biophysical Research Communications, 2000. **276**(1): p. 169.

83. Bisby, R.H., C. Mead, and C.G. Morgan, *Active uptake of drugs into photosensitive liposomes and rapid release on UV photolysis.* Photochemistry and Photobiology, 2000. **72**(1): p. 57.

84. Shi, X., J. Li, C. Sun, and S. Wu, *The aggregation and phase separation behavior of a hydrophobically modified poly(N-isopropylacrylamide).* Colloids and Surfaces, A: Physicochemical and Engineering Aspects, 2000. **175**(1-2): p. 41.

85. Ohya, Y., Y. Okuyama, A. Fukunaga, and T. Ouchi, *Photo-sensitive lipid membrane perturbation by a single chain lipid having terminal spiropyran group.* Supramolecular Science, 1998. **5**(1-2): p. 21.

86. Condorelli, G., L.L. Costanzo, S. Giuffrida, G. De Guidi, S. Sortino, P. Miano, and A. Velardita, *Molecular mechanisms of photosensitivity induced by drugs in biological systems and design of photoprotective systems.* 1998, Dipartimento di Scienze Chimiche,Universita di Catania,Italy. FIELD URL:. p. 26.

87. Da Ros, T., G. Spalluto, A.S. Boutorine, R.V. Bensasson, and M. Prato, *DNA-photocleavage agents.* Current Pharmaceutical Design, 2001. **7**(17): p. 1781.

88. Haubs, M. and H. Ringsdorf, *Photosensitive monolayers, bilayer membranes and polymers.* New J. Chem., 1987. **11**(2): p. 151.

89. Monroe, W.T., M.M. McQuain, M.S. Chang, J.S. Alexander, and F.R. Haselton, *Targeting expression with light using caged DNA.* Journal of Biological Chemistry, 1999. **274**(30): p. 20895.

90. Sortino, S., G. Condorelli, G. De Guidi, and S. Giuffrida, *Molecular mechanism of photosensitization XI. Membrane damage and DNA cleavage photoinduced by enoxacin.* Photochemistry and Photobiology, 1998. **68**(5): p. 652.

91. O'Brien, D.F. and D.A. Tirrell, *Photoinduced reorganization of bilayer membranes*, in *Bioorganic Photochemistry*, H. Morrison, Editor. 1993, John Wiley and Sons: New York. p. 111.

92. Bondurant, B. and D.F. O'Brien, *Photoinduced Destabilization of Sterically Stabilized Liposomes.* J. Am. Chem. Soc., 1998. **120**: p. 13541.

93. Lamparski, H., U. Liman, D.A. Frankel, J.A. Barry, V. Ramaswami, M.F. Brown, and D.F. O'Brien, *Photoinduced Destabilization of Liposomes.* Biochemistry, 1992. **31**: p. 685.

94. Miller, C.R., P.J. Clapp, and D.F. O'Brien, *Visible light-induced destabilization of endocytosed liposomes.* FEBS Letters, 2000. **467**(1): p. 52.

95. Mueller, A., B. Bondurant, and D.F. O'Brien, *Visible-Light-Stimulated Destabilization of PEG-Liposomes.* Macromolecules, 2000. **33**(13): p. 4799.

96. Spratt, T., B. Bondurant, and D.F. O'Brien, *Rapid photoinitiated destabilization of sterically stabilized liposomes.* Polymer Preprints (American Chemical Society, Division of Polymer Chemistry), 2002. **43**(2): p. 779.

97. Lamparski, H. and D.F. O'Brien, *Two-Dimensional Polymerization of Lipid Bilayers:Degree of Polymerization of Sorbyl Lipids.* Macromolecules, 1995. **28**(6): p. 1786.

98. Sisson, T.M., H.G. Lamparski, S. Koelchens, A. Elayadi, and D.F. O'Brien, *Crosslinking Polymerizations in Two-Dimensional Assemblies.* Macromolecules, 1996. **29**(26): p. 8321.

99. Clapp, P.J., B.A. Armitage, and D.F. O'Brien, *Two-Dimensional Polymerization of Lipid Bilayers: Visible-Light-Sensitized Photoinitiation.* Macromolecules, 1997. **30**(1): p. 32.

100. Bennett, D.E. and D.F. O'Brien, *Photoactivated Enhancement of Liposome Fusion.* Biochemistry, 1995. **34**: p. 3102.

101. Armitage, B., P. Klekotka, E. Oblinger, and D.F. O'Brien, *Enhancement of Energy Transfer on Bilayer Surfaces via Polymerization-Induced Domain Formation.* J. Am. Chem. Soc., 1993. **115**: p. 7920.

102. Lei, J. and D.F. O'Brien, *Two-Dimensional Polymerization of Lipid Bilayers: Rate of Polymerization of Acryloyl and Methacryloyl Lipids.* Macromolecules, 1994. **27**: p. 1381.

103. Bondurant, B., *Photoinduced Release of Contents from Sterically Stabilized Liposomes*, in *Department of Chemistry*. 2000, University of Arizona: Tucson. p. 325.

104. O'Brien, D.F., K. McGovern, T. Spratt, and A. Mueller, *Radiation sensitive PEG-liposomes for drug delivery.* Polymer Preprints (American Chemical Society, Division of Polymer Chemistry), 2002. **43**(2): p. 705.

105. Lamparski, H., Y.S. Lee, T.D. Sells, and D.F. O'Brien, *Thermotropic properties of model membranes composed of polymerizable lipids. 1. Phosphatidylcholines containing terminal acryloyl, methacryloyl, and sorbyl groups.* J. Am. Chem. Soc., 1993. **115**(18): p. 8096.

106. O'Brien, D.F., K. McGovern, B. Bondurant, A. Mueller, and A. Spratt, *Ionizing radiation induced destabilization of PEG-liposomes.* Abstr. Pap. - Am. Chem. Soc., 2001. **221st**: p. PMSE.

107. Tannock, I.F., *The Basic Science of Oncology.* 2nd ed, ed. R.P. Hill. 1992, New York: McGraw-Hill. 420.

108. Ohno, H., Y. Ogata, and E. Tsuchida, *Gamma-ray polymerization of phospholipids having diene or triene groups as liposomes.* J. Polym. Sci. Polym. Chem. Ed., 1986. **24**: p. 2959.

109. Takeoka, S., N. Kimura, H. Ohno, and E. Tsuchida, *Polymerization of liposomes evaluated from molecular weight distribution of diene-type phospholipid polymers.* Polymer Journal, 1990. **22**: p. 867.

110. Sells, T.D. and D.F. O'Brien, *Degree of polymerization in two-dimensional assemblies.* Macromolecules, 1991. **21**: p. 226.

111. Sells, T.D. and D.F. O'Brien, *Two-dimensional polymerization of lipid bilayers: degree of polymerization of acryloyl lipids.* Macromolecules, 1994. **27**: p. 226.

112. Sisson, T.M., *Crosslinking polymerization in supramolecular assemblies*, in *Univ. of Arizona, Tucson, AZ, USA. FIELD URL:*. 1997. p. 279 pp.

113. Chapman, C.J., W.L. Eradahl, R.W. Taylor, and D.R. Pfeiffer, *Factors affecting solute entrapment in phospholipid vesicles prepared by the freeze-thaw extrusions method: A possible general method for improving the efficiency of entrapment.* Chem. Phys. Lipids, 1990. **55**: p. 73.

114. Mayer, L.D., M.J. Hope, and P.R. Cullis, *Vesicles of variable sizes produced by a rapid extrusion procedure.* Biochimica et Biophysica Acta, 1986. **858**: p. 161.

115. Perkins, W.R., S.R. Minchey, P.L. Ahl, and A.S. Janoff, *The determination of liposome captured volume.* Chem. Phys. Lipids, 1993. **64**(197-217).

116. Efremova, N.V., B. Bondurant, D.F. O'Brien, and D.E. Leckband, *Measurements of Interbilayer Forces and Protein Adsorption on Uncharged Lipid Bilayers Displaying Poly(ethylene glycol) Chains.* Biochemistry, 2000. **39**: p. 3441.

117. Brown, R.E., *Cholesterol-induced interfacial area condensations of galactosylceramides and sphingomyelins with identical acyl chains.* Biochemistry, 1996. **35**: p. 5696.

118. Edwards, K., M. Johnsson, G. Karlsson, and M. Silvander, *Effect of Polyethyleneglycol-Phospholipids on Aggregate Structure in Preparations of Small Unilamellar Liposomes.* Biophysical Journal, 1997. **73**: p. 258.

119. Matsumoto, A., Y. Isizy, and K. Yokoi, *Solid-State Photopolymerization of Octadecyl Sorbate to Yield an Alternating Copolymer with Oxygen.* Macromolecular Chemistry and Physics, 1998. **199**: p. 2511.

120. Odian, G., *Principals in Polymerization.* 1991, New York: John Wiley and Sons, INC.

121. Babilis, D., P. Dias, L.H. Margaritis, and C.M. Paleos, *Polymerization of oriented monomers. VIII. Polymerization of allyl and diallyl vesicle-forming quaternary ammonium salts.* J. Polym. Sci. Polym. Chem. Ed., 1984. **23**: p. 3383.

122. Paleos, C.M., P. Dias, and A. Malliaris, *Polymerization of allyldimethyldodecylammonium bromide in micellar and isotropic media.* J. Polym. Sci. Polym. Chem. Ed., 1984. **22**: p. 3383.

123. Paleos, C.M., C. Christias, and G.P. Evangelatos, *Polymerization of oriented monomers. VI. Polymerization of monomeric di(undecenyl) phosphate vesicles to stable polymeric vesicles.* J. Polym. Sci. Polym. Chem. Ed., 1982. **20**: p. 2565.

124. Tsuchida, E., E. Hasegawa, N. Kimura, M. Hatashita, and C. Makino, *Polymerization of unsaturated phospholipids as large unilamellar liposomes at low temperature.* Macromolecules, 1992. **25**: p. 207.

125. Lasic, D.D. and D. Papahadjopoulos, *Medical Applications of Liposomes.* 1998, Amsterdam: Elsivier Science.

126. Gabizon, A., D. Goren, Z. Fuks, Y. Barenholz, A. Dagan, and A. Meshorer, *Enhancement of adriamycin delivery to liver metastatic cells with increased tumoricidal effect using liposomes as drug carriers.* Cancer Research, 1983. **43**: p. 4730.

127. Jones, M.N. and M.J.H. Hudson, *The targeting of immunoliposomes to tumour cells (A431) and the effects of encapsulated methotrexate.* Biochimica et Biophysica Acta, 1993. **1152**: p. 231.

128. Konigsberg, P.J., R. Godtel, T. Kissel, and L.L. Richer, *The development of IL-2 conjugated liposomes for therapeutic purposes.* Biochimica et Biophysica Acta, 1998. **1370**: p. 243.

129. Erdlenbruch, B., M. Nier, W. Kern, W. Hiddemann, A. Pekrum, and M. Lakomek, *Pharmacokinetics of cisplatin and relation to nephrotoxicity in paediatric patients.* European Journal of Clinical Pharmacology, 2001. **57**: p. 393.

130. Schramel, P., I. Wendler, and S. Lustig, *Capability of ICP-MS (pneumatic nebulization and ETV) for Pt-analysis in different matrices at ecologically relevant concentrations.* Fresenius' Journal of Analytical Chemistry, 1995. **353**: p. 115.

131. Milacic, R., M. Cemazar, and G. Sersa, *Determination of platinum in tomour tissues after cisplatin therapy by electrothermal atomic absorption spectrometry.* Journal of Pharmaceutical and Biomedical Analysis, 1997. **16**: p. 343.